Niemann-Pick Type C Disease: Molecular Mechanisms of Neurodegeneration and Targets for Therapeutic Intervention

by

Ting Yu

A dissertation submitted in partial fulfillment
of the requirements for the degree of
Doctor of Philosophy
(Molecular and Cellular Pathology)
in the University of Michigan
2013

Doctoral Committee:

Associate Professor Andrew P. Lieberman, Chair
Professor Roger L. Albin
Professor Gregory R. Dressler
Professor Miriam H. Meisler
Associate Professor Anuska Andjelkovic-Zochowska

Dedication

This dissertation is dedicated to all Niemann-Pick Type C patients and their families, for their optimism and persistence in fighting this devastating disease. They are a great inspiration and a motivation behind my thesis work.

Acknowledgements

First, I would like to thank my mentor Andy Lieberman for his invaluable guidance and support along my five-year PhD journey. I am both grateful and honored to have the opportunity to work with him, who always makes himself available to me, who encourages me to think independently and broadly, and who gives me full support to pursue my scientific interest. His wisdom in both scientific research and laboratory management is exemplary. I am hoping to grow into a scientist who could make an impact on students the way he has done to me.

I also want to thank all the former and current members of the Lieberman lab, for making my PhD life such an enjoyable memory. In particularly, I thank Nahid Dadgar and Satya Reddy, for their incredible technical support as superb lab managers; Matt Elrick and Christ Pacheco, for their helpful scientific discussions with me, as well as the conditional NPC mouse model they developed, without which my thesis would not be made possible; Chan Chung, for giving me the chance to learn how to work closely with a junior graduate student. Finally a special thank you to Zhigang Yu, who has given me numerous valuable tips on how to do experiments efficiently and is always there to offer me advice whenever I encounter a problem.

It is my luck to have Roger Albin, Greg Dressler, Miriam Meisler and Anuska Zochowska serving on my thesis committee. I thank them for spending valuable time and offering insightful inputs on my thesis projects. I enjoyed the time discussing science with them.

I would like to extend my thankfulness to many other people who have helped me and who I have collaborated with throughout the whole course. This includes, but not limited to,

Vikram Shakkottai, Dongbiao Shen, John Dishinger, Huilin Shi, Yu Liu, and Lisa Sharkey. I am also grateful to the staff at the Microscopy and Imaging Laboratory, especially Chris Edwards, Bruce Donohoe, Jeff Harrison and Shelley Almburg, for their superb training and assistance on various microscopes. Thank you also goes to the MCP program, as well as Laura Hessler and Laura Labut, for their tremendous assistance in all kinds of student affairs.

My life in Ann Arbor would not be so colorful without all the friends I have met here. Thank you so much for sharing the ups and downs with me. Please accept my best wishes as you guys are pursuing the dreams all over the world. I am also incredibly indebted to my aunt Qinxian Miao, uncle Hanjin Miao and their families, for their warm hospitality and always treating me like their own daughter. Finally, I would like to express my deepest gratitude to my parents Genfa Yu and Qinbao Miao, whose unconditional love and support is behind every progress I have made.

Table of Contents

List of Figures

Figure

Abstract

Niemann-Pick Type C disease (NPC) is a childhood-onset neurodegenerative disorder characterized by the accumulation of unesterified cholesterol and glycosphingolipids in late endosomes and lysosomes. Ninety-five percent of cases of NPC are caused by loss-of-function mutations in the ubiquitously expressed *NPC1* gene, which encodes a multi-pass transmembrane protein essential for mobilizing cholesterol from the endolysosomal system. How disruption of NPC1 function leads to progressive neurodegeneration remains unknown and effective treatment is lacking.

I used a conditional knockout mouse model of NPC to define the timing and cell type underlying neurodegeneration due to *Npc1* deficiency. Global deletion of *Npc1* in adult mice leads to progressive weight loss, impaired motor function and early death in a time course similar to that resulting from germline deletion. Additionally, the disease can be recapitulated when *Npc1* is deleted specifically in neurons. In contrast, Npc1 deficiency in mature astrocytes does not produce any detectable defects. These findings demonstrate that neurons, but not astrocytes, play a critical role in the pathogenesis of NPC.

I also explored the contribution of exogenously derived cholesterol to the formation of CNS myelin, a specialized extension of the oligodendrocyte plasma membrane that serves as an electrical insulator to ensure proper nerve conduction. By using the conditional knockout mouse model of NPC, I unexpectedly found that *Npc1* deficiency in neurons alone leads to an arrest of

oligodendrocyte maturation and to subsequent failure of myelin synthesis in selective brain regions. This defect is associated with decreased activation of Fyn kinase, an integrator of axon-glial signals that normally promotes myelination. In parallel, I showed that loss of *Npc1* specifically in oligodendrocytes results in delayed myelination at early postnatal days. These mice, when aged, also exhibit progressive motor deficits accompanied by late stage demyelination and secondary Purkinje neuron loss. These data demonstrate that lipid uptake by neurons and oligodendrocytes through an Npc1-dependent pathway is required for both the formation and maintenance of CNS myelin.

In addition, I explored a potential treatment strategy that targets mutant NPC1 protein containing missense mutations. I identified ryanodine receptor (RyR) antagonists as effective disease-modifying compounds in patient fibroblasts harboring the NPC1 I1061T mutation. My data demonstrate that by increasing ER calcium levels, RyR antagonists increase the steady-state levels of the NPC1 I1061T protein, promote its trafficking to the late endosomes and lysosomes, and rescue the cholesterol storage and sphingolipid trafficking defects. Similar rescue is achieved by over-expressing calnexin, a calcium-dependent ER chaperone. My work highlights the utility of proteostasis regulators to remodel the protein-folding environment in the ER to recover function in the setting of disease-causing missense alleles. In summary, the findings presented here provide new insights into the pathogenic mechanisms underlying NPC and suggest a possible approach for therapeutic intervention.

Chapter 1

Introduction

1.1 Niemann-Pick Type C (NPC) disease

1.1.1 NPC pathology

Lysosomal storage diseases are a group of ~50 rare genetic disorders that result in lysosomal dysfunction (Gieselmann, 1995). Most of these diseases are caused by deficiencies of either a lysosomal hydrolase or an integral lysosomal membrane protein. In both cases, lysosomal dysfunction leads to the aberrant accumulation of lipids, proteins or other macromolecules in lysosomes (Winchester et al., 2000). Among this group is Niemann-Pick type C disease (NPC), an autosomal recessive neurodegenerative disorder characterized by the accumulation of unesterified cholesterol and glycosphingolipids in late endosomes and lysosomes (LE/LYs) (Vanier, 2010).

Among NPC patients, disease onset and phenotype severity vary greatly (Fink et al., 1989; Vanier et al., 1991; Vanier et al., 1988), with no clear genotype-phenotype correlation (Runz et al., 2008). The classic form of NPC presents in early childhood, but disease can also present in both the perinatal period and adults (Vanier and Millat, 2003). Although visceral involvement such as hepatosplenomegaly is frequent in NPC, all patients eventually develop progressive and fatal neurological symptoms, including cerebellar ataxia, cataplexy, dystonia, dysarthria,

dysphagia, dementia and vertical supranuclear gaze palsy (Wraith et al., 2009). Patients with adult onset NPC also suffer from psychiatric disturbances (Imrie et al., 2002; Shulman et al., 1995). The average lifespan of NPC patients is between 10 to 25 years, with the adult patients often surviving until their late 30's or 40's (Vanier, 2010).

1.1.2 NPC1 and NPC2

NPC can be caused by mutations in either the *NPC1* (Carstea et al., 1997) or *NPC2* (Naureckiene et al., 2000) genes, both of which encode cholesterol-binding proteins that are essential for mobilizing LDL-derived cholesterol from LE/LYs. *NPC1* encodes a large glycoprotein that is localized to the limiting membranes of LE/LYs (Davies and Ioannou, 2000; Garver et al., 2000; Higgins et al., 1999; Neufeld et al., 1999). It contains 13 transmembrane domains, 3 large luminal domains and a cytoplasmic tail (Davies and Ioannou, 2000) **(Figure 1.1)**. The sequences of five transmembrane helices in NPC1 resemble the steroid sensing domain of several other membrane proteins (Carstea et al., 1997), including HMG-CoA reductase, the rate-limiting enzyme in cholesterol sythesis (Chin et al., 1984), SREBP cleavage-activating protein (SCAP), which transports SREBP from the ER to the Golgi under low sterol conditions (Hua et al., 1996), and Patched, a negative regulator in the Sonic Hedgehog signaling pathway (Johnson et al., 1996). The precise function of the steroid sensing domain in NPC1 remains unknown. Crystal structure of the amino-terminal domain (luminal domain 1) of NPC1 revealed the role of this domain as binding cholesterol, with the 3β-hydroxyl end buried within NPC1 and the isooctyl side chain exposed (Kwon et al., 2009).

Figure 1.1 The structure of the NPC1 protein. (Adapted from Vanier and Millat, 2003)

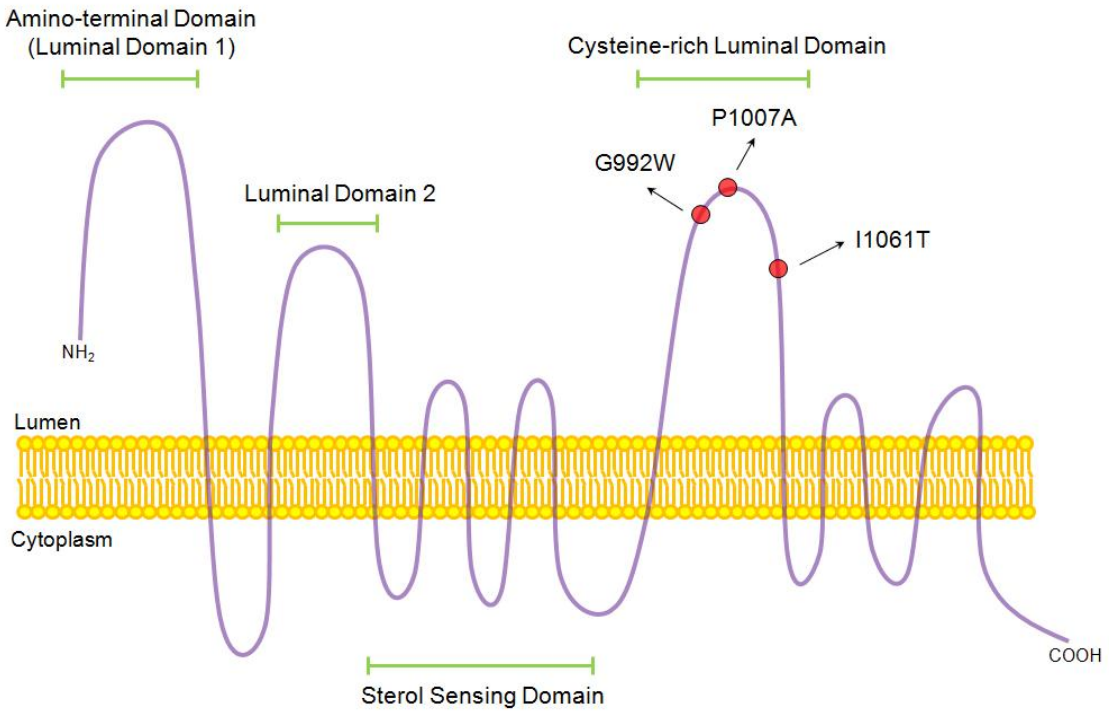

NPC2 is a small soluble glycoprotein that resides in the lumen of LE/LYs (Blom et al., 2003; Naureckiene et al., 2000; Zhang et al., 2003). It can also be secreted from the cell (Kirchhoff et al., 1996; Mutka et al., 2004). NPC2 binds cholesterol with much higher affinity than NPC1, but in an opposite orientation (Friedland et al., 2003; Infante et al., 2008a; Ko et al., 2003; Liou et al., 2006; Okamura et al., 1999; Xu et al., 2007). As such, NPC2 binds cholesterol via the isooctyl side chain, leaving the 3β-hydroxyl end exposed, thereby enabling transfer between NPC1 and NPC2 (Infante et al., 2008b; Kwon et al., 2009).

That loss-of-function mutations in either NPC1 or NPC2 yield identical cellular defects suggests that the two proteins function in a coordinated manner (Vanier et al., 1996). Consistent with this notion, deletion of both genes in mice causes a similar phenotype to the deletion of either gene alone (Sleat et al., 2004). Additionally, biochemical evidence suggests that NPC2

binds to the luminal domain 2 of NPC1 and can mediate the transfer of cholesterol both to and from NPC1. The binding of NPC2 to NPC1 is optimal at pH 5.5, and requires the presence of cholesterol on NPC2 (Deffieu and Pfeffer, 2011). This supports the idea that the transfer of cholesterol is directed from NPC2 to the amino-terminal domain of NPC1 in LE/LYs (Kwon et al., 2009).

Based on these structural and biochemical studies, a cellular model has been proposed for how NPC1 and NPC2 facilitate the egress of LDL-derived cholesterol from LE/LYs **(Figure 1.2)**. Exogenously-derived cholesterol, present mainly as the form of cholesterol esters within lipoprotein particles, enters cells through receptor-mediated endocytosis. After arriving in LE/LYs, cholesterol esters are hydrolyzed to unesterified cholesterol by lysosomal acidic lipase. Unesterified cholesterol is first transferred to NPC2, with the 3β-hydroxyl end exposed. Cholesterol-loaded NPC2 then binds to the luminal domain 2 of NPC1, and delivers cholesterol to NPC1's amino-terminal domain in a "hydrophobic handoff", with the 3β-hydroxyl end interacting with NPC1 and the isooctyl side chain inserted into the outer lysosomal membrane. From there, cholesterol is released from NPC1 and exits LE/LYs, a process that is less well characterized and may involve the participation of oxysterol-binding protein-related protein 5 (ORP5) (Du et al., 2011). After exit from LE/LYs, cholesterol is redistributed to other organelles including the ER, Golgi and plasma membrane (Maxfield and van Meer, 2010).

Figure 1.2 The "handoff" model of NPC1 and NPC2 in cholesterol efflux from LE/LYs. (Adapted from Kwon et al., 2009)

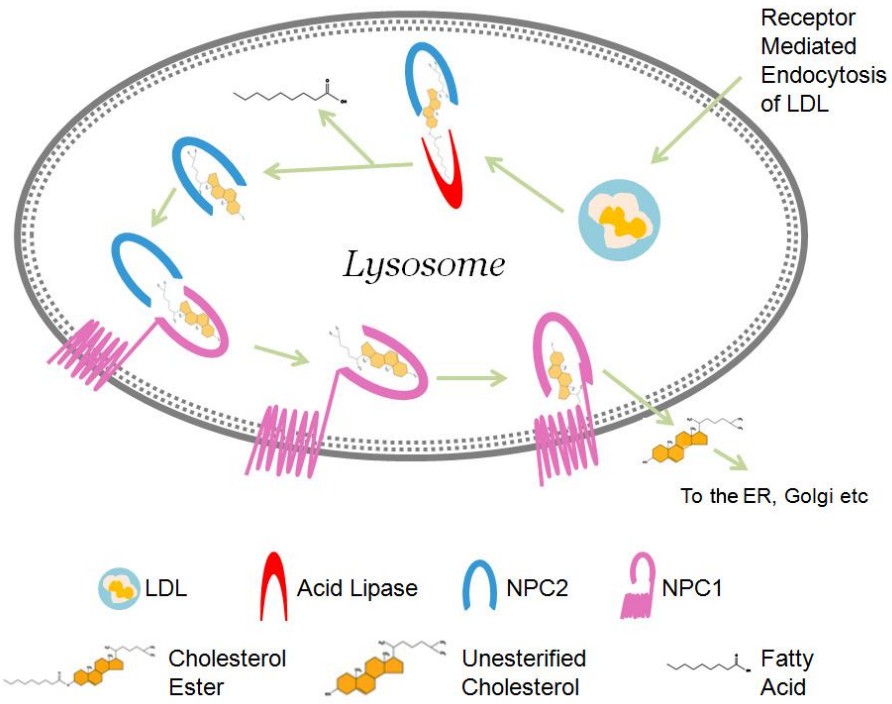

In *NPC1* or *NPC2* deficient cells, the intracellular trafficking of LDL-derived cholesterol is dramatically altered. Although the endocytosis of LDL cholesterol and subsequent lysosomal hydrolysis of cholesterol esters are normal in these mutant cells (Pentchev et al., 1985), the egress of unesterified cholesterol from LE/LYs is greatly impaired (Liscum et al., 1989; Sokol et al., 1988). In addition, glycosphingolipids, sphingosine and other lipids also accumulate in the same compartments (Rodriguez-Lafrasse et al., 1994; Vanier, 1999). The impaired egress of cholesterol and other lipids from LE/LYs causes a two-fold problem: the excessive storage of these lipids within LE/LYs interferes with the activities of lysosomal hydrolases (Elrick et al., 2012), and causes a paucity of these lipids in other organelles. It has been shown that the movement of unesterified cholesterol to the endoplasmic reticulum (ER) in NPC1 deficient cells is reduced, resulting in perturbed cholesterol homeostasis in the ER including diminished cholesterol esterification (Pentchev et al., 1985) and enhanced cholesterol synthesis (Liscum et

al., 1989; Liu et al., 2009). The cholesterol content in the plasma membrane of *NPC1* deficient cells is also reduced (Hawes et al., 2010; Liscum et al., 1989; Sokol et al., 1988; Wojtanik and Liscum, 2003), which may alter the fluidity and function of the plasma membrane.

1.1.3 Genetics

The estimated prevalence of NPC is 1 in 150,000 individuals (Vanier and Millat, 2003). Approximately 95% cases of NPC are caused by loss-of-function mutations in the *NPC1* gene and the remaining 5% are caused by mutations in the *NPC2* gene (Park et al., 2003).

There are ~250 disease-causing mutations identified in the *NPC1* gene that include missense, nonsense, deletion, insertion and frameshift mutations (Niemann-Pick type C disease gene variation database, http://npc.fzk.de/). They are scattered throughout most of the NPC1 functional domains, with more than 1/3 concentrated in luminal domain 3 (Greer et al., 1999; Millat et al., 2001). The disease is most commonly caused by missense mutations, with several frequent ones identified **(Figure 1.1)**. The most prevalent mutation, I1061T, is found in ~20% of patients of Western European ancestry, and in 15% of patients from the US (Millat et al., 1999). Other frequent mutations include P1007A, the second most prevalent one in Europe (Greer et al., 1999; Millat et al., 2005; Millat et al., 2001), and G992W, typical of patients from Nova Scotia (Greer et al., 1998).

How missense mutations in *NPC1* lead to a loss of functional protein has been studied in detail for the I1061T mutation (Gelsthorpe et al., 2008). Metabolic labeling and biochemical experiments suggested that NPC1 I1061T is synthesized but fails to advance in the secretory pathway. Instead of being targeted to LE/LYs, it gets quickly degraded by proteasomes, probably due to misfolding and subsequent recognition by ER protein quality control machinery. If NPC1

I1061T is overexpressed, a fraction of the mutant protein is able to escape ER protein quality control and traffic to LE/LYs. Once localized to LE/LYs, NPC1 1061T functions normally and the cholesterol storage phenotype is suppressed. These data suggest that NPC1 I1061T, although misfolded, is functional if gets to LE/LYs, and a small amount of functional NPC1 protein is sufficient to overcome the cholesterol storage defect. This raises the possibility that strategies to promote protein folding and trafficking might enable functional recovery of NPC1 I1061T. In Chapter 4, I will explore this possibility by modulating the ER proteostasis network in patient fibroblasts with the I1061T mutation.

1.1.4 Models for NPC

Several cellular models have been used to understand the pathogenesis of NPC, including skin fibroblasts derived from NPC patients with various mutations in *NPC1* or *NPC2*, and Chinese hamster ovary (CHO) cells harboring deletion mutations in *NPC1* (Cruz et al., 2000; Pentchev et al., 1985). Mutant cells in both models display cholesterol storage in LE/LYs that can be detected by filipin, a fluorescent dye that specifically recognizes unesterified cholesterol (Bornig and Geyer, 1974). In addition, U18666A, a cell-permeable, amphiphilic amino-steroid, has also been widely used to quickly induce a cholesterol storage phenotype that mimics *NPC1/NPC2* deficiency (Liscum and Faust, 1989), although the exact mechanism underlying this effect is not clear.

In addition to the above cellular models, animal models are another valuable source for probing NPC neurodegeneration. Since NPC1 is a highly conserved protein in eukaryotes (Higaki et al., 2004), a wide range of model organisms have been developed to study its function, including yeast (Malathi et al., 2004), nematode (Li et al., 2004; Sym et al., 2000), drosophila

(Fluegel et al., 2006; Huang et al., 2005; Phillips et al., 2008), zebrafish (Louwette et al., 2012; Schwend et al., 2011), feline (Lowenthal et al., 1990), canine (Kuwamura et al., 1993) and murine models. Due to the faithful recapitulation of the human disease, mouse models of NPC are the most commonly used in animal studies.

Five mouse models of NPC have been reported to date. Three of these carry spontaneous mutations in the mouse *Npc1* gene, including C57BLKS/J-*Npc1*^{spm}/J (Miyawaki et al., 1982; Yamamoto et al., 1994), BALB/c-*Npc1*^{nih} (Morris et al., 1982), and C57BL/6J-*Npc1*^{nmf164}/J (Maue et al., 2012). Both *Npc1*^{spm} and *Npc1*^{nih} mice have null mutations in *Npc1* with very similar phenotypes. *Npc1*^{nih} mice, the better characterized line, have an insertional mutation in exon 9 of *Npc1*, resulting in premature truncation of the protein (Loftus et al., 1997). They develop progressive degenerative symptoms starting around 4-5 weeks, including weight loss and motor dysfunction, followed by early death around 10-12 weeks (Morris et al., 1982). In the liver and spleen, foamy macrophages are abundant in these mutant mice, reminiscent of the histopathological changes seen in human patients (Morris et al., 1982). In the CNS, aberrant accumulation of cholesterol (Xie et al., 2000) and other lipids (Zervas et al., 2001a) leads to swollen axons (Zervas et al., 2001a), neuron loss (German et al., 2001; Yamada et al., 2001), gliosis (Baudry et al., 2003; German et al., 2002; Pressey et al., 2012) and myelin defects (Takikita et al., 2004; Weintraub et al., 1987; Weintraub et al., 1985), with selective Purkinje neuron loss as a prominent feature of the cerebellar pathology(Sarna et al., 2003). *Npc1*^{nmf164} mice carry a missense mutation (D1005G) in *Npc1* and develop a milder, yet progressive phenotype that may resemble the late-onset form of the human disease (Maue et al., 2012).

In addition to spontaneous-occurring mutants, two genetically engineered mouse models have been developed. This includes one in which the cholesterol binding function of NPC1 is

abolished by substitutions of 2 amino acids to alanine in the amino-terminal domain of NPC1 (Xie et al., 2011). This mouse model reproduced the phenotype of *Npc1*^{nih} mice, confirming *in vivo* that the cholesterol binding site in NPC1 is crucial for cholesterol export from LE/LYs.

Mice with a conditional null allele of *Npc1* have been recently developed in our laboratory to accommodate the need for studying the effects of gene deletion in a temporal and spatial specific manner (Elrick et al., 2010). In this mouse model, exon 9 of *Npc1* is flanked by loxP sites (*Npc1*^{flox}), and Cre recombinase-mediated deletion of exon 9 generates a frameshit mutation, resulting in premature truncation of the protein. It has been shown that deletion of *Npc1*^{flox} in the germline recapitulates all the features of *Npc1*^{nih} mice. In Chapters 2 and 3, I will use this mouse model to establish the timing and cell type that underlie neurodegeneration due to *Npc1* deficiency.

1.1.5 Therapeutic efforts

Since the discovery of the genes underlying NPC, much effort has been devoted to develop therapeutic approaches for treatment of this disease. Due to limited blood brain barrier permeability, strategies used to treat other lysosomal storage diseases with only visceral involvement, such as enzyme replacement therapy (Beck, 2007), are not suitable for NPC, in which the primary defect occurs in the CNS. Similarly, bone marrow transplantation (Hsu et al., 1999) does not improve the neurological manifestations of NPC, although visceral symptoms regress.

Other strategies for treating lysosomal storage diseases include substrate reduction therapy. Initial attempts at applying this strategy to NPC focused on correcting the cholesterol accumulation defect. This includes the application of cholesterol lowering agents such as

lovastatin, nicotinic acid and pravastatin in both NPC patients (Patterson et al., 1993) and an NPC mouse model (Erickson et al., 2000). Although these studies showed reduced cholesterol levels in the liver and other peripheral organs, neurological symptoms were not significantly affected. These disappointing results are likely attributable to several causes:1) all the compounds inhibit the synthesis of cholesterol, while the defect in NPC lies in the uptake of exogenous cholesterol through the endocytic pathway; and 2) some of the cholesterol lowering agents have very limited blood brain barrier permeability and therefore do not gain access to directly target the primary defect in the CNS. Similarly, dietary cholesterol restriction in a feline model of NPC yielded no beneficial outcome (Somers et al., 2001), due to the fact that cholesterol in the CNS is solely made *in situ* (discussed in Chapter 1.2).

Following the observation that glycosphingolipids also accumulate in NPC cells, sphingolipid lowering agents were tested as a substrate reduction therapy strategy. This led to the identification of miglustat (Zavesca) as the first specific drug approved for treating NPC. Miglustat, originally used to treat type I Gaucher's disease (Cox, 2005; Lachmann, 2003), reportedly acts as both an inhibitor of glucosylceramide synthase, the enzyme catalyzing the first step of glycosphingolipid synthesis (Platt et al., 1994), and a chemical chaperone (Abian et al., 2011). Miglustat treatment of NPC mice and cats led to decreased glycosphingolipid accumulation, delayed neurological symptoms and mild lifespan extension (Zervas et al., 2001b). Several clinical trials have suggested that miglustat stabilizes the disease course in NPC patients, with the late onset patients showing greater benefits (Chien et al., 2007; Di Rocco et al., 2012; Galanaud et al., 2009; Lachmann et al., 2004; Paciorkowski et al., 2008; Patterson et al., 2010; Patterson et al., 2007; Pineda et al., 2010; Pineda et al., 2009; Santos et al., 2008).

Additional efforts to develop drug therapy include the identification of hydroxypropyl-β-cyclodextrin, a sugar compound able to rescue the cholesterol storage defect in both cellular and animal models (Abi-Mosleh et al., 2009; Davidson et al., 2009; Griffin et al., 2004; Liu et al., 2008; Liu et al., 2009; Ramirez et al., 2010). While the precise mechanism underlying this effect is still under investigation, it is proposed that cyclodextrin enters LE/LYs through endocytosis and facilitates the efflux of cholesterol without the need of NPC1 or NPC2 (Abi-Mosleh et al., 2009; Rosenbaum et al., 2010). However, relative inability of cyclodextrin to cross the blood brain barrier limits its broad clinical application (Aqul et al., 2011; Camargo et al., 2001). Other compounds identified include HDAC inhibitors (Kim et al., 2007; Munkacsi et al., 2011; Pipalia et al., 2011) and δ-tocopherol (Xu et al., 2012), both of which are able to rescue the cholesterol storage defect in NPC patient fibroblasts though mechanisms that are not well understood. Testing of these small molecules in a disease-relevant cell type or an animal model is needed to further assess their beneficial effects. At the current time, no effect disease-modifying treatment has been developed for NPC patients. In Chapter 4, I will explore the possibility of using proteostasis regulators to modulate the disease phenotype in NPC patient fibroblasts.

1.2 Cholesterol metabolism in the brain

A comprehensive knowledge of cholesterol metabolism in the brain is important for understanding NPC pathogenesis. Cholesterol is highly enriched in the brain, with an average concentration of 15-20 mg/g fresh tissue, compared to that of the whole animal body in which the concentration equals ~2.2 mg/g (Dietschy and Wilson, 1968). Within the cholesterol pool in the adult brain, 70%-80% of the sterol is present as the form of unesterified cholesterol in

compact myelin, with the remaining in the membranes of various cellular organelles (Dietschy, 2009).

Since no evidence so far supports the uptake of plasma lipoprotein cholesterol across the blood brain barrier into the CNS, it is generally accepted that the cholesterol required for brain development and function comes entirely from *de novo* synthesis within the CNS (Dietschy and Turley, 2004). Similarly, excess cholesterol in the brain has to be first converted to 24-hydroxycholesterol before it crosses blood brain barrier and gets delivered to the liver for bile excretion. This conversion only takes place in some types of neurons, including pyramidal neurons and Purkinje neurons, with little in glia (Lund et al., 1999; Lund et al., 2003).

Neurons and glia are both able to synthesize cholesterol by themselves. In the mouse brain, the highest rate of cholesterol synthesis is found during the first 4 weeks after birth, and is occurring mostly in oligodendrocytes during myelin production. The rate of cholesterol synthesis decreases significantly in mature animals, after myelination has completed, and primarily reflects the synthesis of cholesterol in astrocytes and neurons (Dietschy and Turley, 2004).

In addition to synthesizing their own cholesterol, neurons and glia are able to take up extracellular lipoprotein cholesterol produced and released by neighboring CNS cells. Astrocytes are thought to be the major cell type responsible for ApoE-associated cholesterol secretion (Gong et al., 2002). They supply neurons, especially the distal part of axons, with a source of cholesterol for the formation and maintenance of synapse (Vance et al., 2005). In addition to neurons, oligodendrocytes have also been suggested to utilize exogenous cholesterol during the peak of myelin formation (Saher et al., 2005). Since NPC1 is an essential for the endocytosis of lipoprotein cholesterol, it would be of great interest to see how *Npc1* deficiency in individual

CNS cell types affects brain function. In chapters 2 and 3, I will investigate the contributions of neurons, astrocytes and oligodendrocytes to the pathogenesis of NPC.

1.3 Cell autonomous and non-cell autonomous neurodegeneration

It has been of widespread interest to define what cell type is responsible for neurodegeneration in diseases where the mutated gene is ubiquitously expressed. The most detailed studies come from models of amyotrophic lateral sclerosis (ALS), a neurodegenerative disorder with premature death of brain and spinal cord motor neurons. Approximately 2% of familial ALS cases are caused by gain-of-functions mutations in the ubiquitous *SOD1* gene (Rosen et al., 1993). Attempts to reproduce the neuropathology by over-expression of mutant *SOD1* in only motor neurons or astrocytes failed, suggesting that the disease cannot be explained solely by defects within a single cell type; rather, these results suggested the possibility that neuron death is a result of an interplay between multiple cell types. Indeed, studies of a transgenic mouse model with a floxed allele of mutant *SOD1* gene showed that deletion of mutant *SOD1* in motoneurons delayed the disease onset, while the same action in astrocytes or microglia slowed disease progression, revealing a complex pathogenic process with contributions from both neurons and glia.

Another example comes from studies of synucleinopathies, a group of neurodegenerative diseases characterized by aberrant accumulation of fibrillary α-synuclein inclusions in the CNS, including Parkinson's disease (PD) and multiple system atrophy. In a PD transgenic mouse model, over-expression of human wild type α-synuclein in neurons under the promoter for platelet-derived growth factor β (PDGF-β) resulted in inclusion body formation within neurons, selective loss of dopaminergic terminals and motor impairment, demonstrating the leading role

of neurons in the pathogenesis of PD (Masliah et al., 2000). On the other hand, in a transgenic mouse model mimicking multiple system atrophy, over-expression of the same human wild type α-synuclein specifically in oligodendrocytes under the promoter of 2', 3' -cyclic nucleotide 3' -phosphodiesterase (CNP) leaded to accumulation of α-synuclein inclusions in oligodendrocytes, degeneration of both glia and neurons, and progressive motor deficits (Yazawa et al., 2005). This suggests that defects solely arising from glia are sufficient to cause neurodegeneration, at least in synucleinopathy.

Prior efforts to establish the extent of neuronal cell autonomous degeneration in NPC have yielded contradictory findings. Two studies demonstrated cell autonomous death of Purkinje cells in NPC mice. This includes the analysis of a chimeric mouse model in which mutant Purkinje cells were surrounded by wild-type neurons and glia (Ko et al., 2005), and studies in a conditional mouse model with *Npc1* deletion specifically in Purkinje cells (Elrick et al., 2010). In contrast, attempts to address the role of glia in disease pathogenesis yielded contradictory findings. Two studies reintroduced *Npc1* back into *Npc1*$^{-/-}$ mice using various promoters. In one study, presumed neuronal or astrocytic-specific expression of *Npc1* in *Npc1*$^{-/-}$ mice delayed disease onset and extended lifespan, with expression in both cell types nearly completely correcting the phenotype (Borbon et al., 2012; Zhang et al., 2008). However, the specificity of transgene expression in this study was not well controlled, and work from another laboratory showed that mutant mice could only be rescued by expression of *Npc1* in neurons (Lopez et al., 2011). Other studies favoring a role of astrocytes in NPC pathology came from a *Drosophila* model of NPC where expression of *dnpc1a* in glia provided limited rescue of lethality (Phillips et al., 2008), and a neuron-glia co-culture experiment in which neurons showed decreased growth of neurites when cultured with *Npc1* deficient astrocytes (Chen et al., 2007).

Apparently, new approaches are needed to solve the discrepancy regarding the roles of glia in NPC pathogenesis. This will be the aim of Chapters 2 and 3 of this dissertation.

1.4 Myelin and oligodendrocyte development

1.4.1 Myelin composition

Myelin is a specialized structure generated by the spiral extension of the plasma membranes of oligodendrocytes in the CNS and of Schwann cells in the PNS. The ensheathment of axons by myelin is a unique feature of the vertebrate nervous system to ensure high-speed nerve conduction with fidelity of signaling along long distances. As an electrical insulator of axons, myelin is a poorly hydrated structure with high lipid content. Compared to other tissues with 70% water by weight, myelin contains only 40% water. Myelin has also a high lipid-to-protein ratio, with 70% lipids and 30% proteins by dry weight; these numbers are generally reversed in other cellular membranes (Baumann and Pham-Dinh, 2001). A recent study suggests the lipid-rich property of the myelin sheath is possibly achieved by employing myelin basic protein (MBP), one of the most abundant myelin proteins, as a physical barrier to prevent the diffusion of membrane proteins with large cytosolic domains into compact myelin (Aggarwal et al., 2011).

Of all the lipids found in myelin sheath, unesterified cholesterol is a major component. The molar ratio of cholesterol:phospholipids:glycolipids ranges from 4:4:2 to 4:3:2. Cholesterol esters are not present in myelin. Because of the lipid-rich property of myelin, cholesterol in myelin accounts for ~70% of the total cholesterol pool in the brain (Baumann and Pham-Dinh, 2001).

Cholesterol for myelin synthesis was originally thought to be entirely supplied by endogenous synthesis within oligodendrocytes. Consistent with this idea, the highest rate of cholesterol synthesis in the mouse brain occurs during the first 4 weeks after birth, a period when myelination is taking place within the CNS (Dietschy and Turley, 2004). The role of endogenous cholesterol in myelination has been studied in two mouse models. In one, deletion of the squalene sythase, the first enzyme dedicated to sterol biosyntheis, in oligodendrocytes led to perturbed myelination in early postnatal days, demonstrating that cholesterol availability is a rate limiting step in myelination (Saher et al., 2005). However, these mice lacking cholesterol synthesis in oligodendrocytes were able to partially recover as adults, assembling myelin with only slightly reduced cholesterol content. This raised the possibility that oligodendrocytes are also able to use exogenous cholesterol for myelin production. In another mouse model, the gene encoding sterol regulatory element-binding protein cleavage activation protein was mutated in Schwann cells, leading to a disruption of cholesterol and fatty acid synthesis (Verheijen et al., 2009). Delayed but not complete absence of myelination in the PNS was observed. Similarly, this suggests that an alternative source of cholesterol exists in the PNS for myelin synthesis. However, whether exogenous uptake of cholesterol by myelinating glia is a physiological process under normal conditions or just a compensatory strategy when the endogenous source of cholesterol is lacking, is not clear.

1.4.2 Regulation of oligodendrocyte development and myelination

Much effort has also been devoted to study myelination, a process involving oligodendrocyte proliferation, differentiation and maturation in the CNS, with the hope that this would inform our knowledge of dysmyelinating/demyelinating disorders. Myelination starts with oligodendrocyte precursor cells (OPCs) generated from the subventricular zone. OPCs, which

express lineage specific markers PDGFR-α and NG2 proteoglycan, migrate extensively throughout the CNS before settling along the fiber tracts of future white matter. During the differentiation stage, OPCs stop proliferating and transform into postmitotic oligodendrocytes. Oligodendrocytes no longer express OPC markers; instead, they upregulate myelin related genes, among which 2', 3' -cyclic nucleotide 3' -phosphodiesterase (CNP) is the earliest myelin specific protein to be synthesized by oligodendrocytes. During the maturation period, oligodendrocytes compete for axons. They either win by ensheathing axons with myelin, or lose and go into apoptosis (Barres and Raff, 1999).

It is now known that myelination is a highly dynamic process requiring a tight coordination between axons and oligodendrocytes. Within oligodendrocytes, myelination is controlled by both transcriptional and posttranscriptional mechanisms. A number of transcription factors have been identified for their importance in oligodendrocyte development, including Olig2 which is required for OPC specification (Ligon et al., 2006), Olig1 for oligodendrocyte differentiation (Lu et al., 2002), MRF (Myelin gene Regulatory Factor) for oligodendrocyte maturation and myelin maintenance (Emery et al., 2009; Koenning et al., 2012) and ZFP191 for final stages of oligodendrocyte development (Howng et al., 2010). Oligodendrocytes also employ miRNAs as a posttranscriptional mechanism to repress expression of genes that maintain OPCs at the undifferentiated stage, thereby promoting oligodendrocyte differentiation. Several miRNAs in this category have been identified using a conditional *Dicer* knockout mouse model (Dugas et al., 2010; Shin et al., 2009; Zhao et al., 2010). Epigenetic remodeling of chromatins through histone deacetylases (HDACs) is another way oligodendrocytes inhibit the expression of differentiation blockers (Shen et al., 2005; Ye et al., 2009).

Given the importance of myelination for proper functioning of axons, it is not surprising to see that axons also participate in the regulation of this process. A number of inhibitory cues expressed by axons have been identified that inhibit oligodendrocyte differentiation, probably to ensure the proper temporal and spatial arrangement of oligodendrocytes. This includes extracellular ligands PSA-NCAM (Charles et al., 2000), Jagged1 (Wang et al., 1998) and Lingo1 (Lee et al., 2007), as well as the secreted molecule Wnt (Fancy et al., 2009; Tawk et al., 2011). Myelination is also regulated by neuronal activity (Barres and Raff, 1993; Demerens et al., 1996). In a recent neuron-glia co-culture study, action potentials were shown to stimulate myelination through increased formation of cholesterol-rich membrane domains between axons and oligodendrocytes and subsequent up-regulation of MBP synthesis (Wake et al., 2011). This effect of axonal electrical activity was further shown to be mediated by oligodendroglial Fyn kinase, one of the Src family members that is thought to integrate signals from axons for myelination (Kramer-Albers and White, 2011) **(Figure 1.3)** (also see discussions in Chapter 5.2) .

Figure 1.3 Axon-glial signalings in regulating myelination. (Adapted from Kramer-Albers and White, 2011)

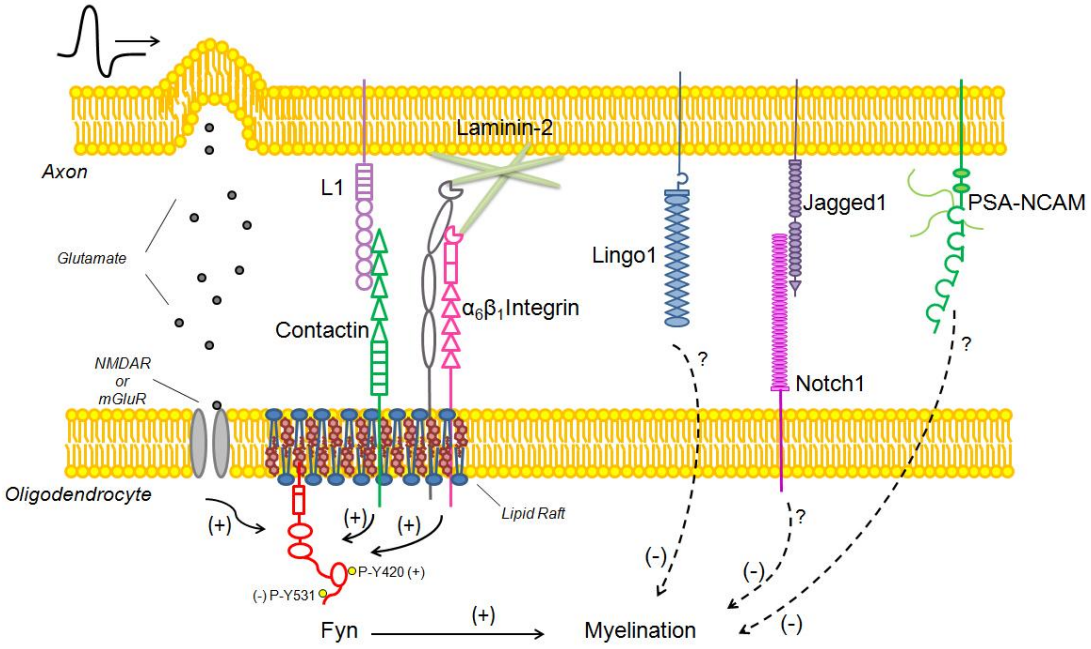

1.4.3 NPC mice as a model to study myelination

Since NPC1 is an essential protein for lipoprotein cholesterol uptake through endocytosis, mice with mutations in *Npc1* are a powerful tool to dissect the role of exogenous cholesterol for myelination. Several studies have suggested $Npc1^{nih}$ mice exhibit a dysmyelination phenotype (Takikita et al., 2004; Weintraub et al., 1987; Weintraub et al., 1985). Along with this line, MRI studies also suggested a defect in the white matter of NPC patients (Trouard et al., 2005; Walterfang et al., 2010). However, the fact that *Npc1* is absent in both neurons and oligodendrocytes in $Npc1^{nih}$ mice makes it difficult to interpret these results, as it is unclear whether dysmyelination in NPC mice is attributable to its axonal pathology or a primary defect in oligodendrocytes. To address this question, in chapter 3 I will use the conditional knockout mouse model of *Npc1* to dissect the contribution of individual cell types in NPC dysmyelination.

1.5 Proteostasis

Protein homeostasis, or proteostasis, is the process that cells use to regulate the physiological functions of proteins in order to adapt to intrinsic and environmental challenges. Proteostasis is maintained by a complex network involving multiple signaling pathways that control protein synthesis, folding, trafficking, aggregation/disaggregation and degradation. Some of the regulatory pathways participating in the proteostasis network include the heat shock response, the unfolded protein response and the ubiquitin-proteasome system. Loss of function diseases are often a result of perturbed proteostasis, in which missense mutations lead to protein instability, mistrafficking and degradation. Therefore, strategies to restore the proteostasis network have been a focus for many conformational diseases, including several lysosomal storage diseases with mutated enzymes (Powers et al., 2009).

The best example of work adapting proteostasis in lysosomal storage diseases is in Gaucher's disease, which is most often caused by loss-of-function mutations in the lysosomal hydrolase glucocerebrosidase. As a result, glucosylceramide, the enzyme's substrate, accumulates in the lysosomes and leads to visceral pathology including hepatosplenomegaly. In Type II and III Gaucher's Disease, the central nervous system is also severely affected. Enzyme replacement therapy is being used to treat Type I Gaucher's Disease; however, due to the inability of the recombinant enzyme to cross the blood brain barrier, other therapeutic approaches are needed for Type II and III Gaucher's Disease patients with neurological symptoms (Sawkar et al., 2006a).

Several clinically important mutations, including N370S, the most prevalent mutation for Type I Gaucher's Disease, and L444P, the most common one causing CNS involvement, impede proper folding of glucocerebrosidase in the ER and target the enzyme for ER associated degradation (ERAD) (Grabowski and Horowitz, 1997). Both mutations, however, do not affect the enzymatic activity of glucocerebrosidase in lysosomes (Sawkar et al., 2006b). Based on these observations, several strategies have been developed to enhance ER proteostasis in Gaucher's Disease. In one study, proteostasis was targeted by increasing Ca^{2+} store in the ER lumen to enhance the folding capacity of ER chaperones whose activities are Ca^{2+} dependent (Mu et al., 2008a; Ong et al., 2010; Wang et al., 2011). This was achieved by application of several L-type calcium channel blockers and ryanodine receptor antagonists. In another study, the unfolded protein response was activated to enhance the ER folding capacity for glucocerebrosidase by application of celastrol or MG-132 (Mu et al., 2008b). In both studies, proteostasis regulators promoted the folding and trafficking of mutant glucocerebrosidase to enable its functional recovery in patient fibroblasts. In addition, a synergistic effect was achieved by co-application

of a proteostasis regulator (celastrol or MG-132), which increases the ER concentration of correctly folded glucocerebrosidase , and a chemical chaperone (NN-DNJ), which binds to and stabilizes the correctly folded glucocerebrosidase in the ER (Mu et al., 2008b). The compounds used to restore glucocerebrosidase proteostasis have also been successfully applied to patient fibroblasts derived from other lysosomal storage diseases, including α-mannosidosis, mucopolysaccharidosis type IIIA and Tay-Sachs disease, all of which involve misfolding of a lysosomal hydrolase (Mu et al., 2008a; Mu et al., 2008b).

While the strategies described above have been successfully applied to lysosomal storage diseases with enzyme deficiencies, they have not been tested in those with mutations in integral lysosomal membrane proteins, whose folding and stability are generally more difficult to achieve. In Chapter 4, I will test this idea using NPC patient fibroblasts harboring the NPC1 I1061T mutation.

1.6 Research objectives

Despite the growing understanding of NPC pathology and efforts to develop therapeutic interventions, the link between NPC1/NPC2 deficiencies and neurodegeneration remains elusive and effective, disease modifying therapies are not yet available. The work presented in this dissertation takes two approaches to address these challenges. The first objective is to define the timing and cell type critical for NPC neuropathology. In Chapter 2, I show that mice with global *Npc1* deletion in adults recapitulates the pathology of those with germline deletion. The disease can also be reproduced when *Npc1* is deleted in only neurons, while deletion in astrocytes does not lead to any CNS pathology. This work demonstrates that neurons, but not astrocytes, are the critical cell type for NPC neurodegeneration. As an extension of these data, Chapter 3 explores

the contribution of different CNS cell types to dysmyelination, a specific aspect of NPC neuropathology. I show that *Npc1* deficiency in oligodendrocytes leads to forebrain dysmyelination in early postnatal days, followed by global demyelination and secondary Purkinje neuron loss in adult stages, demonstrating the critical role of exogenous cholesterol uptake in both myelin formation and maintenance. Unexpectedly, *Npc1* deficiency in only neurons also disrupts myelination. This effect is mediated by Fyn kinase-dependent mechanisms. Taken together, these data establish that Npc1 is required by both neurons and oligodendrocytes for CNS myelin formation and maintenance. The second objective of my thesis is to identify therapeutic strategies that might benefit NPC patients. In Chapter 4, I seek to modulate the cellular proteostasis machinery to achieve functional recovery in patient fibroblasts harboring an NPC1 I1061T mutation. This work shows that targeting ER proteostasis network using ryanodine receptor antagonists promotes the folding and trafficking of NPC1 I1061T protein, and rescues the cholesterol storage and sphingolipid mistrafficking defects in patient fibroblasts. In conclusion, adapting NPC1 proteostasis might be a successful strategy in NPC disease.

Chapter 2

Temporal and cell-specific deletion establishes that neuronal Npc1 deficiency is sufficient to mediate neurodegeneration[1]

2.1 Abstract

Niemann-Pick type C disease (NPC) is an autosomal recessive lysosomal storage disorder caused by mutations in the *NPC1* or *NPC2* genes. Loss of function mutations in either gene disrupt intracellular lipid trafficking and lead to a clinically heterogeneous phenotype that invariably includes neurological dysfunction and early death. The mechanism by which impaired lipid transport leads to neurodegeneration is poorly understood. Here we used mice with a conditional null allele to establish the timing and cell type that underlie neurodegeneration due to *Npc1* deficiency. We show that global deletion of *Npc1* in adult mice leads to progressive weight loss, impaired motor function, and early death in a time course similar to that resulting from germline deletion. These phenotypes are associated with the occurrence of characteristic neuropathology including patterned Purkinje cell loss, axonal spheroids and reactive gliosis, demonstrating that there is not a significant developmental component to NPC

[1] This chapter was published as:
Yu T, Shakkottai VG, Chung C, Lieberman AP. Temporal and cell-specific deletion establishes that neuronal Npc1 deficiency is sufficient to mediate neurodegeneration. *Hum Mol Genet.* 2011 Nov 15;20(22):4440-51.

neurodegeneration. Furthermore, we show that these same changes occur when *Npc1* is specifically deleted only in neurons, establishing that neuronal deficiency is sufficient to mediate CNS disease. In contrast, astrocyte-specific deletion does not impact behavioral phenotypes, CNS histopathology or synaptic function. We conclude that defects arising in neurons, but not in astrocytes, are the determining factor in the development of NPC neuropathology.

2.2 Introduction

Niemann-Pick type C disease (NPC) is a childhood-onset neurodegenerative disorder characterized biochemically by the accumulation of unesterified cholesterol and glycosphingolipids in late endosomes and lysosomes (Vanier, 2010). Loss of function mutations in the *NPC1* gene, which encodes a multipass transmembrane protein that is essential for mobilizing cholesterol from the endolysosomal system, disrupt intracellular lipid trafficking in ~95% of NPC patients (Carstea et al., 1997; Kwon et al., 2009; Park et al., 2003). The resulting disease exhibits progressive neuropathology in which intracellular lipid accumulation, abnormally swollen axons, neuron loss and demyelination underlie the occurrence of cognitive impairment, ataxia, seizures and early death (Higgins et al., 1992). Although disease-causing mutations were identified over a decade ago, it remains unknown how disruption of intracellular lipid transport leads to the severe, progressive neurological impairment characteristic of NPC.

Insights into the pathogenesis of central nervous system (CNS) disease have been gleaned from studies of NPC mouse models. Recent pre-clinical therapeutic trials in mice with an insertional mutation that abolishes *Npc1* gene function highlight cyclodextrin as a promising therapeutic candidate. Cyclodextrin circumvents the requirement for Npc1 to clear stored lipids from diseased cells (Abi-Mosleh et al., 2009), and several studies have shown that a single

injection at postnatal day 7 markedly prolongs the lifespan of mutant mice (Davidson et al., 2009; Griffin et al., 2004; Liu et al., 2009). In contrast, injections at later ages are less effective (Davidson et al., 2009; Griffin et al., 2004; Liu et al., 2009). Although cyclodextrin's therapeutic mechanism remains incompletely understood, this time-sensitive beneficial effect raised the possibility of a critical developmental window for disease.

Much effort has also focused on defining the cell types responsible for CNS degeneration, with the expectation that this is an important first step toward identifying pathogenic mechanisms. Following the demonstration that transgenic expression of Npc1 predominantly in the CNS diminishes disease severity in *Npc1* null mice (Loftus et al., 2002), several models systems were used to explore the contributions of neurons and glia. Transgenic rescue experiments in NPC mouse and *Drosophila* models (Phillips et al., 2008; Zhang et al., 2008), and co-culture experiments with neurons and glia (Chen et al., 2007), raised the possibility that astrocytes contribute to neurodegeneration. However, conditional deletion of *Npc1* only in cerebellar Purkinje cells and an analysis of chimeric mice demonstrate that *Npc1* deficiency triggers cell autonomous Purkinje cell loss (Elrick et al., 2010; Ko et al., 2005). Furthermore, recent studies show that transgenic expression of Npc1 in neurons, but not astrocytes, delays CNS disease, indicating that Npc1 expression by neurons is necessary for nervous system function (Lopez et al., 2011). Whether neuronal or glial deficiency of Npc1 is sufficient to cause NPC neuropathology has not been addressed previously.

To determine the extent to which *Npc1* deficiency during CNS development is necessary for NPC neuropathology, and to help define the cell type critical for disease pathogenesis, we used mice containing a conditional null allele of the *Npc1* gene. By employing various Cre lines, we achieved deletion of the *Npc1* gene in a spatial and temporal specific manner. Our findings

demonstrate that deletion of *Npc1* in the adult is sufficient to cause disease, and show that neurons, but not astrocytes, are the critical cell type for NPC neurodegeneration.

2.3 Results

2.3.1 Adult deletion of *Npc1* recapitulates NPC neuropathology

We first sought to determine the extent to which Npc1 deficiency during CNS development is necessary for NPC neuropathology. To answer this question, we utilized mice with a floxed allele of the *Npc1* gene ($Npc1^{flox}$), in which exon 9 is flanked by *loxP* sites. We have shown previously that Cre-mediated deletion of exon 9 yields a null allele that is functionally indistinguishable from the spontaneous null mutant found in the widely used npc^{nih} $(Npc1^{-/-})$ model (Elrick et al., 2010). These mice were bred with transgenic animals expressing a tamoxifen regulated Cre recombinase under the control of the CMV promoter ($Cre\text{-}ER^{TM}$) (Hayashi and McMahon, 2002). Our breeding strategy generated littermates expressing Cre recombinase that were compound heterozygotes of the conditional *Npc1* allele. To induce Cre-mediated deletion of experimental ($Npc1^{flox/-}$, $Cre\text{-}ER^{TM+}$) and control ($Npc1^{flox/+}$, $Cre\text{-}ER^{TM+}$) mice, both groups were injected with tamoxifen at 6 weeks, an age at which mice are sexually mature and have a fully developed CNS. Following injections, we verified diminished Npc1 expression in the brain by western blot **(Figure 2.1A)**. Similar to mice with germline deletion ($Npc1^{\Delta/-}$), mice with adult deletion ($Npc1^{flox/-}$, $Cre\text{-}ER^{TM+}$) expressed no detectable Npc1 protein in all brain regions examined. Additionally, control mice ($Npc1^{flox/+}$, $Cre\text{-}ER^{TM+}$) expressed reduced protein levels after tamoxifen treatment. Our data indicate that this strategy successfully triggered widespread recombination throughout the brain.

The phenotypic consequences of *Npc1* deletion in adults were weight loss, impaired motor function and early death. Following tamoxifen injections at 6 weeks, $Npc1^{flox/-}$, $Cre\text{-}ER^{TM+}$ males and females, but not $Npc1^{flox/+}$, $Cre\text{-}ER^{TM+}$ controls, started to lose weight around 16 weeks **(Figure 2.1B, C)**. By 12 weeks, $Npc1^{flox/-}$, $Cre\text{-}ER^{TM+}$ mice exhibited impaired balance beam performance, indicating a motor deficit, which progressed with age **(Figure 2.1D)**. The average lifespan of $Npc1^{flox/-}$, $Cre\text{-}ER^{TM+}$ mice was 109 days post-tamoxifen injections, and comparison of the survival curves of $Npc1^{flox/-}$, $Cre\text{-}ER^{TM+}$ mice (adult deletion) with that of $Npc1^{\Delta/-}$ mice (germline deletion) revealed slightly longer survival **(Figure 2.1E)**, a finding that may reflect differences in the extent of gene deletion between these groups.

Figure 2.1 Phenotype of mice following *Npc1* deletion at 6 weeks.
(A) Western blots of Npc1 protein in mouse brain lysates from three different regions. **(B, C, D)** Weight curves for male (B) and female (C) mice, and age-dependent performance on balance beam (D). Data are mean +/- SD. * $p<0.05$, ** $p<0.01$. **(E)** Kaplan-Meyer survival curves for mice following *Npc1* deletion at 6 weeks ($Npc1^{flox/-}$, $Cre\text{-}ER^{TM+}$) and for littermate controls ($Npc^{flox/+}$, $Cre\text{-}ER^{TM+}$). For reference, the previously reported survival of mice with germline deletion ($Npc1^{\Delta/-}$) is shown (Elrick et al., 2010).

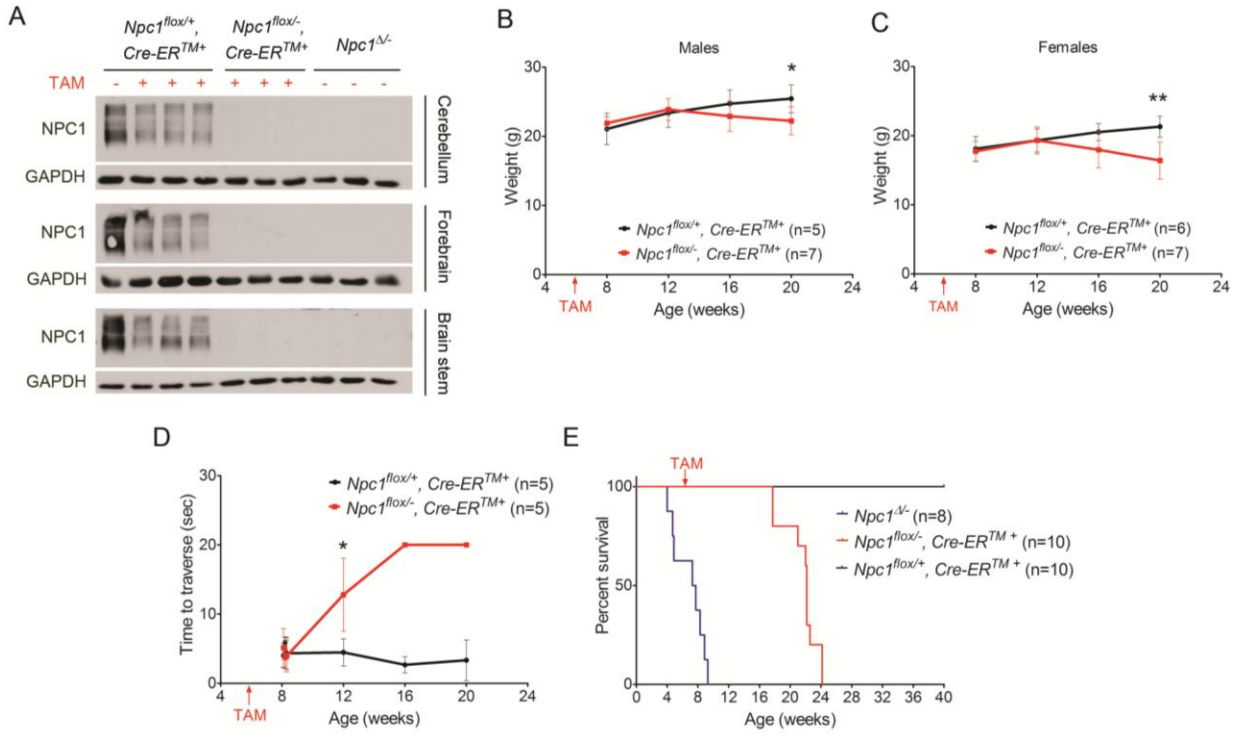

Based on prior analyses of the neuropathology of mice in which *Npc1* deletion occurred in the germline, we next determined whether similar changes occurred following adult deletion. Calbindin staining of sagittal midline cerebellar sections revealed progressive anterior-to-posterior Purkinje cell loss in tamoxifen treated *Npc1*$^{flox/-}$, *Cre-ER*$^{TM+}$ mice **(Figure 2.2A)**. This patterned Purkinje cell loss has been documented previously in *Npc1*$^{-/-}$ and *Npc1* $^{\Delta/-}$ mice (Elrick et al., 2010; Sarna et al., 2003). Quantification of Purkinje cell density demonstrated that the rate of neuron loss fits well into a model incorporating a plateau followed by exponential decay **(Figure 2.2B)**. The occurrence of an initial plateau was confirmed by comparing *Npc1*$^{flox/-}$, *Cre-ER*$^{TM+}$ mice at 8 weeks with *Npc1*$^{flox/+}$, *Cre-ER*$^{TM+}$ controls at 21 weeks, indicating that there was no Purkinje cell loss 2 weeks after tamoxifen injections **(Figure 2.2C)**. Quantification of Purkinje cell density by lobule revealed selective vulnerability of Purkinje cell subpopulations, with cells in anterior lobules degenerating early and those in posterior lobules exhibiting resistance to the toxicity of Npc1 deficiency **(Figure 2.2D)**. This survival of Purkinje cells in posterior lobules occurred despite the accumulation of unesterified cholesterol **(Figure 2.2E)**. All of these findings are similar to those documented in Purkinje cell specific *Npc1* null mice (*Npc1*$^{flox/-}$, *Pcp2-Cre*$^{+}$), further supporting the notion that Purkinje cell loss is independent of events during development (Elrick et al., 2010). In addition to cerebellar pathology, widespread axonal spheroids, secondary demyelination, microgliosis and astrocytosis were also present in *Npc1*$^{flox/-}$, *Cre-ER*$^{TM+}$ mice **(Figure 2.2F)**. We conclude that deletion of *Npc1* in the adult CNS is sufficient to cause disease and that there is not a significant developmental component to NPC neuropathology.

Figure 2.2 *Npc1* deletion in adult mice recapitulates Niemann-Pick C neuropathology. **(A)** Calbindin immunofluorescence shows progressive anterior-to-posterior Purkinje cell loss in the cerebellar midline of *Npc1*$^{flox/-}$, *Cre-ER*$^{TM+}$ mice following tamoxifen treatment at 6 weeks. Cerebellar lobules are labeled by Roman numerals. **(B)** Quantification of Purkinje cell density in the cerebellar midline over time (mean +/- SD). Slope of the decay phase indicates a half-life of 34 days for Purkinje cells. **(C)** Comparison of Purkinje cell density in 8-week-old mutant mice (*Npc1*$^{flox/-}$, *Cre-ER*$^{TM+}$) and 21-week-old littermate controls (*Npc* $^{flox/+}$, *Cre-ER*$^{TM+}$), indicating no Purkinje cell loss 2 weeks after tamoxifen treatment. Data are mean +/- SD. $p>0.05$. **(D)** Quantification of Purkinje cell density in midline cerebellar lobules over time. Data are mean +/- SD. **(E)** Calbindin and filipin co-staining reveals accumulation of unesterified cholesterol in cerebellar lobule X of 18-week-old *Npc1*$^{flox/-}$, *Cre-ER*$^{TM+}$ mice (right column), but not in littermate controls (left column). **(F)** Neurofilament (NF) and luxol fast blue (LFB) stains highlight swollen axons in the cortex (NF) and demyelination in the corpus callosum (LFB) of *Npc* $^{flox/-}$, *Cre-ER*$^{TM+}$ mice (bottom row) compared to littermate controls (top row) at 22 weeks. Immunofluorescence demonstrates microgliosis (Iba1) and astocytosis (GFAP) in the cerebellum of *Npc* $^{flox/-}$, *Cre-ER*$^{TM+}$ mice at 18 weeks (bottom row).

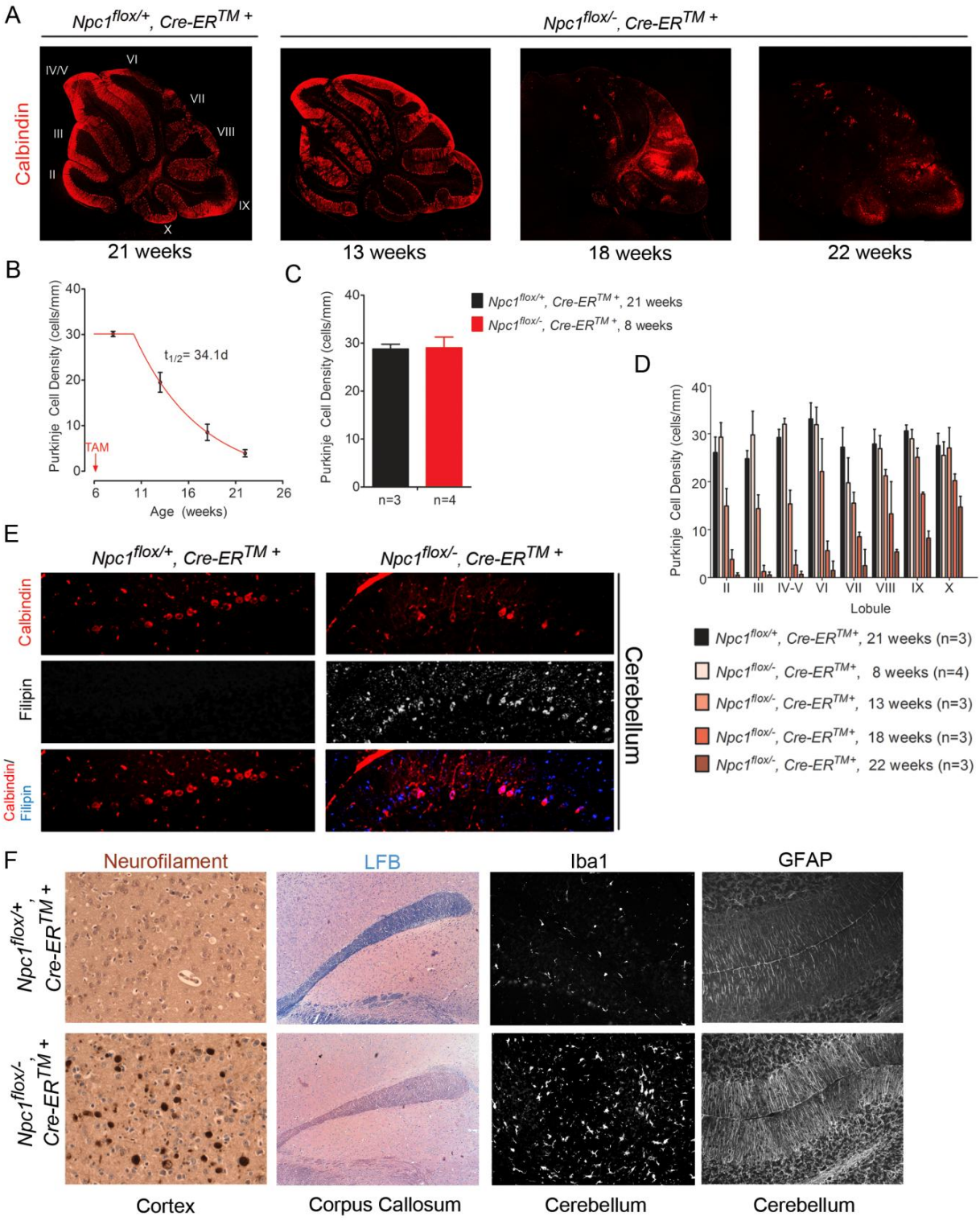
A
Npc1flox/+, Cre-ERTM +
Npc1flox/-, Cre-ERTM +
Calbindin
IV/V
VI
VII
VIII
III
II
IX
X
21 weeks
13 weeks
18 weeks
22 weeks
B
Purkinje Cell Density (cells/mm)
t1/2= 34.1d
TAM
Age (weeks)
C
Npc1flox/+, Cre-ERTM +, 21 weeks
Npc1flox/-, Cre-ERTM +, 8 weeks
n=3
n=4
D
Lobule
Npc1flox/+, Cre-ERTM+, 21 weeks (n=3)
Npc1flox/-, Cre-ERTM+, 8 weeks (n=4)
Npc1flox/-, Cre-ERTM+, 13 weeks (n=3)
Npc1flox/-, Cre-ERTM+, 18 weeks (n=3)
Npc1flox/-, Cre-ERTM+, 22 weeks (n=3)
E
Calbindin
Filipin
Calbindin/
Filipin
Cerebellum
F
Neurofilament
LFB
Iba1
GFAP
Cortex
Corpus Callosum
Cerebellum
Cerebellum

2.3.2 Astrocyte-specific deletion of Npc1 does not lead to CNS pathology

We next sought to establish the contribution of distinct CNS cell populations to NPC neuropathology, and began by deleting *Npc1* only in astrocytes. To achieve astrocyte-specific deletion, we used mice expressing a tamoxifen regulated Cre recombinase under the control of the human GFAP promoter (*GFAP-CreER*$^{T2+}$) (Casper et al., 2007). To avoid confounding effects due to GFAP expression by neuronal precursors during development (Casper and McCarthy, 2006), Cre activation was induced by tamoxifen injections at 6 weeks. We confirmed gene deletion by staining brain sections with filipin, a fluorescent dye that marks accumulations of unesterified cholesterol (Bornig and Geyer, 1974). By performing GFAP and filipin co-staining, we confirmed that *Npc1*$^{flox/-}$*, GFAP-CreER*$^{T2+}$ mice, but not *Npc1*$^{flox/+}$*, GFAP-CreER*$^{T2+}$ controls, contained widespread filipin-positive astrocytes throughout the brain **(Figure 2.3A-C)**.

Figure 2.3 Astrocyte-specific deletion of *Npc1* at 6 weeks leads to the accumulation of unesterified cholesterol in astrocytes.
(A, B, C) Filipin and GFAP co-staining identifies the accumulation of unesterified cholesterol in astrocytes of *Npc1* $^{flox/-}$, *GFAP-CreER*$^{T2+}$ mice (bottom rows in A and B) but not in littermate controls (top rows in A and B) after tamoxifen treatment. Shown are representative images of the hippocampus (A), cortex (B) and cerebellum (C). For comparison in panel C, co-staining following Purkinje cell specific deletion (*Npc1*$^{flox/-}$, *Pcp2-Cre*$^{+}$ mice) is shown in the right column.

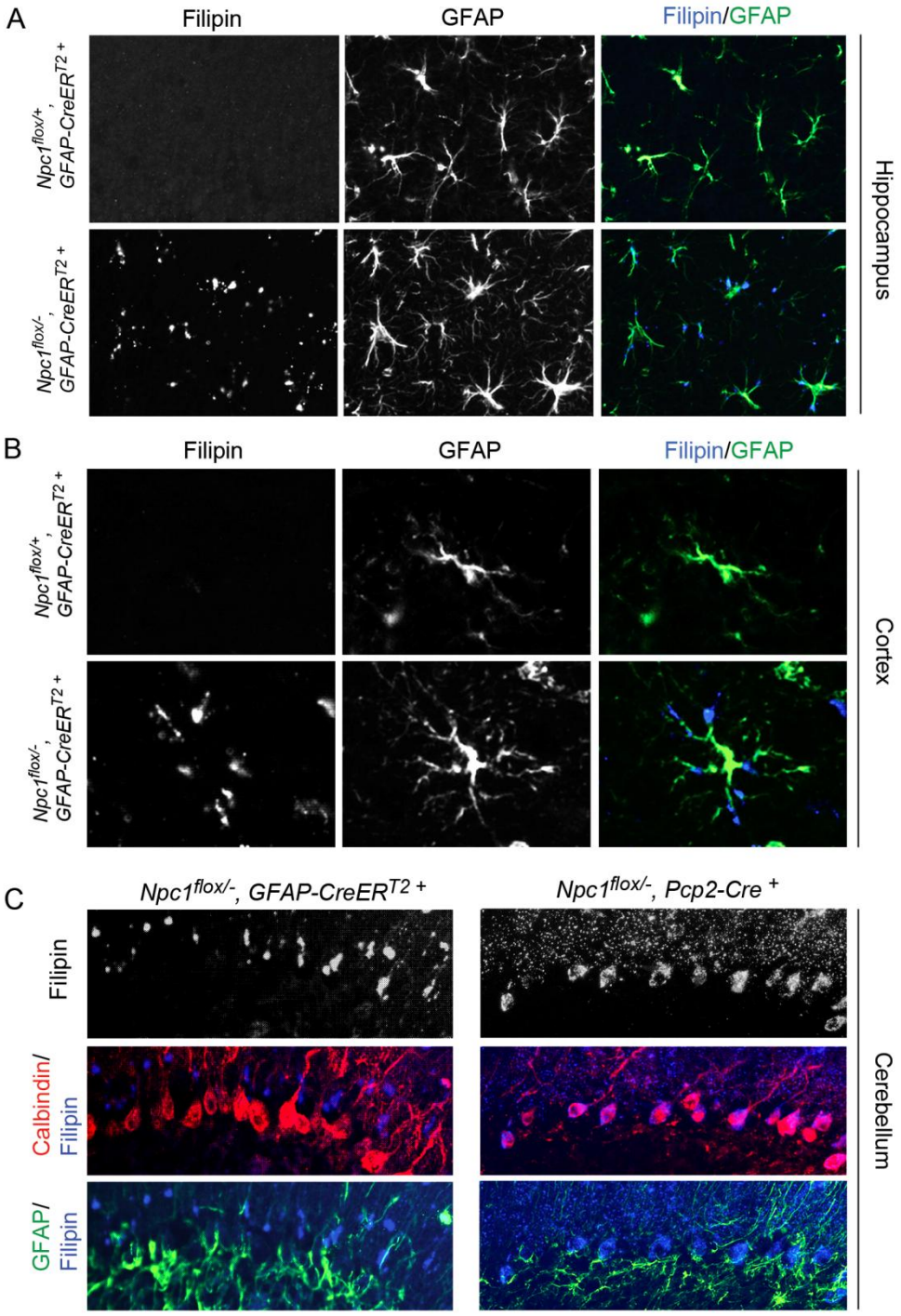

Despite the occurrence of efficient recombination, phenotype analysis did not reveal any differences between astrocyte-specific null mice (*Npc1*$^{flox/-}$, *GFAP-CreER*$^{T2+}$) and their littermate controls (*Npc1*$^{flox/+}$, *GFAP-CreER*$^{T2+}$). Astrocyte-specific null mutants gained weight normally (**Figure 2.4A, B)**, showed unimpaired motor performance **(Figure 2.4C)** and exhibited normal survival **(Figure 2.4D)**. Similarly, histological examination did not uncover abnormalities in the astrocyte-specific null mutants. Compared to controls, there was no Purkinje cell loss in the cerebellar midline, even at 48 weeks **(Figure 2.5A, B)**, nor was there formation of axonal spheroids or evidence of demyelination **(Figure 2.5C)**. Additionally, we did not detect activated astrocytes or microglia (**Figure 2.5C, Figure 2.6A)**, despite *Npc1* deletion in astrocytes, supporting the notion that glial reaction occurred secondary to neuron loss. Similarly, while deletion of *Npc1* in primary astrocytes *in vitro* led to the accumulation of free cholesterol, it did not diminish cell survival **(Figure 2.7)**.

Figure 2.4 Astrocyte-specific deletion of *Npc1* at 6 weeks does not impair weight, motor function or survival.
(A, B) Weight curves for male (A) and female (B) mice. Data are mean +/- SD. **(C)** Age dependent performance on balance beam. Data are mean +/- SD. **(D)** Percent survival at 44 weeks.

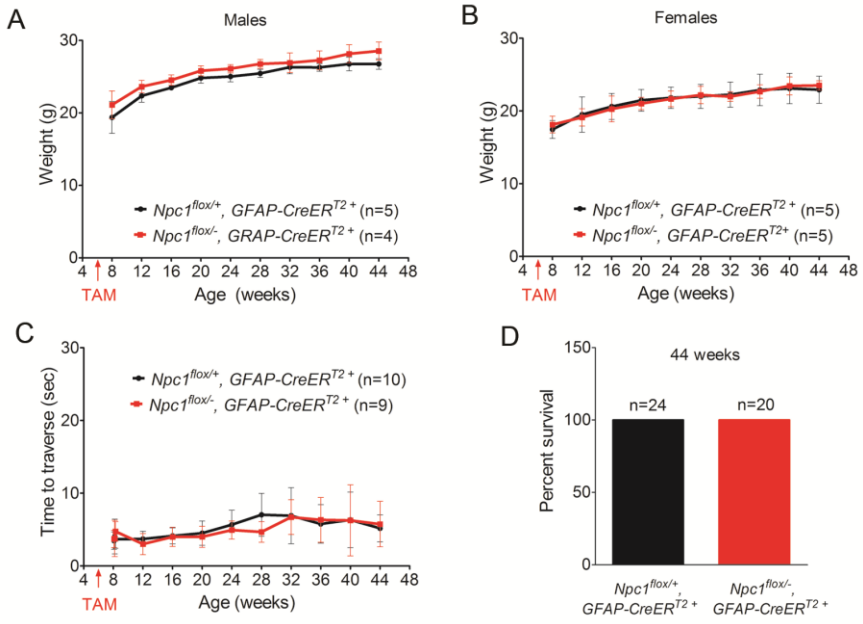

Figure 2.5 Neuropathology and electrophysiology of Purkinje cells following astrocyte-specific *Npc1* deletion.

(A) Calbindin staining shows no Purkinje cell loss in 48-week-old Npc1 $^{flox/-}$, *GFAP-CreER*$^{T2+}$ mice (right) or littermate controls (left) after tamoxifen treatment at 6 weeks. **(B)** Quantification of Purkinje cell density in midline cerebellar lobules (mean +/- SD). **(C)** Neurofilament and luxol fast blue stains reveal no swollen axons (NF) in the brainstem or demyelination (LFB) in the corpus callosum of 48-week-old Npc1 $^{flox/-}$, *GFAP-CreER*$^{T2+}$ mice (bottom row) compared with littermate controls (top row). Iba1 and GFAP immunofluorescence identify no gliosis in the cerebellum of these mice. **(D, E, F)** (D) Representative traces of parallel fiber-mediated excitatory postsynaptic currents (PF-EPSCs) to increasing stimulus intensity in a Purkinje cell (PC) from *Npc1* $^{flox/+}$, *GFAP-CreER*$^{T2+}$ mice (left) and *Npc1* $^{flox/-}$, *GFAP-CreER*$^{T2+}$ mice (right). (E) Quantification of decay time constants of PF-EPSCs with an amplitude of ~ 300 pA from *Npc1* $^{flox/+}$, *GFAP-CreER*$^{T2+}$ mice (n=5 PCs) and *Npc1* $^{flox/-}$, *GFAP-CreER*$^{T2+}$ mice (n=6 PCs). Data are mean +/- SEM, $p>0.05$. (F) Mean decay time constants measured at different EPSC amplitudes, normalized to that of the smallest EPSC for each group. **(G, H)** (G) Representative traces of PF-EPSCs to pairs of stimuli separated by 50ms from *Npc1* $^{flox/+}$, *GFAP-CreER*$^{T2+}$ mice (left) and *Npc1* $^{flox/-}$, *GFAP-CreER*$^{T2+}$ mice (right). (H) Quantification of the paired-pulse facilitation ratio, expressed as the ratio of the amplitude of the second response to the first one (n= 5 PCs from *Npc1* $^{flox/+}$, *GFAP-CreER*$^{T2+}$ mice and n=8 PCs from *Npc1* $^{flox/-}$, *GFAP-CreER*$^{T2+}$ mice). Data are mean +/- SEM, $p>0.05$. The experiments in Figure 2.5D-H were performed by Vikram Shakkottai.

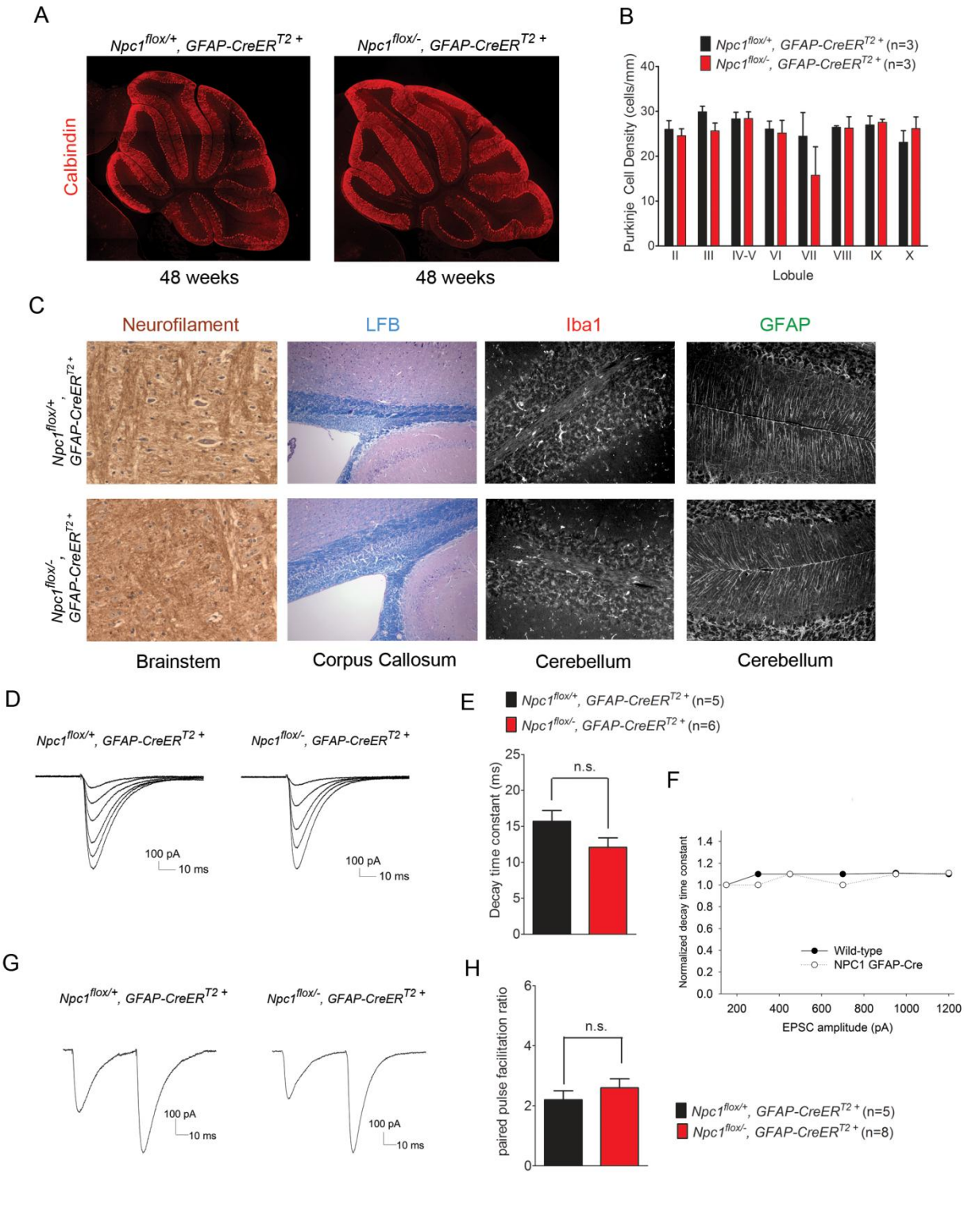
A
Npc1flox/+, GFAP-CreERT2 +
Npc1flox/-, GFAP-CreERT2 +
Calbindin
48 weeks
48 weeks
B
Npc1flox/+, GFAP-CreERT2 + (n=3)
Npc1flox/-, GFAP-CreERT2 + (n=3)
Purkinje Cell Density (cells/mm)
0
10
20
30
40
II
III
IV-V
VI
VII
VIII
IX
X
Lobule
C
Neurofilament
LFB
Iba1
GFAP
Npc1flox/+, GFAP-CreERT2 +
Npc1flox/-, GFAP-CreERT2 +
Brainstem
Corpus Callosum
Cerebellum
Cerebellum
D
Npc1flox/+, GFAP-CreERT2 +
Npc1flox/-, GFAP-CreERT2 +
100 pA
10 ms
100 pA
10 ms
E
Npc1flox/+, GFAP-CreERT2 + (n=5)
Npc1flox/-, GFAP-CreERT2 + (n=6)
Decay time constant (ms)
0
5
10
15
20
25
n.s.
F
Normalized decay time constant
0.0
0.2
0.4
0.6
0.8
1.0
1.2
1.4
200
400
600
800
1000
1200
EPSC amplitude (pA)
Wild-type
NPC1 GFAP-Cre
G
Npc1flox/+, GFAP-CreERT2 +
Npc1flox/-, GFAP-CreERT2 +
100 pA
10 ms
100 pA
10 ms
H
paired pulse facilitation ratio
0
2
4
6
n.s.
Npc1flox/+, GFAP-CreERT2 + (n=5)
Npc1flox/-, GFAP-CreERT2 + (n=8)

Figure 2.6 Reactive gliosis in neuron-specific *Npc1* null mice, but not astrocyte-specific null mutants.
(A) Western blots of Iba1, GFAP and GAPDH from cerebellar homogenates of *Npc1*$^{flox/-}$*, GFAP-CreER*$^{T2+}$ and control mice at 48 wks. **(B)** Western blots of Iba1, GFAP and GAPDH from brainstem homogenates *Npc1*$^{flox/-}$*, Syn1-Cre*$^{+}$ and control mice at 16 wks.

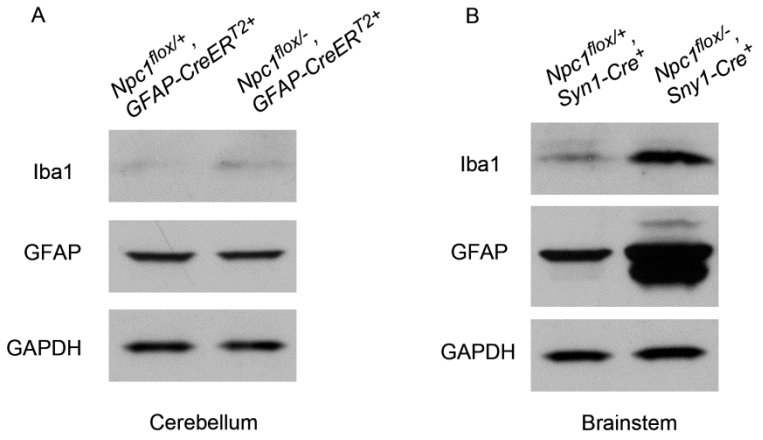

Figure 2.7 Deletion of *Npc1* in astrocytes *in vitro* leads to free cholesterol accumulation, but does not impair survival.
(A) Western blots for Npc1, Cre and GFAP from primary astrocyte cultures after 4-day treatment of 5 uM 4-hydroxytamoxifen (4-OHT) to induce Cre-mediated deletion of *Npc1*.
(B) Filipin and GFAP co-staining shows accumulation of unesterified cholesterol in astrocytes after *Npc1* deletion (bottom row), but not in the control group (top row).
(C) Survival of astrocytes over time after *Npc1* deletion, as measured by XTT assay. The absorbance readings of Npc1 deficient astrocytes are normalized to the mean value of the control group for each time point and are expressed as survival ratio (n=8 wells for each group). Data are mean +/- SD. p>0.05.

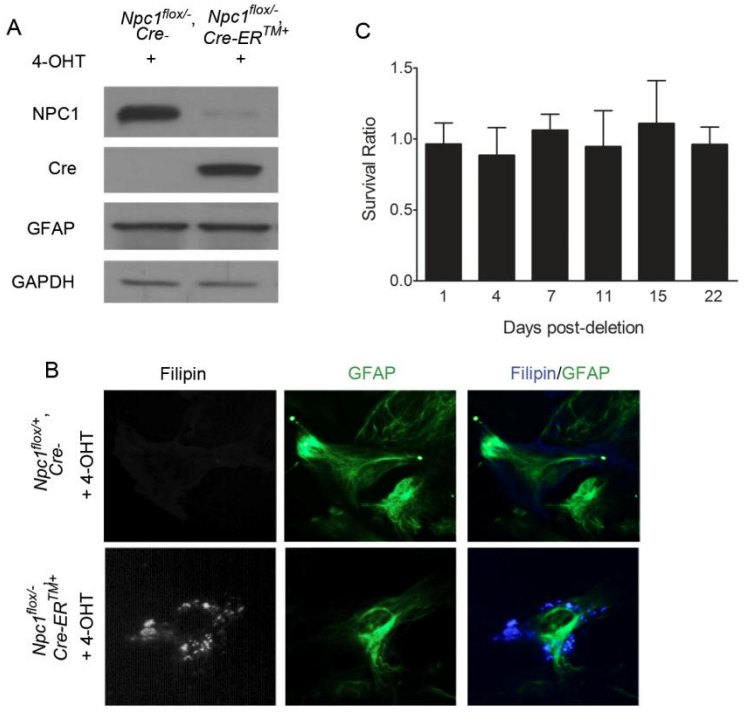

We considered the possibility that *Npc1* deletion in astrocytes impaired neuron function without triggering morphological hallmarks of neuron loss. To test this possibility, we focused on cerebellar glial cells in mice aged less than 4 weeks. To accomplish this, we generated another cohort of *Npc1*$^{flox/-}$, *GFAP-CreER*$^{T2+}$ mice and *Npc1*$^{flox/+}$, *GFAP-CreER*$^{T2+}$ controls which were injected with tamoxifen at postnatal days 12 and 14. As with mice receiving tamoxifen at 6 weeks, these astrocyte specific null mice showed no deficits in weight, motor function or survival **(Figure 2.8)**.

Figure 2.8 Astrocyte-specific deletion of *Npc1* at P12 & P14 does not impair weight, motor function or survival.
(A, B) Weight curves for male (A) and female (B) mice. Data are mean +/- SD. **(C)** Age dependent performance on balance beam. Data are mean +/- SD.

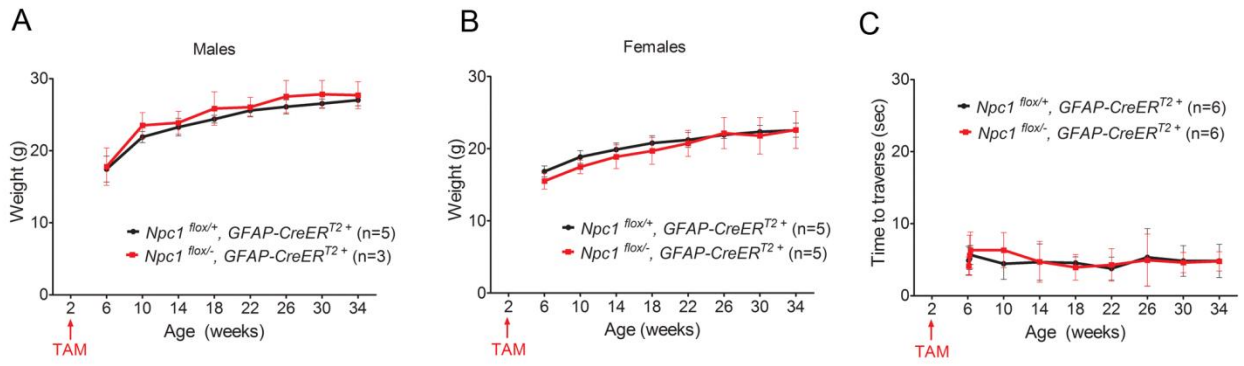

The synapses of cerebellar parallel fibers onto Purkinje cells are strongly wrapped by Bergmann glia, specialized astrocytes in the cerebellum that express a high density of glutamate transporters (Lehre and Danbolt, 1998). We determined whether the absence of Npc1 triggered glial dysfunction that altered the handling of glutamate at the parallel fiber-Purkinje neuron synapse in cerebellar slices. We assessed glutamatergic synaptic responses using whole-cell

patch-clamp recordings from Purkinje neurons in the presence of 50 μM picrotoxin to block inhibitory post-synaptic currents. In response to stimulation of parallel fibers in the molecular layer, we elicited excitatory postsynaptic currents (EPSCs) that increased in amplitude with increasing stimulus strength. Similar responses **(Figure 2.5D)** and decay time constants **(Figure 2.5E)** were detected in *Npc1*$^{flox/-}$*, GFAP-CreER*$^{T2+}$ and *Npc1*$^{flox/+}$*, GFAP-CreER*^{T2} mice. Since inhibiting glial glutamate transporters slows the decay of parallel fiber EPSCs when many nearby parallel fibers are simultaneously activated (Marcaggi et al., 2003), we also determined whether the EPSC decay time constant increased with increasing stimulus strength. However, we detected no significant slowing of EPSC decay with increasing stimulation of parallel fibers (**Figure 2.5F)**. As Bergmann glia may influence presynaptic transmitter release (Bordey and Sontheimer, 2003), we determined whether paired-pulse facilitation was altered in the astrocyte-specific null mutants; no difference was detected **(Figure 2.5G, H)**. These electrophysiologic studies suggest that loss of Npc1 in Bergmann glia was not associated with functional alterations in synaptic transmission. Taken together, our analyses indicate that Npc1 deficiency in astrocytes is not a prime contributor to the NPC disease phenotype.

2.3.3 Deletion of Npc1 in neurons is sufficient to cause neurodegeneration

The fact that mice were not affected by deletion of *Npc1* in astrocytes led us to test whether neurodegeneration in NPC is heavily dependent upon toxicity within neurons. To accomplish neuron-specific *Npc1* deletion, we used transgenic mice expressing Cre recombinase under the control of the *Synapsin1* promoter (*Syn1-Cre*) (Zhu et al., 2001). In these mice, Cre is abundantly and specifically expressed in neurons during late embryonic development in a wide range of brain regions, but is minimally expressed in cerebellar Purkinje cells.

Filipin and NeuN co-staining verified that *Npc1*$^{flox/-}$, *Syn1-Cre*$^{+}$ mice, but not *Npc1*$^{flox/+}$, *Syn1-Cre*$^{+}$ controls, developed filipin-positive neurons in multiple brain regions including the cortex **(Figure 2.9A)** and brainstem **(Figure 2.9B)**. Histological examination of liver sections from *Npc1*$^{flox/-}$, *Syn1-Cre*$^{+}$ mice did not reveal an accumulation of foamy macrophages **(Figure 2.9C)**, consistent with reports that Cre expression is not leaky in visceral organs. Neuron-specific deletion of *Npc1* reproduced the phenotypic features observed following global gene deletion. *Npc1*$^{flox/-}$, *Syn1-Cre*$^{+}$ mice, but not littermate controls, developed progressive weight loss **(Figure 2.10A, B)**, motor deficits in both balance beam **(Figure 2.10C)** and rotarod **(Figure 2.10D)** tests, and early death, with an average lifespan of 105 days **(Figure 2.10E)**.

Figure 2.9 Neuron-specific deletion of *Npc1* leads to accumulation of unesterified cholesterol in neurons.

(A, B) Filipin and NeuN co-staining identifies the accumulation of unesterified cholesterol in neurons of *Npc1*$^{flox/-}$, *Syn1-Cre*$^{+}$ mice (bottom rows) but not in littermate controls (top rows). Shown are representative images of cortex (A) and brainstem (B).

(C) H&E stain shows foamy macrophages in the liver following germline deletion of *Npc1* (*Npc1*$^{-/-}$) but not after neuron-specific deletion (*Npc1*$^{flox/-}$, *Syn1-Cre*$^{+}$).

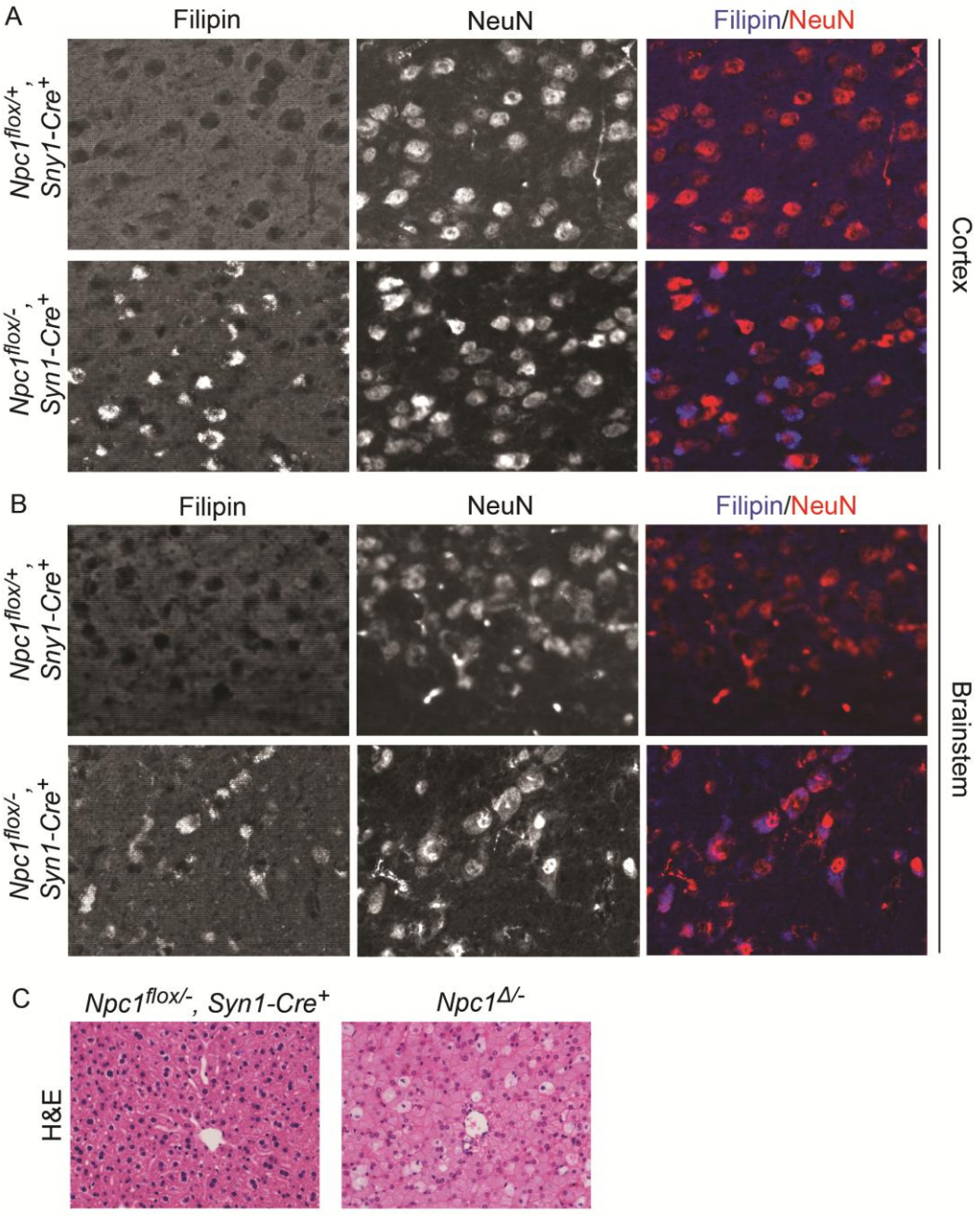

Figure 2.10 Neuron-specific deletion of *Npc1* impairs weight, motor performance and survival.
(A, B) Weight curves for male (A) and female (B) mice. Data are mean +/- SD. * p<0.05, ** p<0.01. **(C, D)** Neuron-specific *Npc1* deletion impairs performance on balance beam (C) and rotarod (D). Data are mean +/- SD. * p<0.05, ** p<0.01. **(E)** Kaplan-Meyer survival curves for mice following neuron-specific deletion of *Npc1* (*Npc1*$^{flox/-}$, *Syn1-Cre* $^{+}$) or littermate controls (*Npc1*$^{flox/+}$, *Syn1-Cre* $^{+}$). For reference, the previously reported survival of mice with germline deletion (*Npc1*$^{\Delta/-}$) is shown (Elrick et al., 2010).

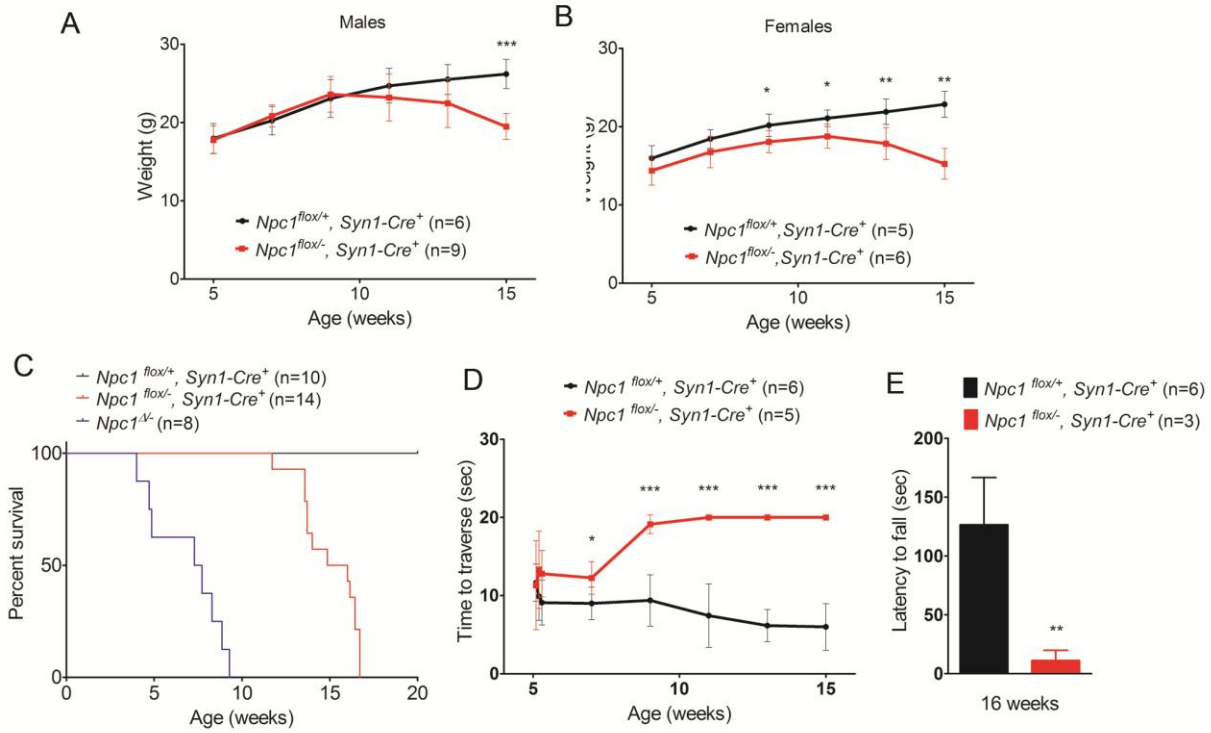

The development of motor impairment occurred in the absence of Purkinje cell degeneration. Histological examination of sagittal midline cerebellar sections revealed no Purkinje cell loss in end stage *Npc1*$^{flox/-}$, *Syn1-Cre*$^{+}$ mice at 16 weeks **(Figure 2.11A, B)**. This finding is consistent with the fact that the *Syn1-Cre* transgene is poorly expressed by Purkinje cells (Zhu et al., 2001). The occurrence of motor deficits in these animals indicates that pathology elsewhere in the nervous system is sufficient to cause this phenotype. In support of

this conclusion, *Npc1*$^{flox/-}$, *Syn1-Cre*$^{+}$ mice, but not *Npc1*$^{flox/+}$, *Syn1-Cre*$^{+}$ controls, showed severe axonal pathology with frequent axonal spheroids in the brainstem, loss of myelinated fibers in the corpus callosum, and activated microglia and astrocytes in many brain regions **(Figure 2.11C, Figure 2.6B)**. We conclude that deletion of *Npc1* in neurons is sufficient to recapitulate the neuropathological features of NPC mice.

Figure 2.11 Neuropathology following neuron-specific deletion of *Npc1.*
(A) Calbindin staining shows no Purkinje cell loss in 16-week-old *Npc1*$^{flox/-}$, *Syn1-Cre*$^{+}$ mice (right) compared to littermate controls (left). **(B)** Quantification of Purkinje cell density in midline cerebellar lobules. Data are mean +/- SD. **(C)** Neurofilament (NF) and luxol fast blue (LFB) stains highlight swollen axons in the brainstem (NF) and loss of myelinated axons in the corpus callosum (LFB) of 16-week-old *Npc1*$^{flox/-}$, *Syn1-Cre*$^{+}$ mice (bottom row) but not littermate controls (top row). Immunofluorescence demonstrates microgliosis (Iba1) in the brainstem and astrocytosis (GFAP) in the cortex in *Npc1*$^{flox/-}$, *Syn1-Cre*$^{+}$ mice (bottom row) at 16 weeks.

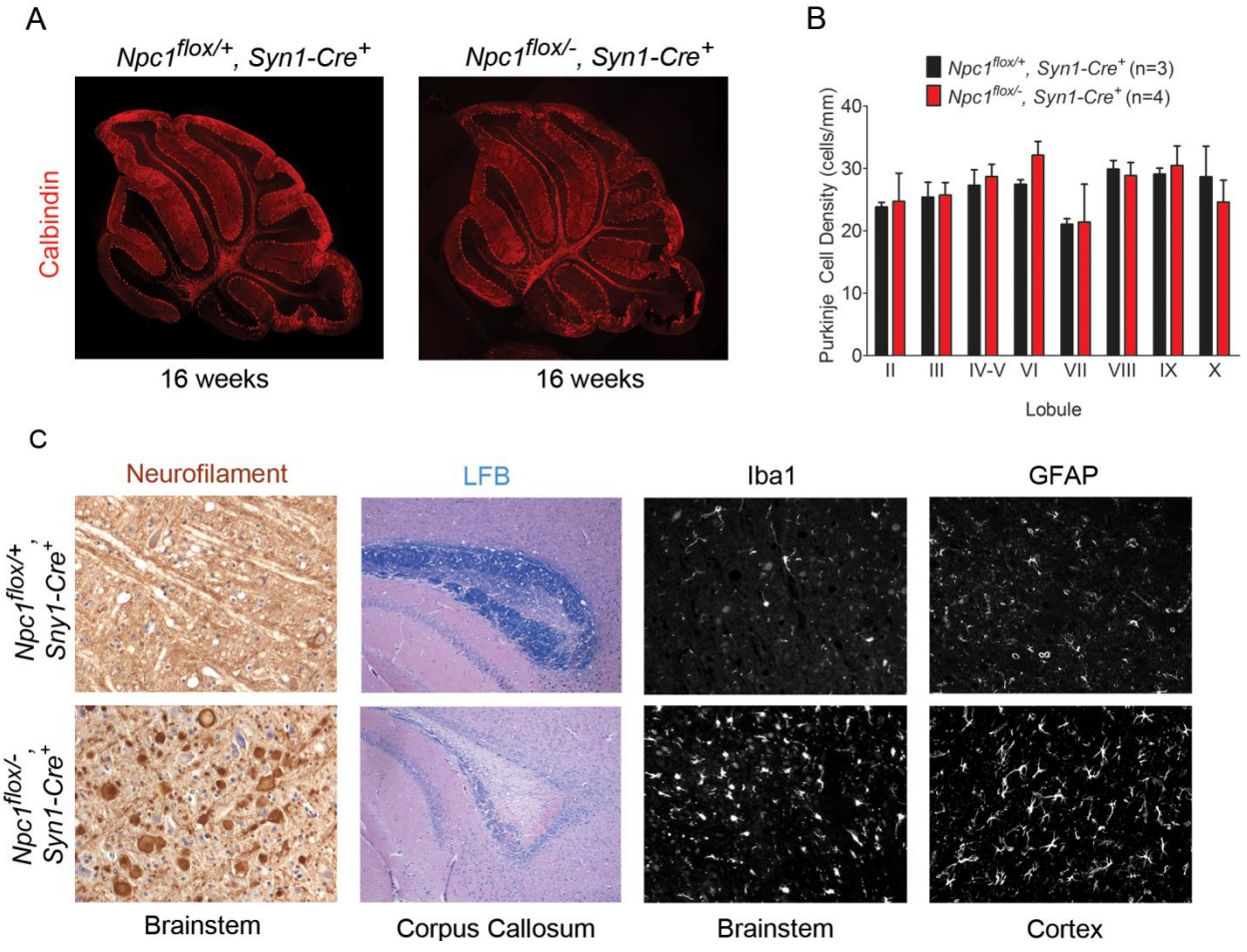

2.4 Discussion

Here we used *Npc1* conditional null mutant mice to achieve global deletion of the *Npc1* gene in adults as well as restricted deletion in specific CNS cell types including astrocytes and neurons. Our findings demonstrate that deletion of *Npc1* in adults is sufficient to recapitulate the disease phenotypes of weight loss, motor deficits and early death. Pathological changes in the CNS of mice following adult deletion were similar to those triggered by germline deficiency and included patterned Purkinje cell loss, axonal pathology and glial activation. Our findings indicate that an impairment of developmental events is not necessary for the occurrence of CNS pathology. Furthermore, our data establish that deletion of *Npc1* in neurons, but not in astrocytes, is sufficient to cause neurodegeneration. The observation that neuronal loss of Npc1 is the primary cause of neuropathology in mice identifies neurons as the critical target cell for future therapeutic interventions.

There has been significant interest in the potential role of astrocytes in the development of NPC neuropathology since the initial observation that these cells robustly express the NPC1 protein (German et al., 2002; Hu et al., 2000; Patel et al., 1999). Astrocytes are an abundant glial cell in the CNS with diverse functions in synaptic transmission (Haydon, 2001), neuroinflammation (Farina et al., 2007) and lipid homeostasis (Vance et al., 2005). Astrocytic processes are closely associated with synapses, and these cells both promote synaptogenesis by secreting factors such as lipoproteins (Mauch et al., 2001) and thrombospondins (Christopherson et al., 2005) and facilitate synaptic function by contributing to the clearance of extracellular neurotransmitters (Danbolt, 2001). Astrocytes are also capable of releasing a variety of cytokines, and these inflammatory mediators have been implicated in the development of CNS disease (Allaman et al., 2011). While Npc1 deficiency in astrocytes *in vitro* results in the sequestration of

cholesterol in late endosomes and lysosomes, it does not impair the secretion of sterols, including cholesterol (Karten et al., 2005; Mutka et al., 2004). Nonetheless, given the importance of astrocytes in maintaining brain homeostasis, they have been implicated in NPC neurodegeneration. This notion was supported by prior studies of transgenic mice in which GFAP-promoter driven expression of an *Npc1* transgene extended lifespan of *Npc1*$^{-/-}$ mice (Zhang et al., 2008). However, a recent analysis of mice expressing a tagged *Npc1* transgene whose expression was clearly restricted to astrocytes showed no phenotypic rescue (Lopez et al., 2011). Here we determined the extent to which deletion of *Npc1* only in astrocytes contributes to CNS disease. Our data show that astrocyte specific null mutants (*Npc1*$^{flox/-}$, *GFAP-CreER* $^{T2+}$) display no phenotypic abnormalities, histopathological changes or evidence of synaptic dysfunction. These unexpected findings demonstrate that *Npc1* deficiency in astrocytes is not sufficient to mediate disease. Furthermore, the observation that astrocyte specific null mutants show no glial activation is consistent with prior work suggesting that gliosis is the consequence, but not the cause of neuronal dysfunction and death.

In marked contrast, neuronal restricted deletion of *Npc1* recapitulates many of the phenotypic and pathological features exhibited by mice with global, germline deficiency. The occurrence of motor impairment in *Npc1*$^{flox/-}$, *Syn1-Cre*$^{+}$ mice was particularly interesting since this occurred in the setting of only limited Cre expression by cerebellar Purkinje cells (Zhu et al., 2001). As such, *Npc1*$^{flox/-}$, *Syn1-Cre*$^{+}$ mice displayed balance beam and rotarod deficits without concurrent Purkinje cell loss. Complementing these findings is our prior analysis of Purkinje cell specific null mutants that demonstrates motor impairment without other features of the NPC phenotype (Elrick et al., 2010). We conclude that although Purkinje cell loss is sufficient to mediate motor dysfunction, it is not required for it, and pathology elsewhere in the brain likely

accounts for this disease manifestation in mice expressing the *Syn1-Cre* transgene. The brainstem, thalamus, cortex and subcortical white matter are abnormal in these mutants, and several of these sites may contribute to the observed phenotype.

The data reported here extend our understanding of disease mechanisms underlying the development of NPC neuropathology. We conclude that neuron dysfunction and loss are the consequence of cell autonomous processes, a notion originally suggested by an analysis of *Npc1* deficient Purkinje cells (Elrick et al., 2010; Ko et al., 2005) and supported by neuron restricted transgenic rescue experiments (Lopez et al., 2011). We find no evidence that astrocytes are primary contributors to disease pathology, despite the existence of multiple potential mechanisms that made them attractive candidates. Finally, our data support the emerging concept that glial reaction and neuroinflammation occur secondary to neuronal injury. Whether the inflammatory mediators they produce contribute to the pathogenic cascade remains to be defined. Taken together, our analysis establishes a critical role for neuronal deficiency of *Npc1* in the development of CNS disease, and compels us to search for therapeutic targets that mediate cell autonomous neurodegeneration.

2.5 Materials and Methods

2.5.1 Mice

Npc1$^{flox/flox}$ and *Npc1*$^{\Delta/-}$ mice were generated as previously described (Elrick et al., 2010). Tamoxifen-inducible *CMV-Cre* mice (*Cre-ER*$^{TM+}$) (#004682) (Hayashi and McMahon, 2002), *Pcp2-Cre* mice (#004146) (Barski et al., 2000) and *Sny1-Cre* mice (#003966) (Zhu et al., 2001) were from the Jackson Laboratories . Tamoxifen-inducible *GFAP-Cre* mice (*GFAP-CreER*$^{T2+}$)

(Casper et al., 2007) were from the Mutant Mouse Regional Resource Center (#016992-MU/H). All mouse strains were backcrossed to C57BL6/J for >10 generations, except *Syn1-Cre* mice which were backcrossed 7 generations. Animal use and procedures were approved by the University of Michigan Committee on the Use and Care of Animals.

2.5.2 Tamoxifen induction

Tamoxifen (Sigma) was dissolved in corn oil (Sigma) at 20 mg/ml and stored at -20 C in the dark. The stock solution was warmed to 37 C before injection. Adult mice were injected intraperitoneally with 3 mg (for *Cre-ER*$^{TM+}$ mice) or 5 mg (for *GFAP-CreER*$^{T2+}$ mice) tamoxifen per 40 g body weight for 5 consecutive days at 6 weeks. Pups were injected intraperitoneally with 5 mg tamoxifen per 40 g body weight at postnatal days 12 and 14.

2.5.3 Phenotype analysis

Motor function was measured using the balance beam and rotarod tests as described previously (Elrick et al., 2010).

2.5.4 Western blot

Brain lysates were homogenized in RIPA buffer (Thermo Scientific) containing complete protease inhibitor cocktail (Roche) and phosphatase inhibitor (Thermo scientific) using a motor homogenizer (TH115, OMNI International). Samples were resolved by 7% SDS-PAGE and transferred to nitrocellulose membranes (BioRad) on a semidry transfer apparatus. Immunoreactivity was detected by Immobilon chemilluminescent substrate (Thermo Scientific). Antibodies used were rabbit anti-NPC1 (1:2000, Abcam), mouse anti-Cre (1:1000, Millipore), rabbit anti-GFAP (1:5000, Dako), rabbit anti-Iba1 (1:2000, Wako), and rabbit anti-GAPDH (1:5000, Santa Cruz).

2.5.5 Histology

Mice were perfused with 0.9% normal saline followed by 4% paraformaldehyde. Brains and livers were removed and post-fixed in 4% paraformaldehyde overnight. Brains were bisected, with the right hemisphere processed for paraffin embedding and the left hemisphere processed for frozen sections. Prior to freezing, brain tissue was cryoprotected in 30% sucrose for 48 hr at 4 C. Brains were frozen in isopentane chilled by dry ice and embedded in OCT (Tissue-Tek). Frozen sections were prepared at 14 μm in a cryostat and used for immunofluorescence staining for calbindin (1:1000, Sigma), GFAP (1:1000, Dako) and NeuN (1:500, Millipore). Sections were subsequently stained with filipin by incubating tissue sections for 90 min in PBS with 10% fetal bovine serum plus 25 μg/ml filipin (Sigma). For visualization of staining, secondary antibodies conjugated to Alexa Fluor 594 or Alexa Fluor 488 (Molecular Probes) were used and images were captured on a Zeiss Axioplan 2 imaging system. Paraffin-embedded sections were prepared at 5 μm and used for staining with H&E staining or Luxol fast blue, neurofilament (1:300, Covance) immunohistochemistry, and Iba1 (1:1000, Wako) and GFAP (1:1000, Dako) immunofluorescence. Quantification of Purkinje cell loss was performed on H&E stained sections. Counts were normalized to the length of the Purkinje layer, as measured by NIH ImageJ software, and reported as Purkinje cell density.

2.5.6 Primary astrocyte culture

Cerebral hemispheres of 1-day-old mouse pups were dissected for the primary astrocyte culture described previously (Kaech and Banker, 2006). Tail DNA samples from pups were used for genotyping. After reaching confluence, cells were trypsinized and plated into 6-well plates for western blot, 12-well plates with coverslips for immunostaining, and 96-well plates for XTT assay. Cells were subsequently treated with 5uM 4-Hydroxytamoxifen (4-OHT, Sigma) after

reaching 80% confluence, for 4 consecutive days to induce Cre-mediated gene deletion. On the following day (designated as 1 day post-deletion), cells were harvested for western blot or immunostaining. XTT assay was performed at different time points as indicated.

2.5.7 XTT assay

XTT assay was carried out using Cell Proliferation Kit II (XTT, Roche) according to manufacturer's instructions with slight modifications. Briefly, 20 uL XTT labeling mixture was added to each 96-well containing 100 uL medium. Cells were then incubated at 37 C for 1 hour, and the absorbance was measured at 490 nm with the reference at 650 nm.

2.5.8 Electrophysiology

Whole-cell recordings were obtained from Purkinje neurons in 300 μm parasagittal cerebellar slices prepared from 25 to 30 day old mice. Vibratome sections were cut in ice-cold solution containing (in mM): 87 NaCl, 2.5 KCl, 25 $NaHCO_3$, 1 NaH_2PO_4, 0.5 $CaCl_2$, 7 $MgCl_2$, 75 sucrose and 10 glucose, bubbled with 5% CO_2/95% O_2. Slices were incubated at 33 C in artificial CSF (ACSF), containing in mM: 125 NaCl, 3.5 KCl, 26 $NaHCO_3$, 1.25 NaH_2PO_4, 2 $CaCl_2$, 1 $MgCl_2$, and 10 glucose, bubbled with 5% CO_2/95% O_2. Purkinje neurons were visualized with infrared differential interference contrast (IR-DIC) optics on a Nikon upright microscope. Borosilicate glass patch pipettes (with resistances of 2–5 MΩ) were filled with internal recording solution containing (in mM): 130 Cs Methanesulfonate, 5 CsCl, 4 NaCl, 2 $MgCl_2$, 5 EGTA, 4 Mg ATP, 0.3 Tris-GTP, 10 Na Phosphocreatine, 5 QX-314, and 10 HEPES, pH 7.3. Whole-cell recordings were made in ACSF containing 50 μM Picrotoxin, 1–5 h after slice preparation using an Axopatch 200B amplifier, Digidata 1400 interface and pClamp-10 software (Molecular Devices, Union City, CA, USA). Series resistance was compensated 50-70%. Cells were rejected if series resistance was greater than 15 mΩ. Excitatory post-synaptic

currents (EPSCs) were recorded in voltage-clamp mode at a holding potential of − 70 mV. EPSCs from were evoked by applying square wave current pulses via a tungsten bipolar electrode to the molecular layer ~100 μm from the Purkinje neuron of interest. Analog current traces were digitized at 100 kHz. EPSC decay time constants were obtained by fitting the current decay between 10% and 80% of the peak current amplitude to a single exponential as previously described (Takahashi et al., 1995).

2.5.9 Statistics

Statistical significance was assessed by unpaired Student's t test (for comparison of two means) or ANOVA (for comparison of more than two mean). The Newman-Keuls post hoc test was performed to carry out pairwise comparisons of group means if ANOVA rejected the null hypothesis. Statistics were performed using the software package Prism 5 (GraphPad Software). *P* values less than 0.05 were considered significant.

2.6 Acknowledgements

We thank Matthew Elrick for helpful discussions and advice, Dr. Kristen Verhey for help with primary astrocyte cultures and Gwen McMichael-Suchanek for help with performing histochemical stains. This work was supported by the National Institutes of Health (R01 NS063967 to A.P.L., K08 NS072158 to V.G.S.).

Chapter 3

Npc1 acting in neurons and glia is essential for the formation and maintenance of CNS myelin

3.1 Abstract

Cholesterol availability is rate-limiting for myelination, and prior studies have established the importance of cholesterol synthesis by oligodendrocytes for normal CNS myelination. However, the contribution of cholesterol uptake through the endocytic pathway has not been fully explored. To address this question, we used mice with a conditional null allele of the *Npc1* gene, which encodes a transmembrane protein critical for mobilizing cholesterol from the endolysosomal system. Loss of function mutations in the human *NPC1* gene cause Niemann-Pick type C disease, a childhood-onset neurodegenerative disorder in which intracellular lipid accumulation, abnormally swollen axons and neuron loss underlie the occurrence of early death. Both NPC patients and *Npc1* null mice exhibit myelin defects indicative of dysmyelination, although the mechanisms underlying this defect are incompletely understood. Here we use temporal and cell type specific gene deletion in order to define effects on CNS myelination. Our results unexpectedly show that deletion of *Npc1* in neurons alone leads to an arrest of oligodendrocyte maturation and to subsequent failure of myelin formation. This defect is

associated with decreased activation of Fyn kinase, an integrator of axon-glial signals that normally promotes myelination. Furthermore, we show that deletion of *Npc1* in oligodendrocytes results in delayed myelination at early postnatal days. Aged, oligodendocyte-specific null mutants also develop late stage demyelination, followed by secondary Purkinje neuron loss. These data demonstrate that lipid uptake by neurons and oligodendrocytes through an Npc1-dependent pathway is required for both the formation and maintenance of CNS myelin.

3.2 Introduction

Ensheathment of axons by myelin is an evolutionary feature of the vertebrate nervous system that is accomplished by the extended and specialized plasma membranes of oligodendrocytes in the CNS and Schwann cells in the PNS. Myelin contains at least 70% lipids by dry weight (Baumann and Pham-Dinh, 2001), and this high ratio of lipid to protein ensures the insulating properties of myelin to maximize the efficiency of nerve conduction. Among all the lipid species found in the myelin sheath, unesterified cholesterol is a major component (Baumann and Pham-Dinh, 2001). In the mouse CNS, cholesterol in compact myelin represents ~78% of the total lipid pool (Dietschy and Turley, 2004), and the availability of cholesterol is the rate-limiting step for myelination (Saher et al., 2005). Since the CNS is shielded by the blood brain barrier, cholesterol required for myelination comes entirely from local synthesis (Dietschy and Turley, 2004). Both neurons and glia obtain the cholesterol they need either through endogenous synthesis or by uptake of lipoprotein particles produced and released within the CNS. That endogenously synthesized cholesterol is critical for CNS myelination in mice is demonstrated by deletion in oligodendrocytes of squalene synthase, the first dedicated enzyme of sterol synthesis (Saher et al., 2005). These mutant mice exhibit delayed myelination, suggesting

that exogenously supplied cholesterol also contributes to CNS myelin formation. However, whether cholesterol from exogenous sources is required for myelin synthesis, or just a compensatory source when endogenous synthesis is lacking in myelinating glia, has not been explored.

An essential component of the pathway through which cholesterol in lipoprotein particles is mobilized from the endolysosomal system is the Npc1 protein (Carstea et al., 1997; Loftus et al., 1997). This multipass transmembrane protein resides in late endosomes and lysosomes (Davies and Ioannou, 2000; Garver et al., 2000; Higgins et al., 1999; Neufeld et al., 1999), and functions cooperatively with the Npc2 protein to facilitate cholesterol efflux (Deffieu and Pfeffer, 2011; Kwon et al., 2009). Loss of functional Npc1 disrupts intracellular lipid trafficking, and leads to the sequestration of unesterified cholesterol and glycosphingolipids in late endosomes and lysosomes (Karten et al., 2009). Mutations in the human *NPC1* gene cause Niemann-Pick type C disease (NPC), a fatal childhood-onset neurodegenerative disorder (Vanier, 2010). Mice with a null mutation in the *Npc1* gene (*Npc1*$^{-/-}$) recapitulate the human disease, and exhibit progressive CNS neuropathology in which intracellular lipid accumulation, abnormally swollen axons, neuron loss and gliosis underlie the occurrence of ataxia and early death (German et al., 2002; Loftus et al., 1997). Notably, both NPC patients and *Npc1*$^{-/-}$ mice exhibit myelin defects indicative of dysmyelination, particularly in the forebrain (Takikita et al., 2004; Trouard et al., 2005; Walterfang et al., 2010; Weintraub et al., 1987; Weintraub et al., 1985). However, the complex pathology resulting from *Npc1* deficiency in both neurons and oligodendrocytes has limited the utility of these global null mutants to provide a detailed understanding of the contribution of exogenous cholesterol to CNS myelination.

Here we use mice with a conditional null allele of the *Npc1* gene to achieve temporal and cell type specific deletion in order to define effects on CNS myelin. We show that deletion of *Npc1* restricted to neurons unexpectedly recapitulates the dysmyelination phenotype of global null mutants. This effect is mediated by a block in maturation of oligodendrocyte lineage cells that is associated with decreased activation of Fyn kinase, an integrator of axon-glial signals that normally promote myelination. Furthermore, we show that deletion of *Npc1* in oligodendrocytes triggers a similar, though less severe impairment of CNS myelination, as well as late-onset demyelination and secondary neurodegeneration. Our analyses suggest that exogenous cholesterol entering cells through an Npc1-dependent pathway is necessary for both the formation and maintenance of CNS myelin.

3.3 Results

3.3.1 Global *Npc1* deficiency leads to CNS dysmyelination, followed by demyelination.

To confirm the requirement of Npc1 for proper myelination in mice during early postnatal stages, we utilized mice with a floxed *Npc1* allele ($Npc1^{flox}$) (Elrick et al., 2010). Cre-mediated deletion yields a null allele that is functionally indistinguishable from the spontaneous null mutation found in $Npc1^{nih}$ mice ($Npc1^{-/-}$) (Elrick et al., 2010; Loftus et al., 1997). To generate mice with *Npc1* deletion in the germline, $Npc1^{flox/flox}$ mice were bred with transgenic mice expressing Cre recombinase under the control of the EIIa promoter (Lakso et al., 1996). Mice mosaic for the conditionally deleted allele were bred with mice carrying the $Npc1^{-}$ allele to generate compound heterozygotes of the conditionally deleted and null *Npc1* alleles ($Npc1^{\Delta/-}$). We also generated mice with *Npc1* deletion in adults by using a tamoxifen-regulated Cre

recombinase under the control of the cytomegalovirus (CMV) promoter (*Cre-ER*$^{TM+}$) (Hayashi and McMahon, 2002). Cre-mediated deletion of *Npc1* in adults was induced by tamoxifen injections at 6 weeks, an age at which myelination is complete. Mice with adult deletion (*Npc1*$^{flox/-}$, *Cre-ER*$^{TM+}$) have been shown to recapitulate most features of NPC neuropathology, and reach end-stage by ~22 weeks (Yu et al., 2011). To determine the effect of the timing of *Npc1* deletion upon myelination, we compared 7-week-old mice with germline deletion (*Npc1*$^{\Delta/-}$), 22-week-old mice with adult deletion (*Npc1*$^{flox/-}$, *Cre-ER*$^{TM+}$) and 7-week-old controls (WT). MBP staining of sagittal midline brain sections revealed a dramatic reduction of myelin in *Npc1*$^{\Delta/-}$ mice, particularly in the forebrain **(Figure 3.1A)**. This pattern is similar to the myelin defects previously reported in *Npc1* $^{-/-}$ mice (German et al., 2002; Takikita et al., 2004; Weintraub et al., 1985). In contrast, *Npc1*$^{flox/-}$, *Cre-ER*$^{TM+}$ mice exhibited a staining pattern morphologically similar to that in controls **(Figure 3.1A)**. The difference in MBP staining patterns between *Npc1*$^{\Delta/-}$ mice and *Npc1*$^{flox/-}$, *Cre-ER*$^{TM+}$ mice suggests that Npc1 is required in early postnatal stages for proper myelin formation. Further analysis of myelin-specific proteins demonstrated a decrease in MBP and CNP protein levels in *Npc1*$^{flox/-}$, *Cre-ER*$^{TM+}$ mice compared to littermate controls **(Figure 3.1B)**. We conclude that myelin was properly formed in *Npc1*$^{flox/-}$, *Cre-ER*$^{TM+}$ mice during postnatal development, but that these mice underwent demyelination at later stages, after *Npc1* deletion at 6 weeks. Late stage demyelination in *Npc1*$^{flox/-}$, *Cre-ER*$^{TM+}$ mice could be secondary to axonal loss, as evidenced by decreased neurofilament levels in these mice **(Figure 3.1B)**. Taken together, our analysis suggests that lack of myelin in NPC mice is caused by dysmyelination at early postnatal days, followed by demyelination at end stage.

Figure 3.1 The effect of timing of *Npc1* deletion on CNS myelination.
(A) MBP immunofluorescence in brain midline sagittal sections of 7-week-old WT (top), 7-week-old *Npc1*$^{\Delta/-}$ (middle), and 22-week-old *Npc1*$^{flox/-}$, *Cre-ER*$^{TM+}$ mice following tamoxifen injections at 6 weeks (bottom). Bar, 1mm. **(B)** Western blots of CNP, MBP, MAG and NF-200 expression levels from cerebral cortex homogenates of 22-week-old *Npc1*$^{flox/-}$, *Cre-ER*$^{TM+}$ mice and their littermate controls following tamoxifen injections at 6 weeks. GAPDH controls for loading.

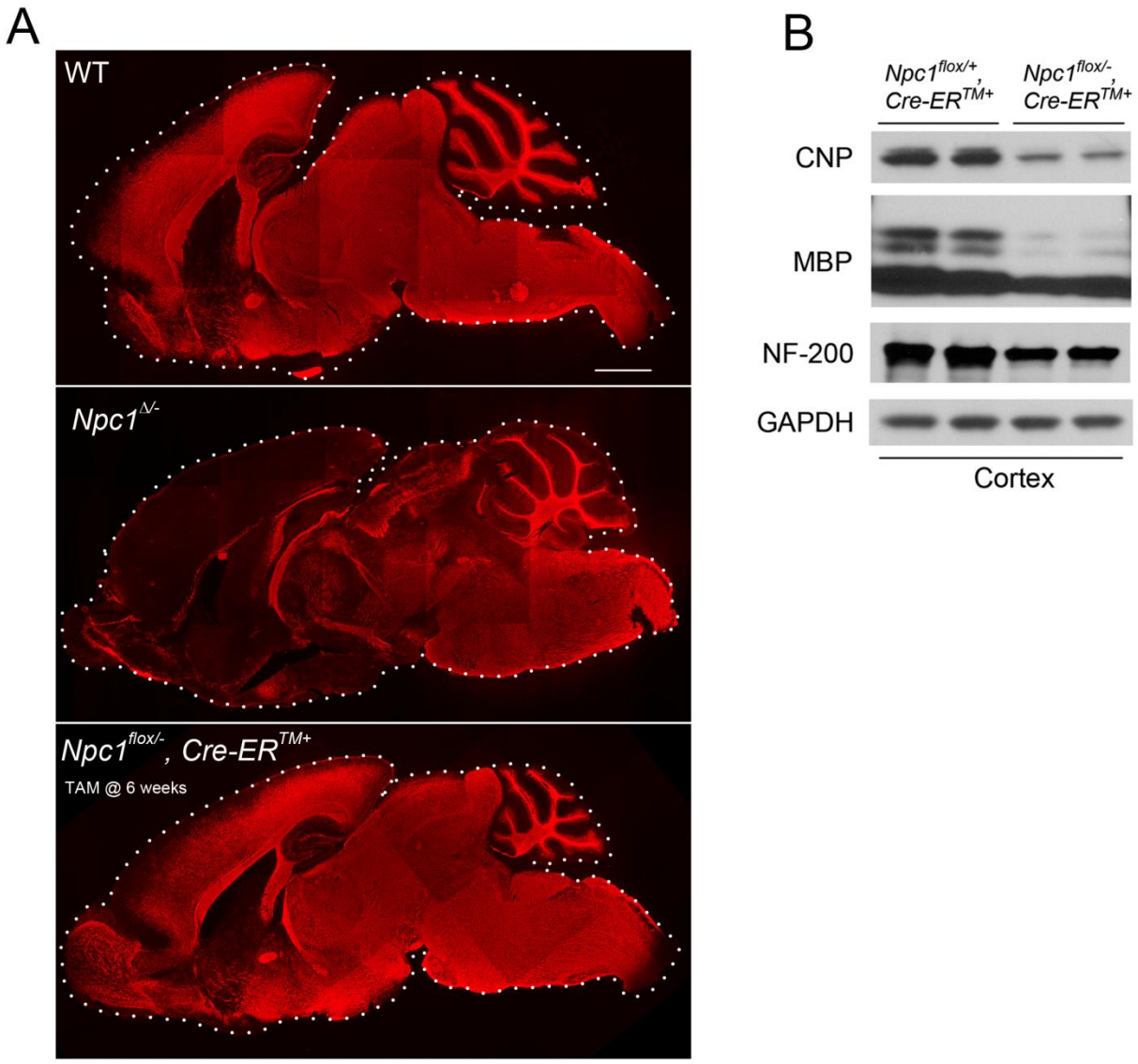

3.3.2 Neuronal deletion of Npc1 leads to blockade of oligodendrocyte maturation and dysmyelination.

We next sought to dissect the contribution of different CNS cell types to NPC dysmyelination. We started by deleting *Npc1* specifically in neurons, using transgenic mice expressing Cre recombinase under the control of the Synapsin1 promoter (*Syn1-Cre*) (Zhu et al., 2001). We confirmed gene deletion by staining brain sections with filipin, a fluorescent dye that specifically marks accumulation of unesterified cholesterol (Bornig and Geyer, 1974). NeuN and filipin co-staining verified that $Npc1^{flox/-}$, $Syn1\text{-}Cre^{+}$ mice, but not $Npc1^{flox/+}$, $Syn1\text{-}Cre^{+}$ controls (Yu et al., 2011), developed widespread filipin-positive neurons throughout the brain, including brainstem and cortex **(Figure 3.2A)**. To further verify neuron-specific gene deletion, $Syn1\text{-}Cre^{+}$ mice were crossed to a Rosa reporter line that has been widely used to demonstrate gene deletion in both neurons and oligodendrocytes (Soriano, 1999). LacZ staining revealed widespread positive cells in many brain regions including the cortex, with minimal staining in the corpus callosum, where neuronal cell bodies are lacking **(Figure 3.2B)**. Co-staining with NeuN or Olig2 showed that these LacZ positive cells were neurons, and not oligodendrocyte lineage cells **(Figure 3.2C)**, further supporting the notion that we achieved neuron-specific deletion by using $Syn1\text{-}Cre^{+}$ mice.

Figure 3.2 Neuron-specific gene deletion in *Syn1-Cre* mice.
(A) Filipin and NeuN co-staining identifies the accumulation of unesterified cholesterol in neurons of 7-week-old *Npc1*$^{flox/-}$, *Syn1-Cre*$^{+}$ mice. Shown are representative images of brainstem (top) and cortex (bottom). Bar, 100 µm. **(B, C)** *Syn1-Cre*$^{+}$ mice were crossed to Rosa reporter mice and LacZ staining was performed as a readout for Cre-mediated recombination. (B) LacZ positive cells are abundant in the cortex but are lacking in the corpus callosum (highlighted by black dots; CC). Bars, 25 µm. (C) Co-staining with NeuN or Olig2 identifies LacZ positive cells as neurons, but not oligodendrocyte lineage cells. Shown are representative images of brainstem (top) and cortex (bottom). Bar, 200 µm.

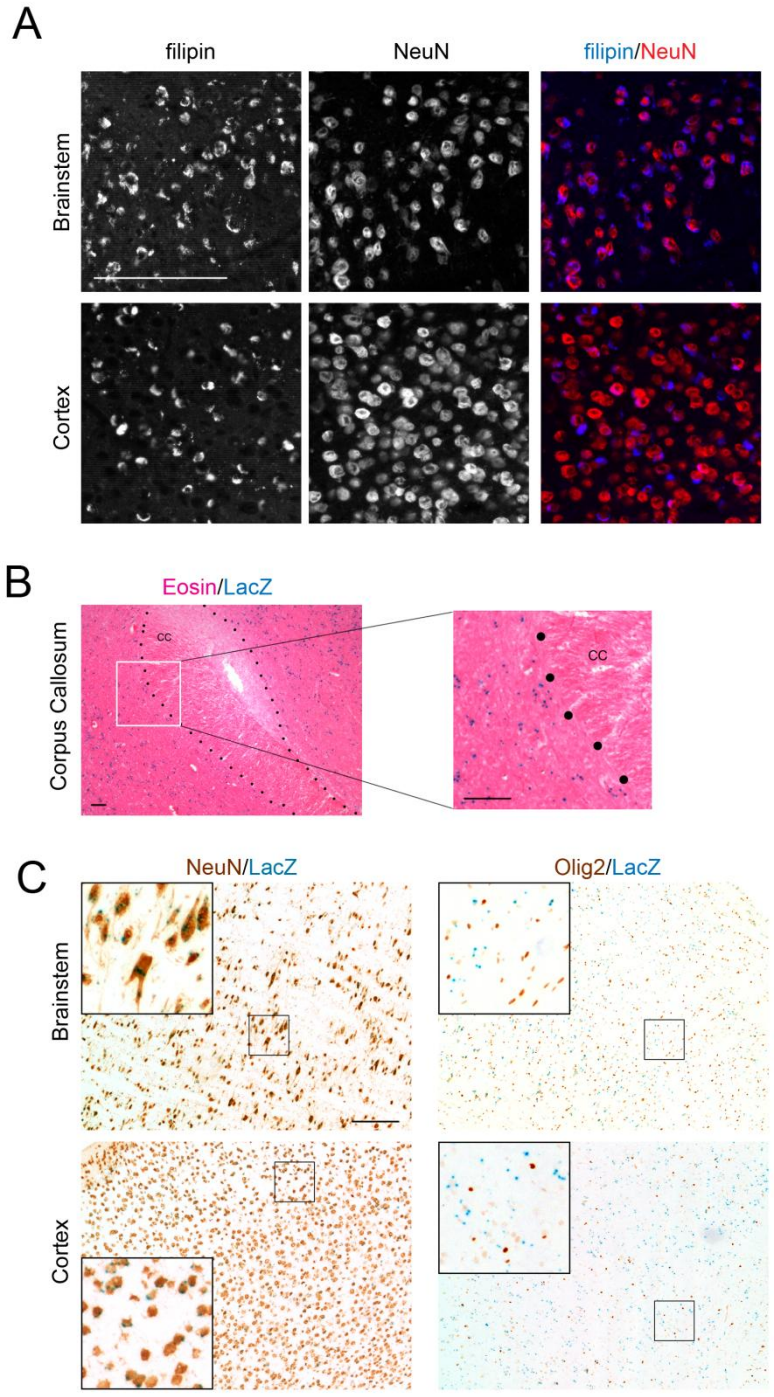

The effect of *Npc1* deficiency in neurons upon myelination was first evaluated by MBP immunofluorescence at 3 different ages. At postnatal day 16 (P16), myelination was actively occurring in the forebrain of $Npc1^{flox/+}$, $Syn1\text{-}Cre^{+}$ controls, with abundant MBP-positive myelinating oligodendrocytes populating the cortex **(Figure 3.3B)**. In contrast, $Npc1^{flox/-}$, $Syn1\text{-}Cre^{+}$ mutants exhibited a severe paucity of myelin in the same region, with most of the MBP positive cells exhibiting the morphology of pre-myelinating oligodendrocytes **(Figure 3.3B)**. At 7 weeks, myelination was completed in $Npc1^{flox/+}$, $Syn1\text{-}Cre^{+}$ controls, but was greatly attenuated in the cortex of $Npc1^{flox/-}$, $Syn1\text{-}Cre^{+}$ mutants. No recovery of myelination was observed in mutants aged to 16 weeks **(Figure 3.3B)**, which is end stage for these mice (Yu et al., 2011). Although MBP staining was markedly decreased in the cortex of $Npc1^{flox/-}$, $Syn1\text{-}Cre^{+}$ mutants, other brain regions exhibited a normal staining pattern, reminiscent of the selective defects in myelination observed after global germline deletion **(Figure 3.1A)**. Regional-specific dysmyelination was further supported by western blots showing decreased levels of myelin-specific proteins including CNP, MBP and MAG in cortex, but not brainstem of $Npc1^{flox/-}$, $Syn1\text{-}Cre^{+}$ mutants **(Figure 3.3C)**. Electron microscopy confirmed that the density of myelinated nerve fibers in the corpus callosum was greatly reduced in $Npc1^{flox/-}$, $Syn1\text{-}Cre^{+}$ mutants at 3 weeks **(Figure 3.3E)**. Notably, neurofilament protein levels in the cortex were similar between $Npc1^{flox/+}$, $Syn1\text{-}Cre^{+}$ controls and $Npc1^{flox/-}$, $Syn1\text{-}Cre^{+}$ mutants at P16 **(Figure 3.3C)**, and neurofilament immnunofluorescence staining showed no significant axonal pathology **(Figure 3.3D)**. These data indicate that dysmyelination in the forebrain of $Npc1^{flox/-}$, $Syn1\text{-}Cre^{+}$ mutants was not secondary to axonal loss.

Figure 3.3 Forebrain dysmyelination in mice following neuron-specific deletion of *Npc1*. **(A)** Schematic of midline sagittal section of the mouse brain, with the area shown in panel B highlighted by the black rectangle. Illustration is from *www.gensat.org.* **(B)** MBP immunofluorescence in forebrain sagittal sections of *Npc1$^{flox/-}$, Syn1-Cre^{+}* and control mice at P16, and at 7 & 16 weeks. Bar, 500 µm. **(C)** Western blots of myelin-specific proteins and NF-200 from brainstem and cerebral cortex homogenates of P16 *Npc1$^{flox/-}$, Syn1-Cre^{+}* mice and controls. GAPDH controls for loading. **(D)** MBP and NF co-staining of P16 *Npc1$^{flox/-}$, Syn1-Cre^{+}* and littermate control mice. Ctx, cortex; CC, corpus callosum; Hp, hippocampus. Bar, 200 µm. **(E)** Electron microscopy of the corpus callosum of P16 *Npc1$^{flox/-}$, Syn1-Cre* and control mice. Bar, 500 nm.

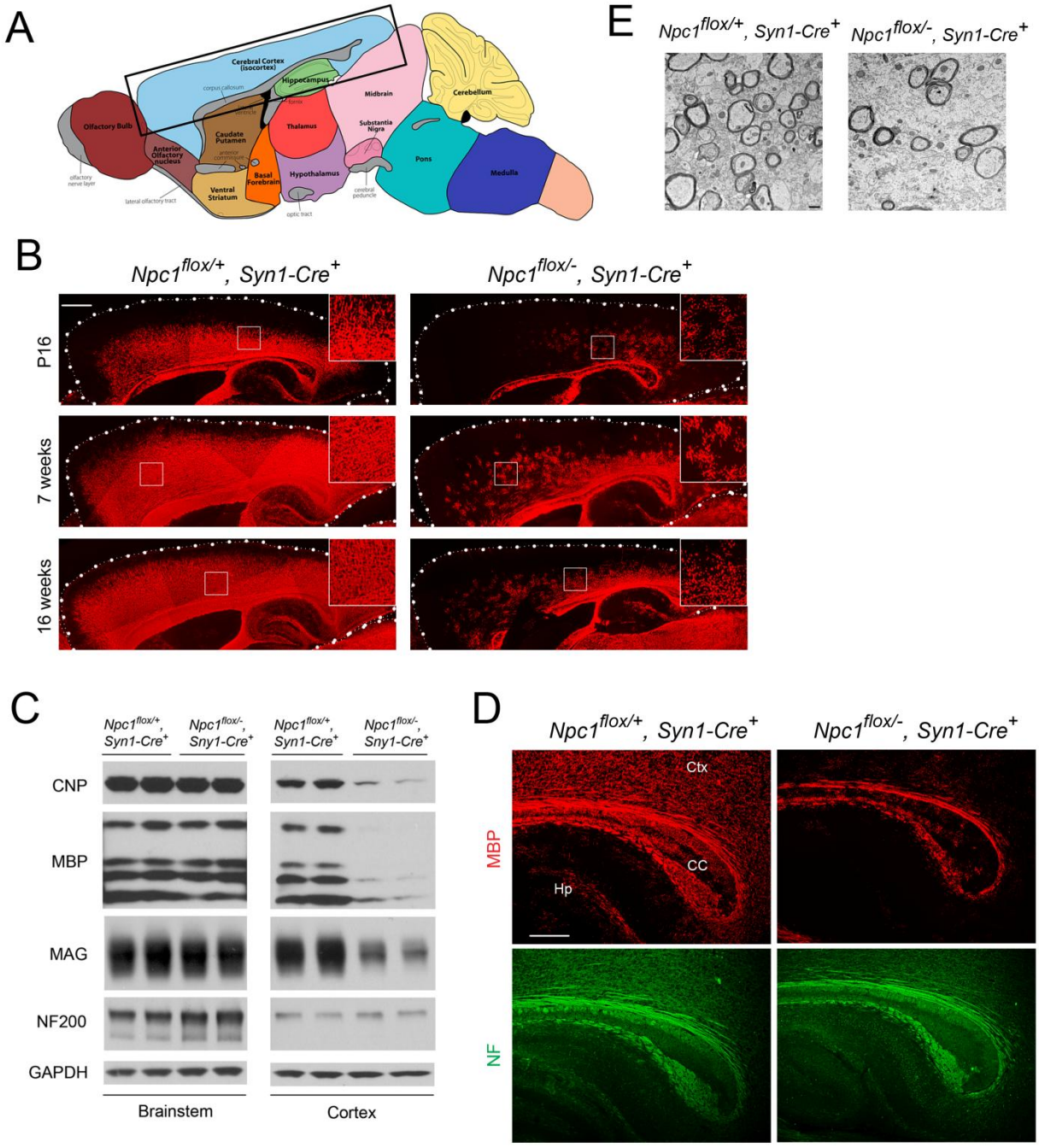

To characterize the mechanism underlying dysmyelination in *Npc1$^{flox/-}$, Syn1-Cre^{+}* mutants, we assessed oligodendrocyte lineage cells at different stages of differentiation. At P16, *Npc1$^{flox/-}$, Syn1-Cre^{+}* mutants showed a significantly reduced number of CC1-positive mature oligodendrocytes in the forebrain **(Figure 3.4A, C)** but a normal density of NG2-positive oligodendrocyte precursor cells (OPCs) **(Figure 3.4A, B)**. As previously reported for global null *Npc1* mutants (Takikita et al., 2004), this deficit of mature oligodendrocytes was not associated with evidence of increased apoptosis (data not shown). The paucity of mature oligodendrocytes was associated with a reduced number of cells in the corpus callosum expressing Sip1, a signaling protein implicated oligodendrocyte differentiation **(Figure 3.4D)** (Weng et al., 2012). These data indicated that *Npc1* deficiency in neurons triggered a block of oligodendrocyte maturation, and prompted us to determine whether signals known to regulate oligodendrocyte maturation and myelination were perturbed in *Npc1$^{flox/-}$, Syn1-Cre^{+}* mutants. We first examined proteins that mediate signaling between axons and oligodendrocyte lineage cells including PSA-NCAM (Charles et al., 2000), Lingo1 (Lee et al., 2007) and Jagged1 (Wang et al., 1998), and found no differences between *Npc1$^{flox/-}$, Syn1-Cre^{+}* mutants and controls at P16 **(Figure 3.5A)**. Similarly, we found no evidence of astrocyte activation in Npc1 mutants **(Figure 3.5B, C)**. In contrast, activity of the non-receptor tyrosine kinase Fyn (Umemori et al., 1994) was reduced in the cortex of *Npc1$^{flox/-}$, Syn1-Cre^{+}* mutants, as evidenced by decreased levels of the active form (phosphorylated at tyrosine 420) and concurrently increased levels of the inactive form (phosphorylated at tyrosine 531) **(Figure 3.4E)**. As oligodendroglial Fyn is an integrator of axonal signals that promote myelination (Kramer-Albers and White, 2011), the decreased activity of Fyn in *Npc1$^{flox/-}$, Syn1-Cre^{+}* mutants suggests that *Npc1* deficiency in axons leads to a

disruption of axon-glial signaling that is crucial for oligodendrocyte differentiation and myelination.

Figure 3.4 Neuron-specific deletion of *Npc1* leads to blockade of oligodendrocyte maturation.
(A) NG2 and CC1 co-staining in the corpus callosum of a P16 *Npc1*$^{flox/-}$, *Syn1-Cre*$^{+}$ and control mice. Bar, 200 μm. **(B)** Western blot of NG2 expression levels from cerebral cortex homogenates of P16 *Npc1*$^{flox/-}$, *Syn1-Cre*$^{+}$ mice and controls. GAPDH controls for loading. **(C)** Quantification of CC1^{+} cell number in the corpus callosum of P16 *Npc1*$^{flox/-}$, *Syn1-Cre*$^{+}$ mice and controls. Data are mean +/- SD. *** *P*<0.001. **(D)** Sip1 and CC1 co-staining in the corpus callosum of a P16 *Npc1*$^{flox/-}$, *Syn1-Cre*$^{+}$ and control mice. Ctx, cortex; CC, corpus callosum; Hp, hippocampus. Bar, 100 μm. **(E)** Cerebral cortex homogenates of P16 control (lane 1) and *Npc1*$^{flox/-}$, *Syn1-Cre*$^{+}$ mice (lane 2) were subject to immunoprecipitation with an anti-Fyn antibody. The resulting lysates were probed for total Fyn, and for Fyn phosphorylated at tyrosine 420 (active form) or tyrosine 531 (inactive form).

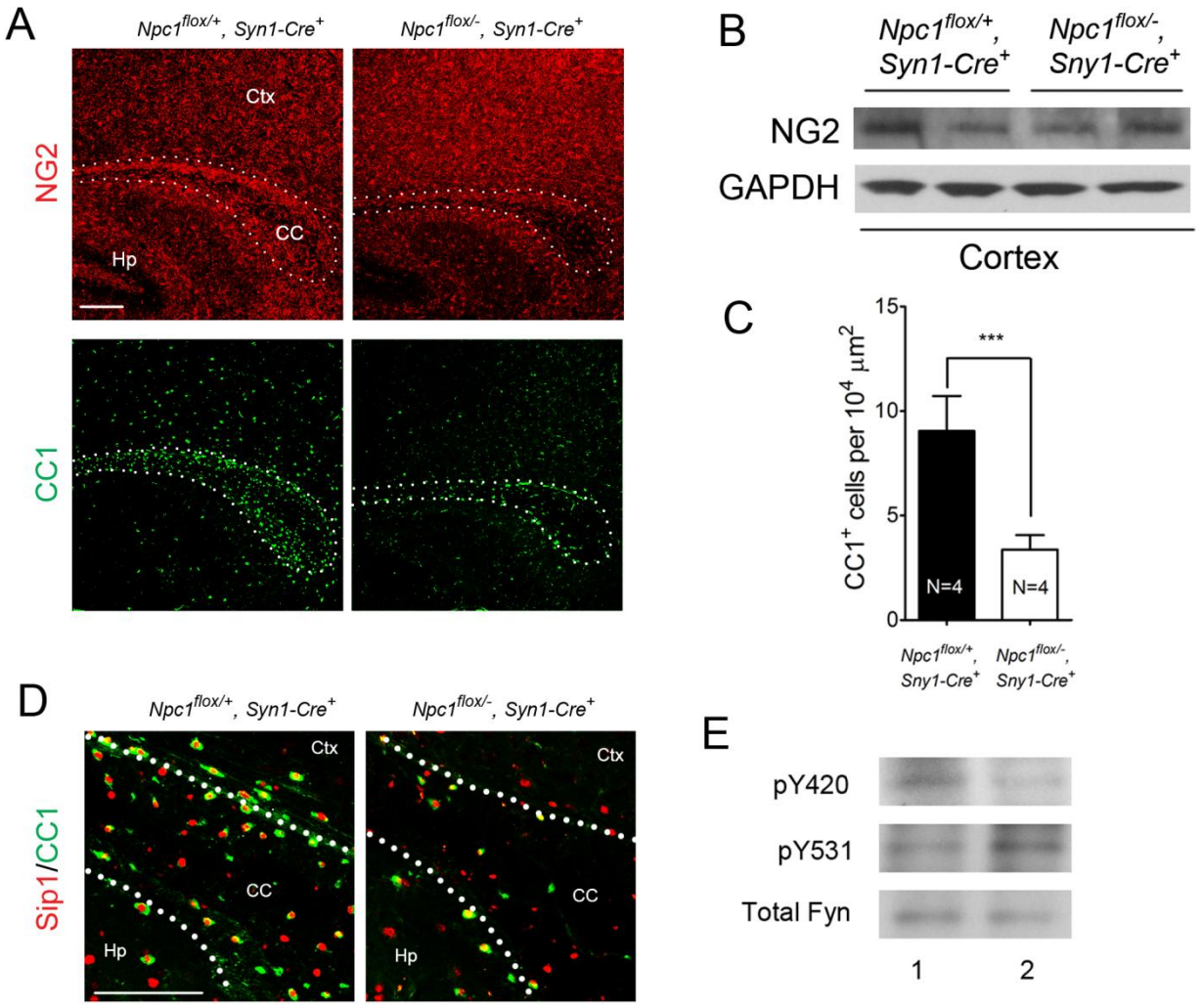

Figure 3.5 No evidence for changes in several axon-glial signaling pathways or induction of reactive gliosis following neuron-specific *Npc1* deletion.
(A) Western blots of PSA-NCAM, Lingo1, and Jagged1 from brainstem and cerebral cortex homogenates of P16 *Npc1*$^{flox/-}$, *Syn1-Cre*$^{+}$ mice and controls. GAPDH controls for loading. **(B, C)** GFAP immunofluorescence (B) and western blots (C) show no evidence for reactive gliosis in the brainstem and cortex of P16 *Npc1*$^{flox/-}$, *Syn1-Cre*$^{+}$ mutants and controls. Hsp90 controls for loading. Bar, 200 μm.

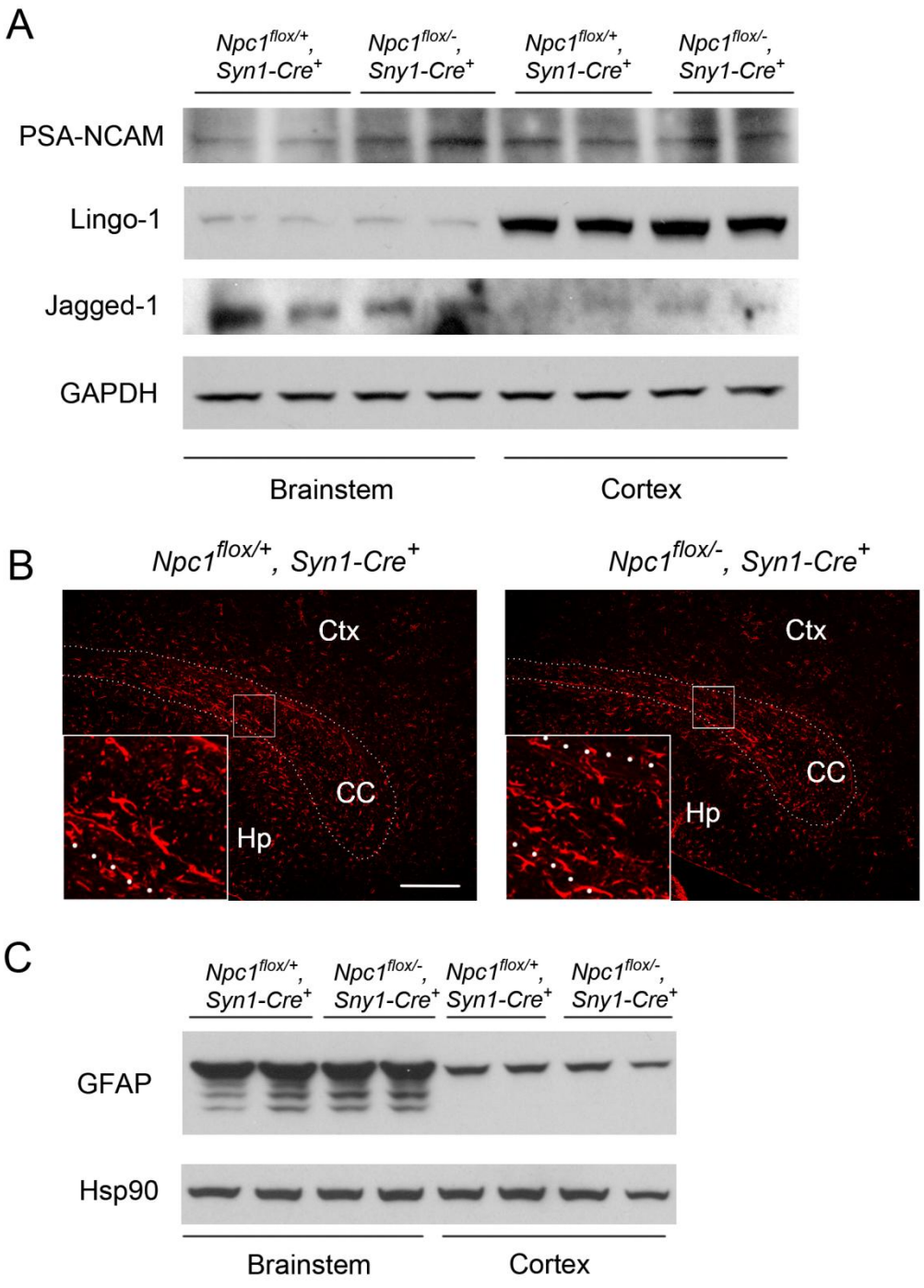

3.3.3 Oligodendrocyte deletion of *Npc1* results in a similar, but milder dysmyelination phenotype during postnatal development.

Next, we tested if *Npc1* deficiency in oligodendrocyte lineage cells contributes to the pathogenesis of dysmyelination in NPC mice. To accomplish this, we used transgenic mice expressing Cre recombinase under the control of the CNP promoter (*CNP* $^{Cre/+}$) (Lappe-Siefke et al., 2003). In these mice, Cre is abundantly and specifically expressed in postmitotic oligodendrocytes. Co-staining for Cre and Olig2 verified that Cre was specifically expressed in a subset of Olig2^{+} oligodendrocyte lineage cells in various brain regions including brainstem and cortex **(Figure 3.6B)**. Filipin staining revealed minimal accumulation of unesterified cholesterol in *Npc1*$^{flox/-}$, *CNP*$^{Cre/+}$ mutants **(Figure 3.6A)**, a finding both consistent with a previous report showing no detectable cholesterol accumulation in oligodendrocytes of *Npc1*$^{-/-}$ mice (Liao et al., 2009) and indicative of the cellular specificity of this Cre line.

Figure 3.6 Oligodendrocyte-specific gene deletion by *CNP*$^{Cre/+}$.

(A) Filipin and NeuN co-staining shows lack of accumulation of unesterified cholesterol in neurons of 7-week-old *Npc1*$^{flox/-}$, *CNP*$^{Cre/+}$ mice, with detection of only rare filipin-positive cortical neurons. Shown are representative images of brainstem (top) and cortex (bottom). Bar, 100 μm. **(B)** Cre and Olig2 co-staining identifies expression of Cre in a subset of oligodendrocyte lineage cells in a P16 *Npc1*$^{flox/+}$, *CNP*$^{Cre/+}$ mouse. Shown are representative images of brainstem (top) and cortex (bottom). Bar, 100 μm. **(C)** Western blots demonstrate expression of Cre in both brainstem and cortex in *Npc1*$^{flox/-}$, *CNP*$^{Cre/+}$ mice and their littermate controls at P16. Hsp90 controls for loading.

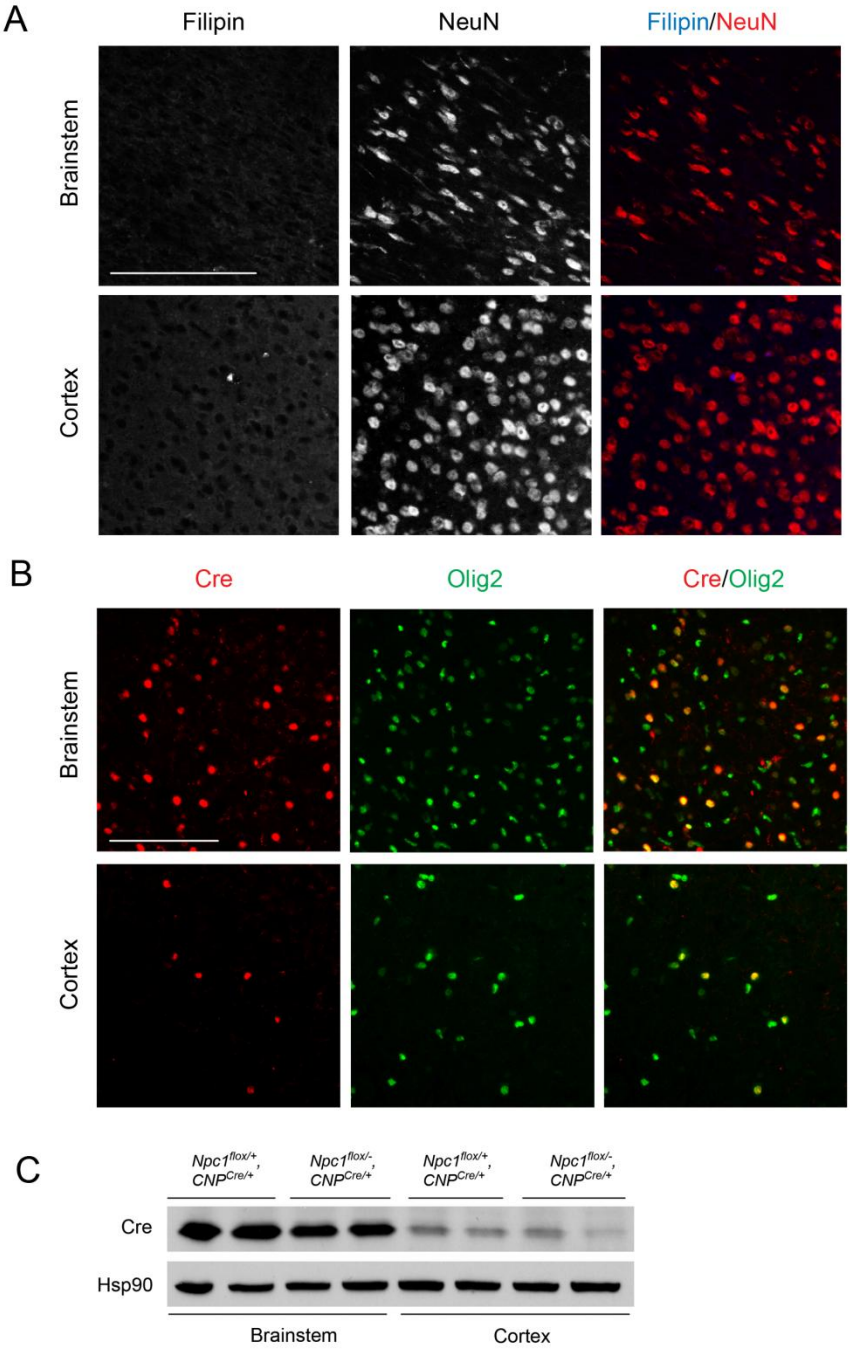

Deletion of *Npc1* in oligodendrocytes resulted in a dysmyelination phenotype that was initially similar to that caused by *Npc1* deletion in neurons. At P16, $Npc1^{flox/-}$, $CNP^{Cre/+}$ mutants expressed markedly reduced levels of myelin-specific proteins including MBP, CNP and MAG in the cortex **(Figure 3.7A, B)**. This dysmyelination phenotype partially recovered by 7 weeks **(Figure 3.7A)**, a finding that indicates oligodendrocyte deletion delayed myelination and contrasts with the block produced by neuronal deletion. Myelination in the brainstem of $Npc1^{flox/-}$, $CNP^{Cre/+}$ mutants was minimally affected **(Figure 3.7B)** despite robust Cre expression in this region **(Figure 3.6B, C)**. Electron microscopy confirmed diminished density of myelinated nerve fibers in the corpus callosum of $Npc1^{flox/-}$, $CNP^{Cre/+}$ mutants at 3 weeks **(Figure 3.7D)**. Similar to neuron-specific mutants, dysmyelination in $Npc1^{flox/-}$, $CNP^{Cre/+}$ mutants occurred without significant axonal pathology **(Figure 3.7B, C)**. The requirement of Npc1 in oligodendrocytes for proper myelination was further confirmed by using an independent line in which Cre was highly expressed in OPCs ($Olig2^{Cre/+}$ mice, **Figure 3.8**) (Schuller et al., 2008). Similar to $Npc1^{flox/-}$, $Syn1\text{-}Cre^{+}$ mutants, $Npc1^{flox/-}$, $CNP^{Cre/+}$ mutants at P16 showed reduced density of mature oligodendrocytes **(Figure 3.9A, C)**, with normal numbers of OPCs in the forebrain **(Figure 3.9A, B)**, indicating arrest of oligodendrocyte maturation.

Figure 3.7 Forebrain dysmyelination in mice with oligodendrocyte-specific deletion of *Npc1*.

(A) MBP immunofluorescence in forebrain sagittal sections of *Npc1*$^{flox/-}$, *CNP*$^{Cre/+}$ mice and controls at P16 and 7 weeks. Bar, 500 μm. **(B)** Western blots of myelin-specific proteins and NF-200 from brainstem and cerebral cortex homogenates of P16 *Npc1*$^{flox/-}$, *CNP*$^{Cre/+}$ mice and controls. GAPDH controls for loading. **(C)** MBP and NF co-staining in the corpus callosum of P16 *Npc1*$^{flox/-}$, *CNP*$^{Cre/+}$ and control mice. Ctx, cortex; CC, corpus callosum; Hp, hippocampus. Bar, 200 μm. **(D)** Electron microscopy of the corpus callosum of a P16 *Npc1*$^{flox/-}$, *CNP*$^{Cre/+}$ and control mice. Bar, 50 nm.

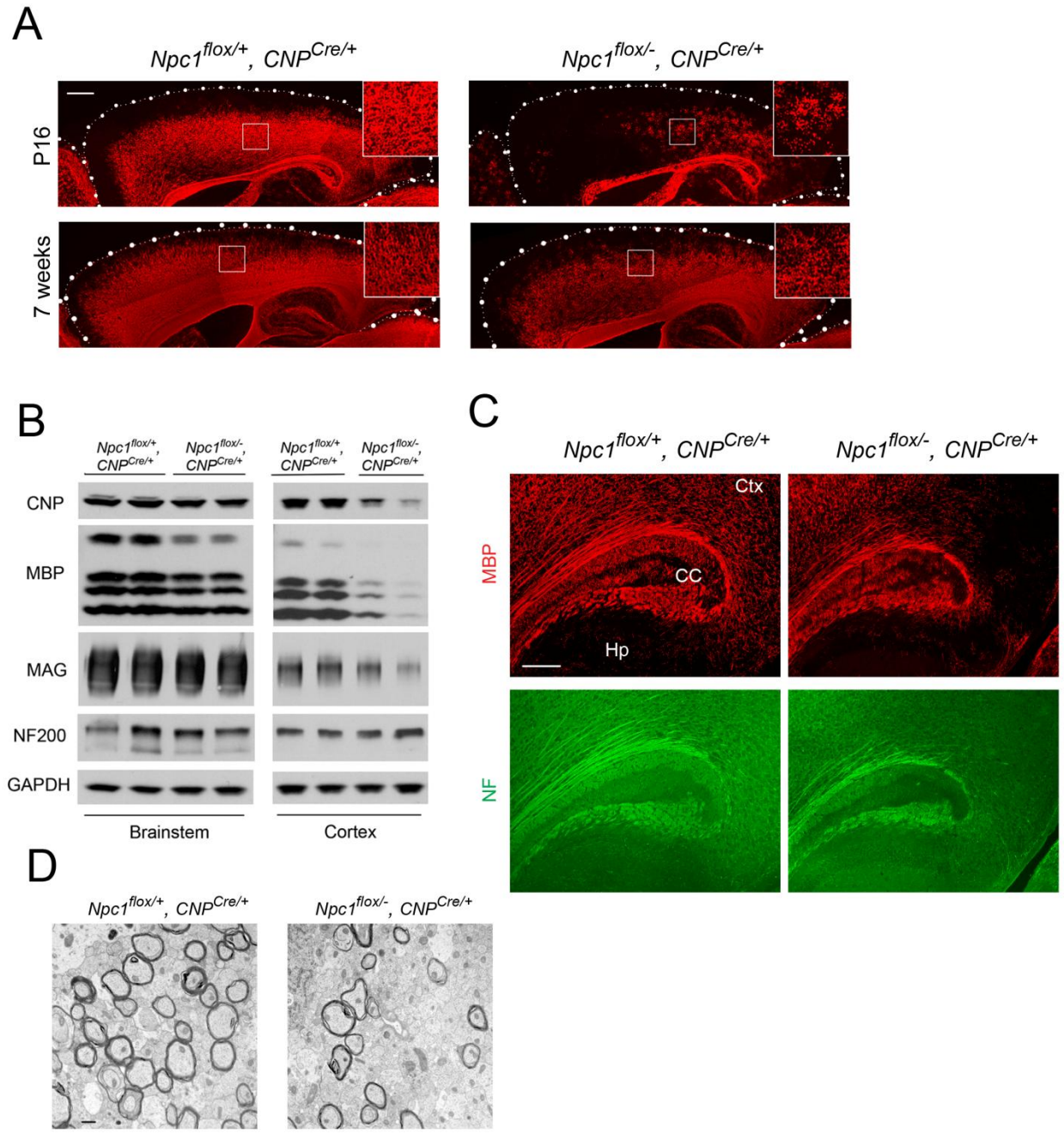

Figure 3.8 Deletion of *Npc1* in OPC by *Olig2*$^{Cre/+}$ results in a similar dysmyelination phenotype

(A) MBP immunofluorescence in forebrain sagittal sections of *Npc1*$^{flox/-}$, *Olig2*$^{Cre/+}$ and control mice at P16. Bar, 1 mm. **(B)** Western blots of myelin-specific proteins from cerebral cortex homogenates of P16 *Npc1*$^{flox/-}$, *Olig2*$^{Cre/+}$ mice and controls. GAPDH controls for loading.

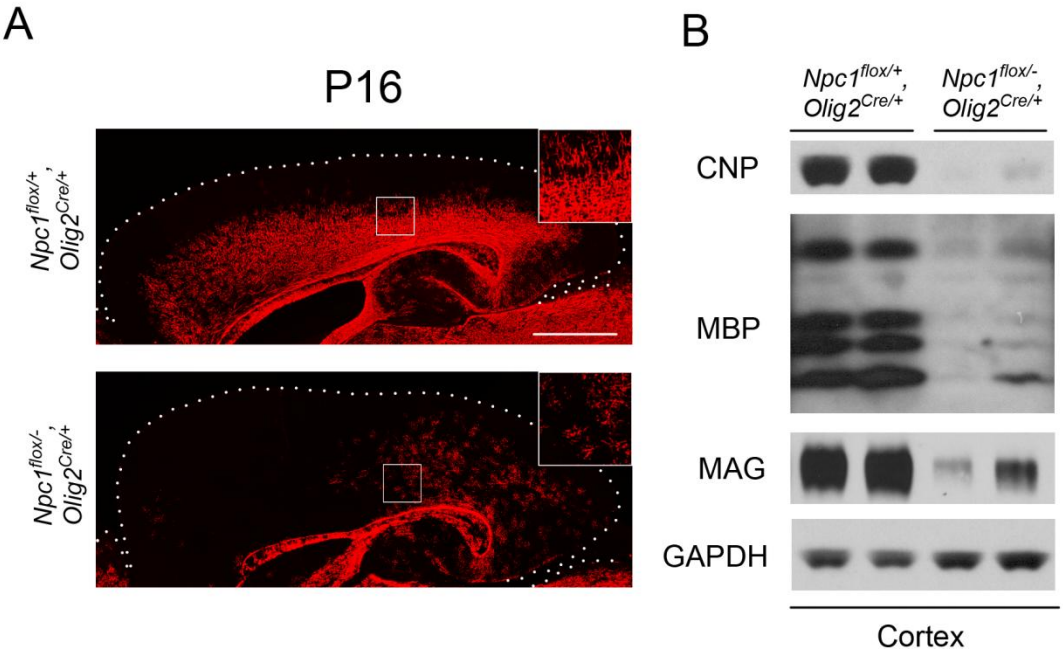

Figure 3.9 Oligodendrocyte-specific deletion of *Npc1* leads to blockade of oligodendrocyte maturation.

(A) NG2 and CC1 co-staining in the corpus callosum of P16 *Npc1*$^{flox/-}$, *CNP*$^{Cre/+}$ and control mice. Ctx, cortex; CC, corpus callosum; Hp, hippocampus. Bar, 200 μm. **(B)** Western blot of NG2 expression levels from cerebral cortex homogenates of P16 *Npc1*$^{flox/-}$, *CNP*$^{Cre/+}$ mice and controls. GAPDH controls for loading. **(C)** Quantification of CC1^{+} cell number in the corpus callosum of P16 *Npc1*$^{flox/-}$, *CNP*$^{Cre/+}$ mice and controls. Data are mean +/- SD. * P<0.05.

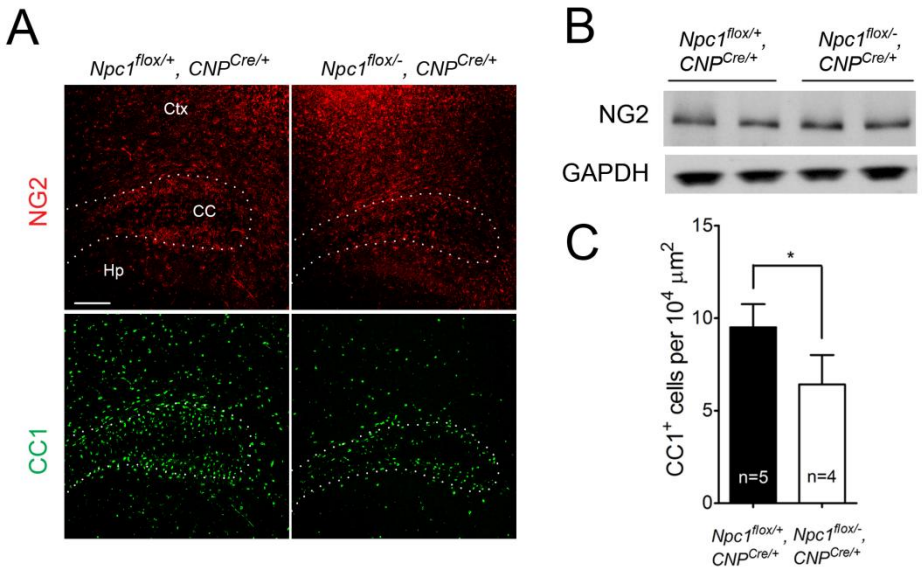

3.3.4 Mice with *Npc1* deletion in oligodendrocytes develop demyelination in late stages.

As the *Npc1*$^{flox/-}$, *CNP*$^{Cre/+}$ mutants aged, they developed progressive motor deficits **(Figure 3.10C)**, although weight was not affected **(Figure 3.10A, B)**. This led us to examine myelin levels in 23-week-old *Npc1*$^{flox/-}$, *CNP*$^{Cre/+}$ mutants. We found decreased levels of myelin proteins not only in cortex, but also in brainstem and cerebellum **(Figure 3.11A)**, where myelination in early postnatal days was nearly normal **(Figure 3.7B)**. This indicated that widespread demyelination was taking place in aged *Npc1*$^{flox/-}$, *CNP*$^{Cre/+}$ mutants. We found this was associated with only mild changes in the pattern of MBP staining **(Figure 3.11B)**. Interestingly, the total number of oligodendrocytes in the cerebellar white matter was unchanged in aged mutants **(Figure 3.11C, D)**, suggesting that loss of Npc1 did not affect the survival of oligodendrocytes in adult mice. This demyelination was associated with secondary neuron loss in the cerebellum. We detected Purkinje cell loss in anterior lobules of 23-week-old but not 7-week-old *Npc1*$^{flox/-}$, *CNP*$^{Cre/+}$ mutants, as demonstrated by calbindin staining of sagittal midline sections **(Figure 3.11E, G)** and by loss of calbindin staining on western blot **(Figure 3.11F)**. We conclude that Npc1 acts in oligodendrocytes both to promote normal myelination and to ensure the maintenance of myelin in the adult CNS.

Figure 3.10 Phenotype of mice following oligodendrocyte-specific deletion of *Npc1*.
(A, B) Weight curves for male **(A)** and female **(B)** mice. Data are mean +/- SD. **(C)** Age-dependent performance on balance beam. Data are mean +/- SD. * p<0.05, *** p<0.001.

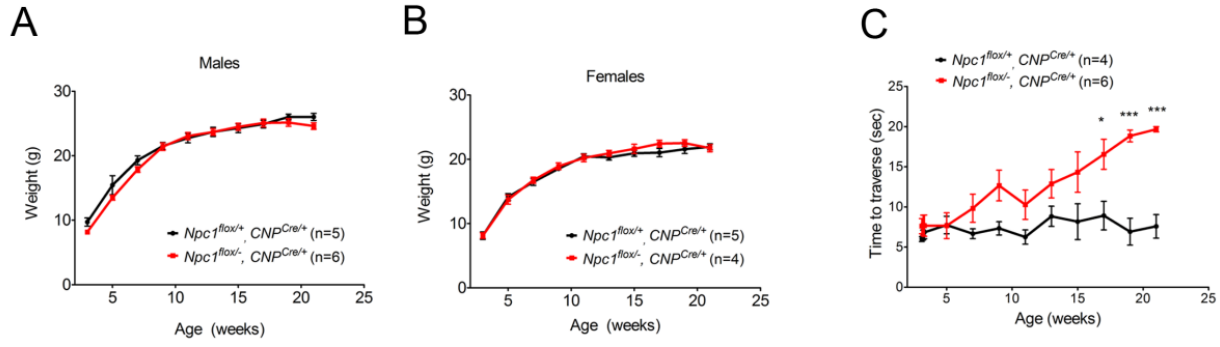

Figure 3.11 Wide-spread demyelination and Purkinje cell degeneration in aged mice with oligodendrocyte-specific deletion of *Npc1*.
(A) Western blots of myelin-specific proteins from brainstem, cerebral cortex and cerebellar homogenates of 23-week-old *Npc1*$^{flox/-}$, *CNP*$^{Cre/+}$ mice and controls. GAPDH controls for loading. **(B)** MBP immunofluorescence in cerebellar lobules III-VI of *Npc1*$^{flox/-}$, *CNP*$^{Cre/+}$ and control mice at 7 & 23 weeks. Bar, 500 μm. **(C, D)** (C) Olig2 immunofluorescence in the cerebellar white matter of *Npc1*$^{flox/-}$, *CNP*$^{Cre/+}$ mice and controls at 23 weeks. Schematic is shown on the left. Quantification of Olig2^{+} cell number is shown in (D). Data are mean +/- SD. n.s., not significant. Bar, 200 μm. **(E)** Calbindin immunofluorescence in the cerebellum of *Npc1*$^{flox/-}$, *CNP*$^{Cre/+}$ mice and controls at 7 & 23 weeks. Roman numerals indicate cerebellar lobules. Bar, 500 μm. **(F)** Western blots of calbindin from cerebellar homogenates of *Npc1*$^{flox/-}$, *CNP*$^{Cre/+}$ mice and controls at 7 & 23 weeks. GAPDH controls for loading. **(G)** Quantification of Purkinje cell density in midline cerebellar lobules at 23 weeks. Data are mean +/- SD. * $p<0.05$, ** $p<0.01$, *** $p<0.001$, n.s., not significant.

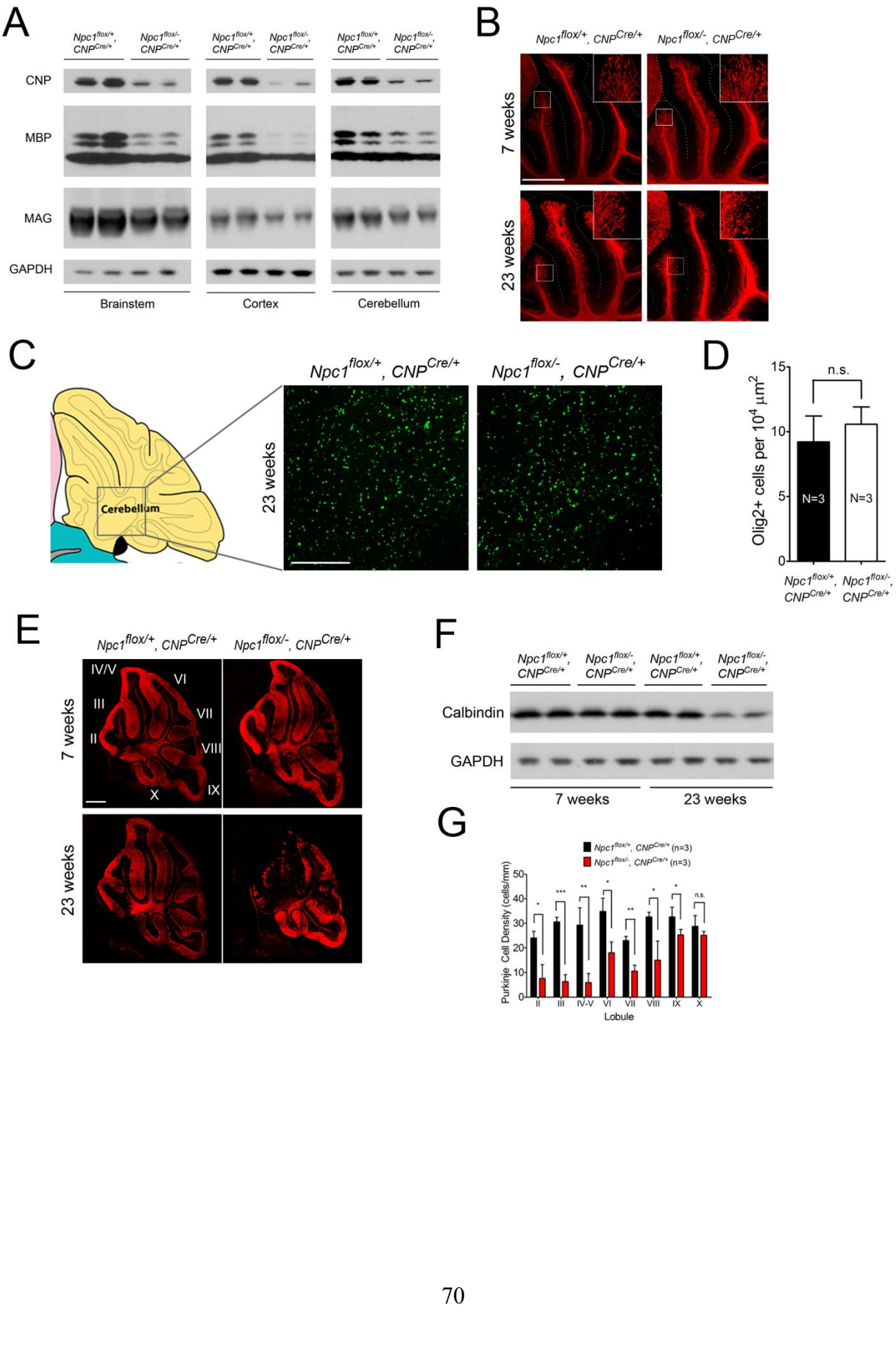
A
Npc1flox/+, CNPCre/+
Npc1flox/-, CNPCre/+
CNP
MBP
MAG
GAPDH
Brainstem
Cortex
Cerebellum
B
Npc1flox/+, CNPCre/+
Npc1flox/-, CNPCre/+
7 weeks
23 weeks
C
Npc1flox/+, CNPCre/+
Npc1flox/-, CNPCre/+
Cerebellum
23 weeks
D
n.s.
Olig2+ cells per 10^4 µm^2
N=3
N=3
E
Npc1flox/+, CNPCre/+
Npc1flox/-, CNPCre/+
7 weeks
23 weeks
IV/V
VI
III
VII
II
VIII
X
IX
F
Calbindin
GAPDH
7 weeks
23 weeks
G
Npc1flox/+, CNPCre/+ (n=3)
Npc1flox/-, CNPCre/+ (n=3)
Purkinje Cell Density (cells/mm)
Lobule
II
III
IV-V
VI
VII
VIII
IX
X
n.s.

3.4 Discussion

Here we used *Npc1* conditional null mice to establish the critical role of Npc1 in both neurons and oligodendrocytes for proper CNS myelination. Our findings demonstrate that deletion of *Npc1* in neurons alone is sufficient to recapitulate the dysmyelination phenotype that occurs following global germline deletion. These mice display a severe phenotype, particularly in the forebrain, characterized by a lack of mature oligodendrocytes but a normal density of OPCs, indicating that *Npc1* deficiency in neurons triggers an arrest of oligodendrocyte maturation. Our data also demonstrate that deletion of *Npc1* in oligodendrocytes leads to similar but milder forebrain dysmyelination that largely recovers by 7 weeks, consistent with a delay rather than a block in myelination. Furthermore, we demonstrate that these oligodendrocyte-specific mutants develop ataxia as they age, and that this is associated with widespread demyelination and Purkinje cell loss in anterior cerebellar lobules, establishing the occurrence of secondary neurodegeneration. Our results highlight the importance of Npc1 in both neurons and oligodendrocytes for the formation and maintenance of CNS myelin.

Oligodendrocyte differentiation and myelination is a highly dynamic process controlled by both intrinsic factors and extrinsic mechanisms (Emery, 2010). Recent studies of axon-glial communication have identified a series of axonal signals important for regulating myelination. Oligodendroglial Fyn, a Src family kinase, has been suggested to play a central role in integrating diverse axonal signals to initiate myelination (Kramer-Albers and White, 2011). Downstream signaling from activated Fyn kinase promotes oligodendrocyte survival, alters cytoskeleton polarity and increases the expression of myelin genes. Our analysis of neuron-specific *Npc1* mutants reveals decreased Fyn activity, and a regionally-restricted dysmyelination phenotype similar to that of Fyn knockout mice (Sperber et al., 2001). We suggest that *Npc1*

deficiency in neurons disrupts an axon-glial signal vital for promoting myelination. The axonal ligand responsible for oligodendroglial Fyn activation remains elusive. The requirement of Npc1 for Fyn activation raises the possibility that a lipid species, such as cholesterol or a sphingolipid, may contribute to this signal. Additionally, recent neuron-glial co-culture studies demonstrate the role of action potentials in stimulating myelination through Fyn-dependent mechanisms (Wake et al., 2011). It is therefore also possible that defective Fyn activation results from decreased electrical activity of axons in *Npc1*$^{flox/-}$*; Syn1-Cre*$^{+}$ mutants. Animal studies of cholesterol metabolism in myelinating glia have highlighted the importance of cell-autonomous production of cholesterol for myelin formation. Mice lacking oligodendroglial squalene synthase, an enzyme required for cholesterol synthesis, exhibit perturbed CNS myelination in early postnatal days (Saher et al., 2005). Similarly, deletion of SCAP (SREBP-cleavage-activating protein) in Schwann cells, a protein that complexes with SREBP to regulate the expression of genes promoting cholesterol synthesis and lipoprotein uptake, leads to PNS hypomyelination (Verheijen et al., 2009). It is notable that both mouse models partially recover at later stages, suggesting that myelinating glia have the capacity to overcome the lack of endogenous cholesterol production, probably through increased uptake. Here we present *in vivo* evidence indicating an important contribution of exogenous cholesterol to myelin synthesis. Our findings show that deletion of *Npc1* in oligodendrocytes, which eliminates their utilization of cholesterol from the endocytosis of LDL or similar lipoprotein particles, leads to perturbed myelin formation in the CNS. Although Npc1 deficiency also impairs intracellular trafficking of sphingolipids, the blockade of exogenous cholesterol utilization and the essential role that cholesterol plays in myelination leads us to conclude that the effects observed here are due to a disruption in the availability of exogenous cholesterol. As shown for other cell types (Karten et al., 2009), we

speculate that the synthesis of endogenous cholesterol is up-regulated in *Npc1* deficient oligodendrocytes. However, this compensatory up-regulation is insufficient to overcome the lack of exogenous cholesterol, especially during the peak phase of myelination. This suggests that extracellularly-derived cholesterol is indispensible for normal CNS myelination.

Although $Npc1^{flox/-}$; $CNP^{Cre/+}$ mutants form myelin in the brainstem and cerebellum during postnatal development, they undergo wide-spread demyelination as adults. Biochemical studies have shown that in the adult CNS, myelin production and cholesterol turnover decrease to very low levels (Dietschy and Turley, 2004). It is therefore unlikely that demyelination in these adult mutants results from impaired access to exogenous cholesterol as a consequence of *Npc1* deficiency. Rather, we speculate that late-stage demyelination stems from the unstable nature of the myelin sheath produced by mutant oligodendrocytes. Studies of cellular models of NPC have shown that cholesterol content is decreased in the plasma membrane of mutant cells (Hawes et al., 2010; Wojtanik and Liscum, 2003). This change may impact myelin by disrupting membrane fluidity, altering lipid rafts or modulating the function of membrane proteins, and thereby increasing vulnerability of aged mutants. Further analysis of the biochemical composition of the myelin sheath generated by *Npc1*-deficient oligodendrocytes will help define the mechanism mediating late-onset demyelination.

In summary, the data reported here extend our understanding of the role of cholesterol metabolism in myelination, and demonstrate that exogenous cholesterol is needed by both neurons and oligodendrocytes for the formation and maintenance of CNS myelin. A characteristic feature of *Npc1* deficient mice, both global nulls and cell-specific knockouts, is the regionally severe dysmyelination that occurs during early postnatal stages. Fate-mapping studies have established that OPCs originate from heterogeneous regions of the subventricular zone,

under the influence of different signaling pathways (Richardson et al., 2006). We speculate that these regional differences in oligodendrocyte lineage cells lead to distinct responses to axonal signals or to the need for exogenously-derived cholesterol for proper myelination, contributing to severe dysmyelination particularly in the forebrain of Npc1 mutants. While the precise mechanism underlying this regional selectivity remains to be defined, our data establish a critical role for Npc1 in both myelin formation and maintenance. Our findings have important implications for understanding the pathogenesis of NPC disease and may also inform our knowledge of other dysmyelinating/demyelinating disorders.

3.5 Materials and Methods

3.5.1 Mice

Npc1$^{flox/flox}$ and *Npc1*$^{\Delta/-}$ mice were generated as previously described (Elrick et al., 2010). Other mice used include tamoxifen-inducible *CMV-Cre* (*Cre-ER*$^{TM+}$) (#004682, Jackson Laboratories), *Sny1-Cre* (#003966, Jackson Laboratories), *CNP*$^{Cre/+}$ mice (Lappe-Siefke et al., 2003), *Olig2*$^{Cre/+}$ mice (Schuller et al., 2008) and Rosa reporter mice (#003474, Jackson Laboratories). All mouse strains were maintained on the C57BL6/J background, except Olig2 $^{Cre/+}$ mice which were maintained on the 129/C3H mixed background. Animal use and procedures were approved by the University of Michigan Committee on the Use and Care of Animals.

3.5.2 Tamoxifen induction

Tamoxifen (Sigma) was dissolved in corn oil (Sigma) at 20 mg/ml and stored at -20 C in the dark. The stock solution was warmed to 37 C before injection. 6-week-old mice were injected intraperitoneally with 3 mg tamoxifen per 40 g body weight for 5 consecutive days.

3.5.3 Phenotype analysis

Motor function was measured using the balance beam test as described previously (Elrick et al., 2010).

3.5.4 Western blot

Brain lysates were homogenized in RIPA buffer (Thermo Scientific) containing *C*omplete protease inhibitor cocktail (Roche) and phosphatase inhibitors (Thermo scientific) using a motor homogenizer (TH115, OMNI International). Samples were resolved by 4-20% Tris-glycine gradient gel and transferred to nitrocellulose membranes (BioRad) on a semidry transfer apparatus. Immunoreactivity was detected by Immobilon chemilluminescent substrate (Thermo Scientific). Antibodies used were rat anti-MBP (1:2000, Abcam), mouse anti-CNP (1:2000, Millipore), mouse anti-MAG (1:5000, Millipore), mouse anti-Neurofilament 200 (1:5000, Millipore), rabbit anti-NG2 (1:1000, Millipore), rabbit anti-GAPDH (1:5000, Santa Cruz), mouse anti-Cre (1:1000, Millipore), rabbit anti-GFAP (1:5000, Dako), mouse anti-PSA-NCAM (1:1000, Millipore), goat anti-Jagged1(1:1000, Santa Cruz) and rabbit anti-Lingo1 (1:1000, Abcam).

3.5.5 Immunoprecipitation

200 µg brain lysates were immunoprecipitated with 10 µg anti-Fyn antibody (FYN3, Santa Cruz) overnight at 4C, followed by incubation with 20 µl Protein A beads (Santa Cruz) for

1h at 4C. The immunoprecipitates were then washed 4 times with protein lysis buffer before being boiled with 2X sample buffer at 100C for 5min. For the subsequent western blot analysis, anti-Fyn (FYN3, Santa Cruz), Src pY418 and pY529 antibodies (Life technologies) were used to detect total Fyn and phosphorylation of Fyn at Y420 and Y531, respectively.

3.5.6 Histology

Mice were perfused with 0.9% normal saline followed by 4% paraformaldehyde. Brains were removed and post-fixed in 4% paraformaldehyde overnight. Brains were bisected, with the right hemisphere processed for paraffin embedding and the left hemisphere processed for frozen sections. Prior to freezing, brain tissue was cryoprotected in 30% sucrose for 48 hr at 4C. Brains were frozen in isopentane chilled by dry ice and embedded in OCT (Tissue-Tek). Frozen sections were prepared at 14 μm in a cryostat and used for LacZ staining and subsequent eosin counter staining or immunohistochemical staining for Olig2 (1:500, Millipore) and NeuN (1:500, Millipore). For filipin staining, frozen sections were first used for immunofluorescence staining for NeuN or Olig2, followed by incubation for 90 min in PBS with 10% fetal bovine serum plus 25 μg/ml filipin (Sigma). Paraffin-embedded sections were prepared at 5 μm and used for staining with H&E staining or MBP (1:100, Abcam), SMI-31P (1:200, Covance), NG2 (1:100, Millipore), CC1 (1:200, Calbiochem), Calbindin (1:1000, Sigma), Sip1 (1:100, Santa Cruz) and GFAP (1:1000, Dako) immunofluorescence. For visualization of staining, secondary antibodies conjugated to Alexa Fluor 594 or Alexa Fluor 488 (Molecular Probes) were used and images were captured on a Zeiss Axioplan 2 imaging system. For NG2 and CC1 co-staining and Olig2 staining, images were captured on an Olympus FluoView 500 Confocal Microscope system. Quantification of $CC1^+$ or $Olig2^+$ cells was performed using NIH ImageJ software.

Quantification of Purkinje cell loss was performed on H&E stained sections. Counts were normalized to the length of the Purkinje layer, as measured by NIH ImageJ software, and reported as Purkinje cell density.

3.5.7 Electron microscopy

Mice were perfused with 0.9% normal saline followed by 3% paraformaldehyde and 2.5% glutaraldehyde in 0.1 M Sorensen's buffer. The corpus callosum was removed and post-fixed in perfusion solution overnight, followed by fixation in 1% osmium tetroxide solution for 1h at room temperature. After dehydration, tissues were embedded in epoxy resin. For transmission electron microscopy, ultrathin sections were cut, and images were captured on a Philips CM-100 imaging system at 10,500X magnification.

3.5.8 Statistics

Statistical significance was assessed by unpaired Student's *t* test. Statistics were performed using the software package Prism 5 (GraphPad Software). *P* values less than 0.05 were considered significant.

3.6 Acknowledgements

We thank Drs. Hisashi Umemori and Roman Giger for helpful discussions. This work was supported by a grant from the N.I.H. (R01 NS063967 to A.P.L.).

Chapter 4

Ryanodine receptor antagonists adapt NPC1 proteostasis to ameliorate lipid storage in Niemann-Pick type C disease fibroblasts[2]

4.1 Abstract

Niemann-Pick type C disease is a lysosomal storage disorder most often caused by loss-of-function mutations in the *NPC1* gene. The encoded multipass transmembrane protein is required for cholesterol efflux from late endosomes and lysosomes. Numerous missense mutations in the *NPC1* gene cause disease, including the prevalent I1061T mutation that leads to protein misfolding and degradation. Here, we sought to modulate the cellular proteostasis machinery to achieve functional recovery in primary patient fibroblasts. We demonstrate that targeting endoplasmic reticulum (ER) calcium levels using ryanodine receptor (RyR) antagonists increased steady state levels of the NPC1 I1061T protein. These compounds also promoted trafficking of mutant NPC1 to late endosomes and lysosomes, and rescued the aberrant storage of cholesterol and sphingolipids that is characteristic of disease. Similar rescue was obtained using three distinct RyR antagonists in cells with missense alleles, but not with null alleles, or by over-expressing calnexin, a calcium-dependent ER chaperone. Our work highlights the utility of

[2] This chapter was published as:
Yu T, Chung C, Shen D, Xu H, Lieberman AP. Ryanodine receptor antagonists adapt NPC1 proteostasis to ameliorate lipid storage in Niemann-Pick type C disease fibroblasts. *Hum Mol Genet*. 2012 Jul 15;21(14):3205-14

proteostasis regulators to remodel the protein-folding environment in the ER to recover function in the setting of disease-causing missense alleles.

4.2 Introduction

Niemann-Pick type C disease is an autosomal recessive neurodegenerative disorder for which there is no effective treatment(Vanier, 2010). Mutations in either of two genes, *NPC1* (Carstea et al., 1997) or *NPC2* (Naureckiene et al., 2000), disrupt efflux of cholesterol from late endosomes and lysosomes, and trigger a clinically heterogeneous phenotype that invariably includes severe neurological dysfunction and early death (Higgins et al., 1992). Most cases of Niemann-Pick C are caused by mutations in *NPC1*, a widely expressed gene encoding a multipass transmembrane glycoprotein localized to late endosome and lysosomes (Davies and Ioannou, 2000; Garver et al., 2000; Higgins et al., 1999; Neufeld et al., 1999). Genetic studies in mice have established that loss of Npc1 in neurons is necessary and sufficient to mediate CNS disease (Elrick et al., 2010; Ko et al., 2005; Lopez et al., 2011; Yu et al., 2011). Despite our growing understanding of disease pathogenesis, strategies to treat the severe, progressive neurodegeneration that is characteristic of this disorder have remained elusive.

The approach to treating Niemann-Pick C patients is complicated by the genetics of the disease. Over 240 sequence variants in the *NPC1* gene have been identified, with reported nucleotide changes occurring in all 25 exons and 14 introns. Disease-causing mutations are scattered throughout the gene, rather than clustering in a single functional domain such as the sterol-sensing region (Vanier and Millat, 2003). Furthermore, despite heterogeneity in clinical presentation, genotype-phenotype correlations have yielded limited information (Runz et al.,

2008), and the functions of most regions of the protein remain poorly understood. Despite these challenges, it has become clear that disease is most commonly caused by missense mutations that lead to non-conservative amino acid substitutions (Vanier and Millat, 2003). The mechanism by which a missense mutation leads to loss of functional NPC1 has been studied in detail for one particular mutant, I1061T, which is found in ~20% of patients of Western European ancestry (Millat et al., 1999). This mutation leads to misfolding of the NPC1 protein in the endoplasmic reticulum (ER) and to its subsequent degradation by the proteasome (Gelsthorpe et al., 2008). That mutant NPC1 is synthesized but fails to fold properly raises the possibility that remodeling of the protein-folding environment in the ER may enable the protein to attain its proper conformation. This approach was first pioneered in studies of Gaucher disease, another lysosomal storage disorder where missense mutations lead to the loss of functional enzyme, glucocerebrosidase (Mu et al., 2008a; Ong et al., 2010; Wang et al., 2011). While misfolded NPC1 I1061T is subject to ER associated degradation, if the mutant protein is over-expressed *in vitro*, some of it transits to late endolysomes/lysosomes and is functional (Gelsthorpe et al., 2008). This suggests that strategies to promote proper folding and trafficking may enable functional recovery of the I1061T mutant.

Here, we present evidence that ryanodine receptor (RyR) antagonists are potent modulators of mutant NPC1 folding and trafficking. We use these small molecules to elevate ER calcium stores and target the proteostasis network, and show that this increases steady-state levels of NPC1 I1061T protein, promotes its trafficking to late endosomes and lysosomes, and ameliorates both the cholesterol storage and sphingolipid trafficking defects in patient fibroblasts. Our findings indicate that proteostasis regulators can be effective therapeutic reagents for Niemann-Pick type C disease caused by missense mutations.

4.3 Results

4.3.1 The ryanodine receptor antagonist DHBP increases steady-state levels of NPC1 I1061T.

To confirm that *NPC1* missense mutations lead to degradation of the mutant, misfolded protein, primary fibroblasts from patients were treated with MG132, an inhibitor of protein degradation through the proteasome, and NPC1 protein levels were determined by western blot **(Figure 4.1A)**. Four patient-derived fibroblast lines were examined, three of which carried at least one copy of the I1061T allele. In each case, basal NPC1 protein levels were lower than in controls and were increased after treatment with MG132. These data are consistent with prior reports that *NPC1* missense mutants, including I1061T, are rapidly degraded by the proteasome (Gelsthorpe et al., 2008).

To test the hypothesis that elevating ER calcium stores will remodel the protein-folding environment so that it is more favorable to mutant NPC1, we examined the effects of several well-characterized RyR antagonists. As this receptor is a channel that mediates calcium efflux from the ER lumen, RyR antagonists are known to increase ER calcium concentration (Ong et al., 2010). We initially tested these small molecules on patient fibroblasts carrying one or two copies of the I1061T allele since this mutant encodes a functionally active protein (Gelsthorpe et al., 2008). We identified the RyR antagonist DHBP (1,1'-diheptyl-4,4'-bipyridium) as a potent inducer of NPC1 protein, increasing its steady-state level in a dose-dependent manner **(Figure 4.1B)**. This occurred without altering *NPC1* mRNA levels **(Figure 4.1C)**, suggesting that DHBP enhanced NPC1 protein stability, an interpretation supported by cycloheximide chase studies **(Figure 4.1D)**.

Figure 4.1 NPC1 I1061T is degraded by the proteasome, and the RyR antagonist DHBP increases its steady-state level.
(A) Primary human fibroblasts with different NPC1 mutations were treated with 10 μM MG132 or vehicle (DMSO) for 24h, and cell lysates were examined by western blot for the expression of NPC1 (top). GAPDH controls for loading (bottom). **(B)** NPC1 I1061T homozygous fibroblasts were treated with increasing concentrations of DHBP or vehicle for 7 days, and cell lysates were analyzed by western blot for the expression of NPC1 (top). GAPDH controls for loading (bottom). **(C, D)** NPC1 I1061T homozygous or control fibroblasts were treated with 5 μM DHBP or vehicle for 5 days. (C) *NPC1* mRNA levels were determined by quantitative real time RT-PCR (mean +/- SD). n.s. = not significant. (D) Cells were treated with 30 μg/ml cycloheximide (CHX) for times indicated and lysates analyzed by western blot for NPC1 expression.

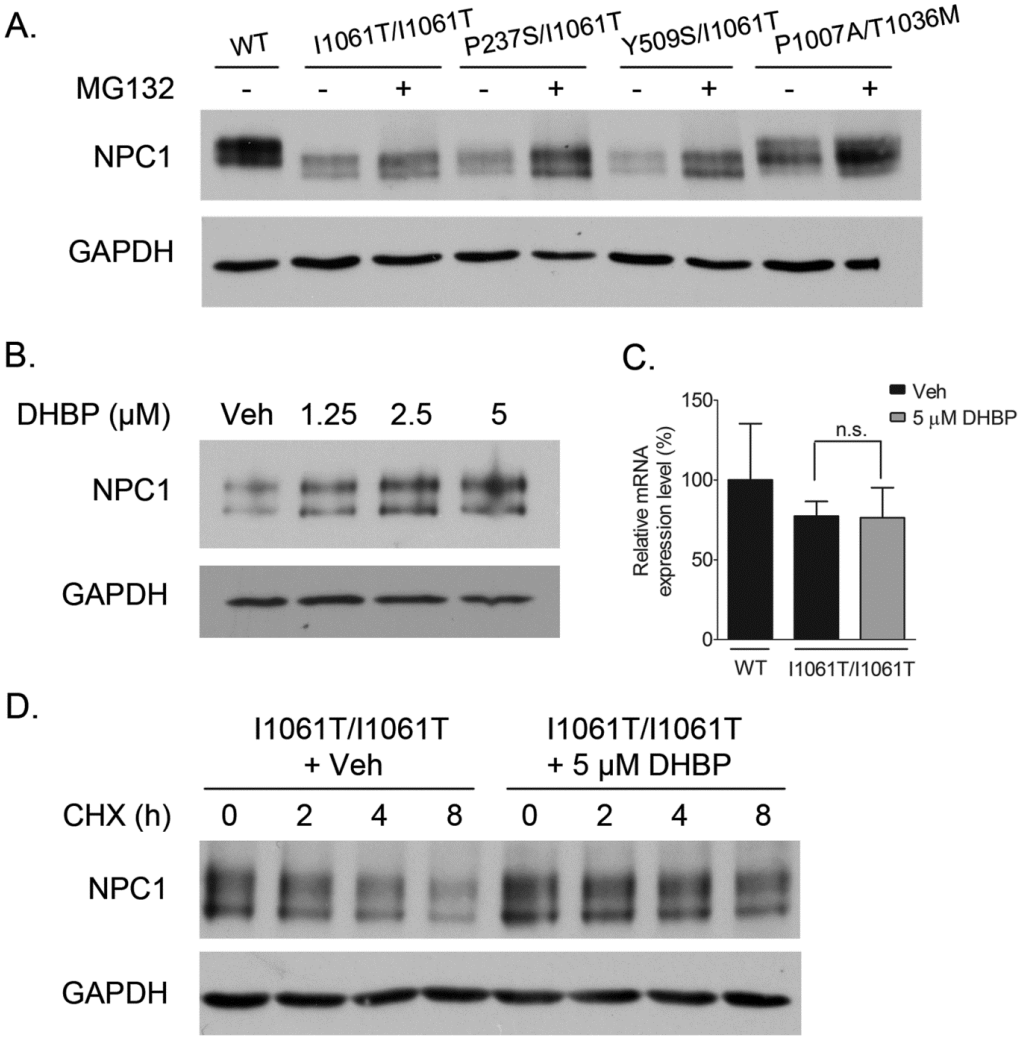

4.3.2 DHBP promotes intracellular trafficking of NPC1 I1061T.

Next we sought to determine whether the increase of NPC1 protein levels mediated by DHBP treatment was accompanied by trafficking of mutant NPC1 to its normal intracellular location in late endosomes and lysosomes. We first employed a biochemical approach to analyze NPC1 trafficking by treating cell lysates with endoglycosidase H (Endo H) or Peptide: N-Glycosidase F (PNGase F). Endo H removes high mannose type N-linked glycans from proteins in the ER, but cannot cleave them after the oligosaccharide chain is further modified in the medial Golgi. Therefore, resistance to Endo H digestion indicates that the glycoprotein has trafficked beyond the ER in the secretory pathway. PNGase F is a glycoamidase that removes all types of N-linked glycans and enables visualization of the unmodified protein. In control fibroblasts, wild type (WT) NPC1 was present as an Endo H-resistant, slow migrating species **(Figure 4.2A)**, indicating that the protein was properly folded and efficiently transported out of ER. In contrast, NPC1 I1061T was present as an Endo H-sensitive, more rapidly migrating species **(Figure 4.2A)**, consistent with the notion that the mutant protein was retained in the ER prior to its degradation. However, after DHBP treatment, NPC1 I1061T showed a detectable increase in the Endo H-resistant band **(Figure 4.2A, B)**, suggesting that a small portion of the mutant protein folded correctly and fluxed through the Golgi.

To gain support for this interpretation, we visualized NPC1 protein by immunofluorescence and assessed its co-localization by confocal microscopy with LAMP1, a marker of late endosomes and lysosomes. In control fibroblasts, WT NPC1 protein was present in cytoplasmic puncta that co-localized with LAMP1 **(Figure 4.2C, top)**, while in mutant fibroblasts, NPC1 I1061T showed a weak and diffuse staining pattern that did not show LAMP1 co-localization **(Figure 4.2C, middle)**. However, DHBP treatment increased the staining

intensity of the mutant protein, and resulted in focal co-localization with LAMP1**(Figure 4.2C, bottom)**. The degree of co-localization between NPC1 I1061T and LAMP1 was quantified by calculating the Pearson correlation coefficient (Rp); this was significantly increased (0.287±0.059 vs. 0.392±0.110, $P< 0.05$) following DHBP treatment. We considered the possibility that this effect might be due to diminished degradation of the Endo H resistant species in lysosomes after DHBP treatment. However, we found that the Endo H resistant species was relatively insensitive to the lysosomal inhibitor chloroquine **(Figure 4.3)**, consistent with prior studies demonstrating that NPC1 I1061T is not significantly degraded in the lysosome (Gelsthorpe et al., 2008). We conclude that DHBP promotes intracellular trafficking of a fraction of the mutant NPC1 protein to late endosomes and lysosomes.

Figure 4.2 DHBP promotes intracellular trafficking of NPC1 I1061T.
(A) NPC1 I1061T homozygous and control (WT) fibroblasts were treated with 5 μM DHBP or vehicle for 7 days. Lysates were digested with Endo H or PNGase F for detection of the post-ER glycoform of NPC1 protein (Endo H resistant).
(B) Quantification of Endo H sensitive and Endo H resistant forms of NPC1 protein levels, as described in (A).
(C) Confocal microscopy shows localization of NPC1 (red) and LAMP1 (green) in NPC1 I1061T homozygous fibroblasts and controls treated with 5 μM DHBP or vehicle for 5 days. Inserts show higher magnification of the boxed regions.

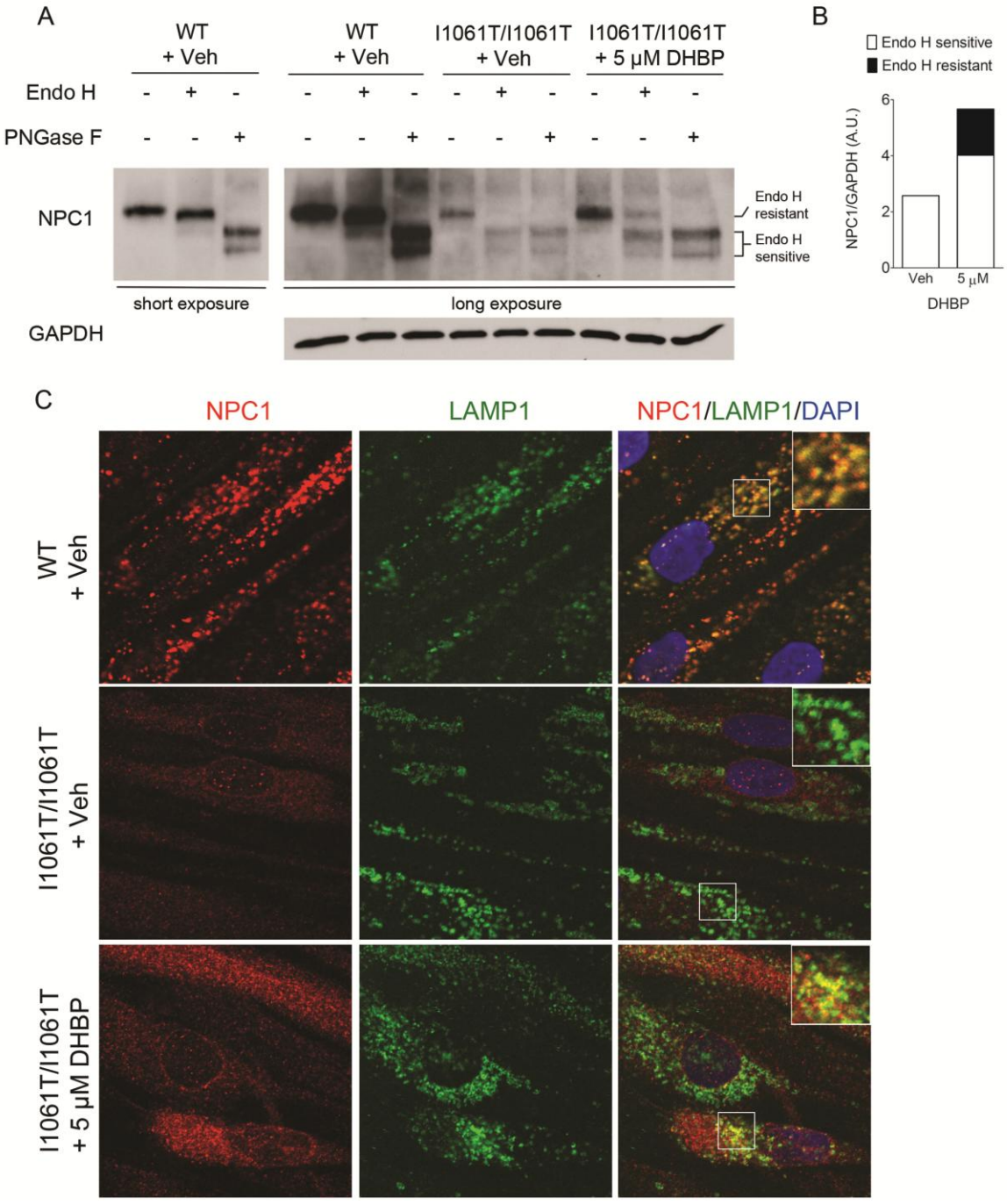

Figure 4.3 Effect of chloroquine on NPC1 I1061T.
NPC1 I1061T homozygous fibroblasts were treated with 5 μM DHBP or vehicle for 7 days. 10 μM chloroquine (Chl) was added on day 6 for 24 hours, and then protein lysates were harvested for Endo H or PNGase F digestion.

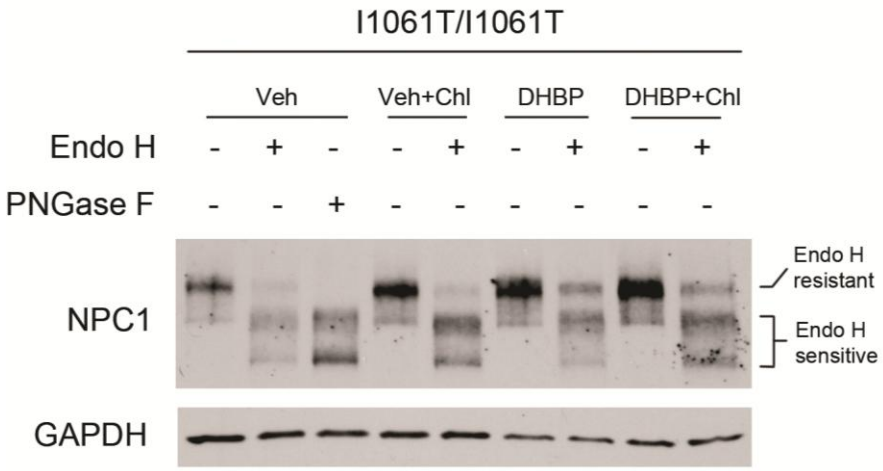

4.3.3 DHBP ameliorates lipid storage in NPC1 I1061T fibroblasts.

To determine the extent to which elevated NPC1 protein levels and enhanced localization to late endosomes and lysosomes were associated with functional recovery, we used quantitative filipin microscopy to evaluate accumulation of unesterified cholesterol, a biochemical hallmark of NPC1 deficient cells. Treatment with DHBP for 5 days significantly decreased filipin staining in fibroblasts homozygous for the NPC1 I1061T allele in a dose-dependent manner **(Figure 4.4A, B)**, demonstrating that treatment diminished lipid storage over the same concentration range that it increased steady-state NPC1 protein levels. Similar results were obtained using an independent line of patient fibroblasts that was a compound heterozygote for the P237S and I1061T alleles **(Figure 4.4C)**. Kinetic analysis established that 5 days treatment was required for DHBP to exert its beneficial effect **(Figure 4.4D)**, likely reflecting time required for protein transit through the secretory pathway and then clearance of accumulated lipids. We confirmed these observations

using an independent assay to measure total free cholesterol in whole cell lysates. Compared to controls, NPC1 I1061T homozygotes showed elevated free cholesterol that was corrected to near WT levels following treatment with DHBP **(Figure 4.4E)**.

Figure 4.4 DHBP ameliorates cholesterol storage in NPC1 I1061T fibroblasts.
(A, B) NPC1 I1061T homozygous fibroblasts were treated with increasing concentrations of DHBP for 5 days and then stained for unesterified cholesterol using filipin. Representative images are shown in (A). Quantification of filipin intensity is shown in (B), and is reported in comparison to controls. Data are mean +/- SD. *** *P<0.001*. **(C)** NPC1 P237S/I1061T fibroblasts were treated with increasing concentrations of DHBP for 5 days, stained with filipin and quantified (mean +/- SD). *** *P<0.001*. **(D)** Quantification of filipin staining of NPC1 I1061T homozygous fibroblasts treated with 5 μM DHBP or vehicle for the indicated times (mean +/- SD). * *P<0.05*. **(E)** NPC1 I1061T homozygous and control fibroblasts were treated with DHBP or vehicle for 5 days. Total free cholesterol was measured by Amplex Red (mean +/- SD). *** *P<0.001*.

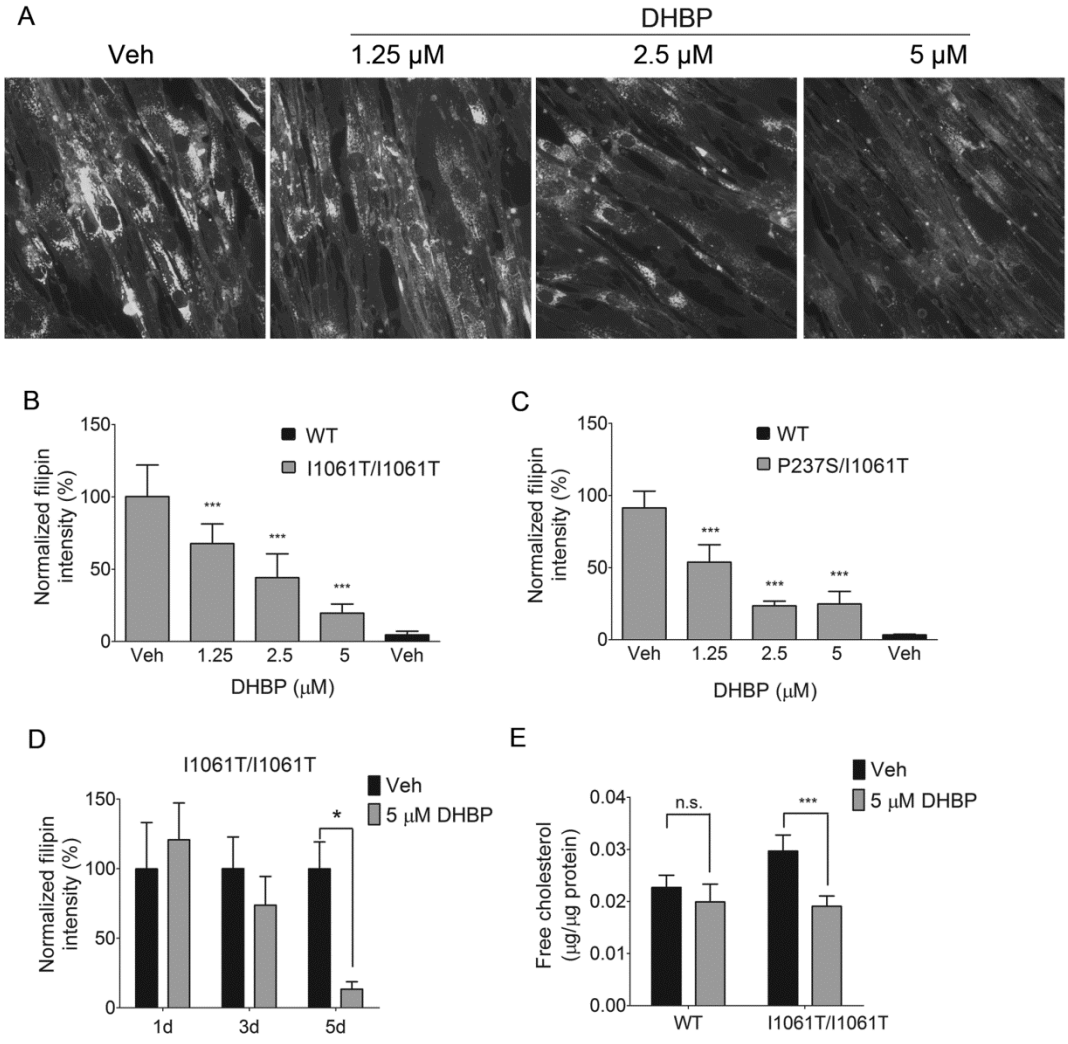

In addition to the storage of unesterified cholesterol, NPC1 deficient cells also display aberrant sphingolipid trafficking. In control fibroblasts, BODIPY-lactosylceramide (BODIPY-LacCer), a synthetic, fluorescent sphingolipid analog, is targeted to the Golgi after endocytosis, but accumulates in endosomes and lysosomes of NPC1 deficient cells (Chen et al., 1999; Sun et al., 2001). We evaluated the intracellular trafficking of BODIPY-LacCer in cells homozygous for the NPC1 I1061T allele, and found that treatment with DHBP for 5 days corrected its transport to the Golgi **(Figure 4.5A, top)**. Similarly, Alexa fluor 594-labeled cholera toxin subunit B (Alexa 594-CtxB), which binds to endogenous monosialotetrahexosylganglioside (GM1) at the cell surface, is transported to the Golgi after internalization in control fibroblasts, but accumulates in endosomes of NPC1 mutant cells (Choudhury et al., 2002; Sugimoto et al., 2001). Treatment with DHBP also corrected this GM1 trafficking defect **(Figure 4.5A, bottom, B)**. Taken together, these data demonstrate that DHBP rescues both the cholesterol and sphingolipid storage phenotypes in mutant NPC1 fibroblasts.

Figure 4.5 DHBP corrects sphingolipid trafficking in NPC1 I1061T fibroblasts.
(A) NPC1 I1061T homozygous fibroblasts and controls were treated with 5 μM DHBP or vehicle for 7 days, then pulse-labeled with BODIPY-LacCer (upper panel) or Alexa 594-CtxB (lower panel) to assess intracellular sphingolipid trafficking. **(B)** NPC1 I1061T homozygous fibroblasts and controls were treated with 5 μM DHBP or vehicle for 7 days. Cells were pulse-labeled with Alexa 594-CtxB, followed by immunofluorescence staining with the Golgi marker GM130. Confocal microscopy was used to assess co-localization.

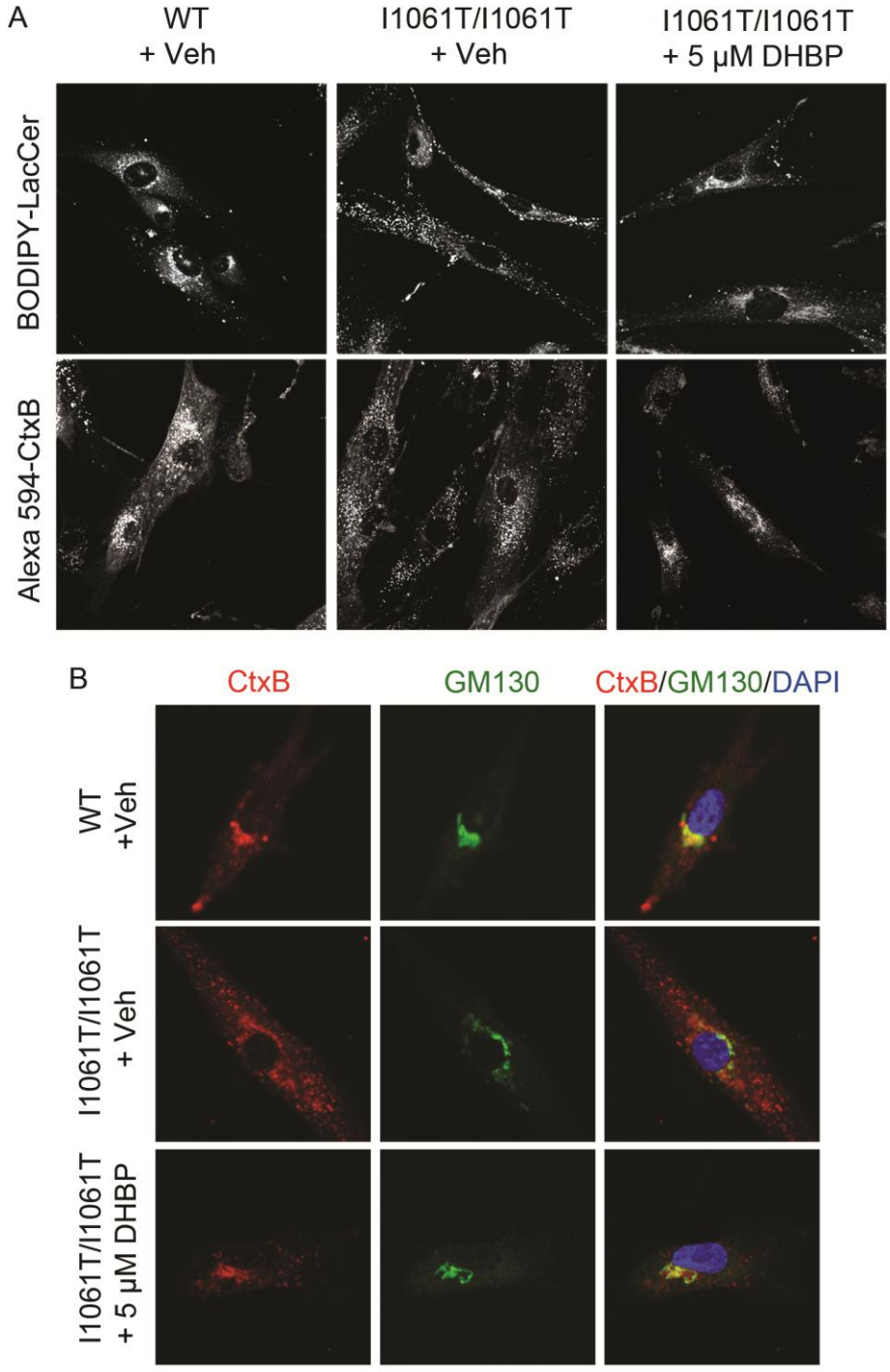

Not all compounds that target calcium levels ameliorated lipid trafficking defects in NPC1 deficient cells. In addition to RyR antagonists, L-type voltage-gated calcium channel blockers modulate ER calcium stores by reducing calcium-induced calcium release. As these small molecules modulate proteostasis of mutant glucocerebrosidase in fibroblasts (Mu et al., 2008a; Ong et al., 2010), we tested their ability to restore mutant NPC1 function. Treatment with diltiazem or verapamil, two L-type calcium channel blockers, resulted in a dose-dependent increase in the steady-state level of NPC1 protein in fibroblasts homozygous for the NPC1 I1061T allele **(Figure 4.6A)**. However, this was not associated with an increase in the Endo H resistant species **(Figure 4.6B)**, and was unexpectedly accompanied by an exacerbation of the cholesterol storage phenotype **(Figure 4.6C, D)**. This may reflect inhibitory effects of these compounds on intracellular lipid metabolism, such as cholesterol esterification (Dushkin and Schwartz, 1995), on off-target effects on other ion channels, or other, less well-characterized actions. These observations focused our efforts on defining the mechanism by which RyR antagonists exerted therapeutic effects.

Figure 4.6 L-type calcium channel blockers exacerbate cholesterol storage in NPC1 I1061T fibroblasts.
(A) Cells were treated with increasing concentrations of diltiazem or verapamil for 7 days, and lysates were examined by western blot for expression of NPC1 (top) and GAPDH (bottom). **(B)** NPC1 I1061T homozygous fibroblasts were treated with 50 μM verapamil for 7 days. Lysates were digested with Endo H or PNGase F for detection of the post-ER glycoform of NPC1 protein (Endo H resistant). **(C, D)** Fibroblasts were treated with increasing concentrations of verapamil for 7 days and then stained with filipin. Representative images are shown in (C). Quantification of filipin intensity is shown in (D), and for comparison, filipin intensity of WT fibroblasts is included (mean +/- SD). * *P*<0.05, *** *P*<0.001.

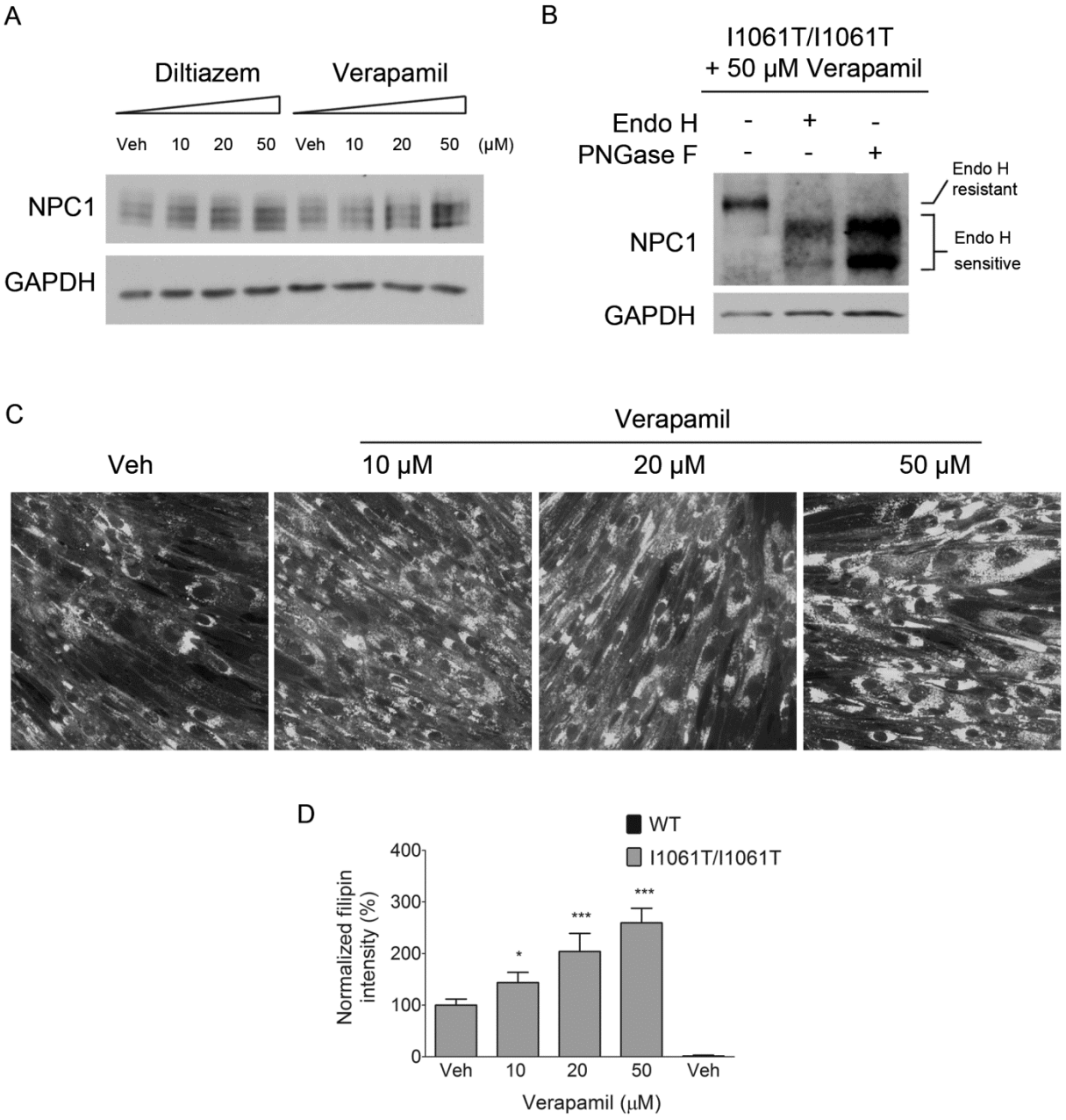

4.3.4 Ryanodine receptor antagonists act through NPC1 protein-dependent mechanisms.

To test our working model that DHBP targets RyRs to enhance mutant NPC1 proteostasis, we examined the effects of additional RyR antagonists on cholesterol storage in fibroblasts homozygous for the NPC1 I1061T allele. Similar to DHBP, both ruthenium red and dantrolene reduced the intensity of filipin staining **(Figure 4.7A, B)**. In contrast, DHBP was ineffective at altering filipin staining of patient fibroblasts carrying two null alleles (*NPC1* 1628delC) of the *NPC1* gene **(Figure 4.7C)**, confirming that NPC1 protein was necessary for its beneficial effects. We also considered the possibility that DHBP exerted its therapeutic effects by targeting other calcium channels, such as those localized to lysosomes that have been implicated in regulating exocytosis (Dong et al., 2009). However, we found that DHBP did not trigger release of lysosomal calcium through the TRPML1 channel **(Figure 4.7D)**. To further test the notion that these small molecules facilitated calcium-dependent ER proteostasis, we transiently over-expressed calnexin **(Figure 4.8A)**, a calcium-dependent ER chaperone. We found that calnexin over-expression was sufficient to promote the appearance of Endo H resistant NPC1 species **(Figure 4.8B)** and significantly reduce filipin staining of NPC1 mutant fibroblasts **(Figure 4.8C, D)**. Taken together, our data demonstrate that genetic or pharmacological manipulation of the protein-folding environment within ER modulates the stability, trafficking and function of mutant NPC1 to yield a functional recovery.

Figure 4.7 Ryanodine receptor antagonists reduce cholesterol storage in *NPC1* missense mutant fibroblasts.
(A, B) NPC1 I1061T homozygous fibroblasts were treated with ruthenium red, dantrolene or vehicle for 5 days, stained with filipin and quantified (mean +/- SD). * P<0.05, *** P<0.001. **(C)** Quantification of filipin intensity in NPC1 null fibroblasts (1628delC) treated with DHBP or vehicle for 5 days (mean +/- SD). P>0.05. **(D)** CHO cells were transfected with a genetically-encoded Ca^{2+} indicator (GCaMP3) fused to the N-terminus of TRPML1 (Shen et al., 2012). TRPML1 mediated lysosomal Ca^{2+} release, as measured by GCaMP3 fluorescence, was examined after sequential application of 50 μM DHBP (in 0 Ca^{2+} Tyrode with <10nM Ca^{2+}), 200 μM Glycyl-L-phenylalanine 2-naphthylamide (GPN, in 0 Ca^{2+} Tyrode with <10nM Ca^{2+}), a cathepsin C substrate that induces lysosomal rupture (Berg et al., 1994), and 1 μM ionomycin (in tyrode with 2mM Ca^{2+}). Shown are data from 5 representative cells, with each cell tracing in a different color. The experiment in Figure 4.7D was performed by Dongbiao Shen.

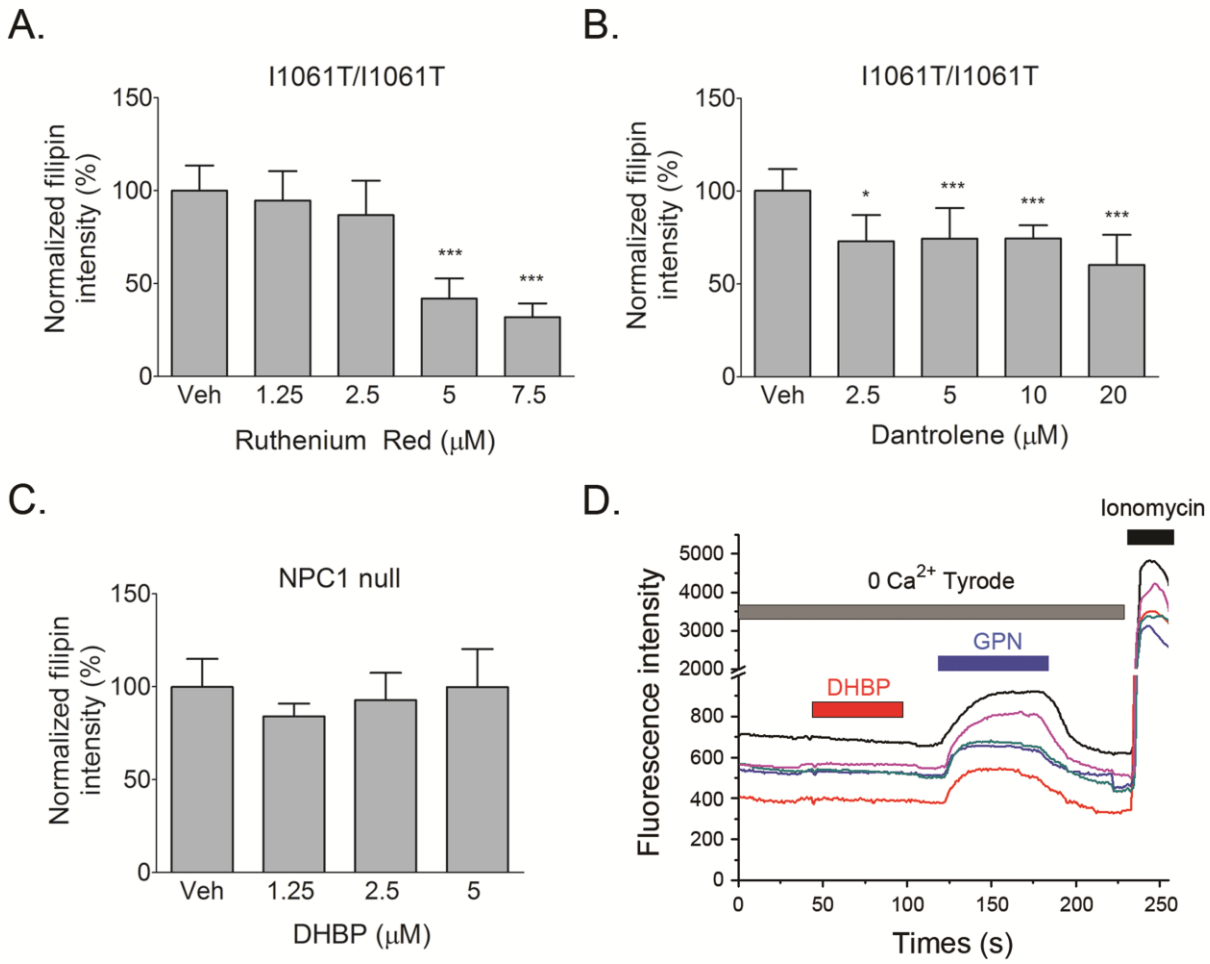

Figure 4.8 Calnexin over-expression promotes mutant NPC1 proteostasis.
(A) NPC1 mutant fibroblasts were transiently transfected with 3XFlag-calnexin for 2 days and cell lysates were analyzed by western blot for the expression of Flag (upper) and calnexin (middle). GAPDH (bottom) controls for loading. **(B)** NPC1 P237S/I1061T fibroblasts were transfected to express 3XFlag-calnexin. Lysates were harvested 6 days later, then digested with Endo H or PNGase F for detection of the post-ER glycoform of NPC1 protein (Endo H resistant). **(C, D)** NPC1 P237S/I1061T fibroblasts were stained with filipin 6 days after 3XFlag-calnexin transfection. Representative images are shown in (C). Quantification of filipin intensity is shown in (D), and is reported in comparison to controls. Data are mean +/- SD. *** *P*<0.001.

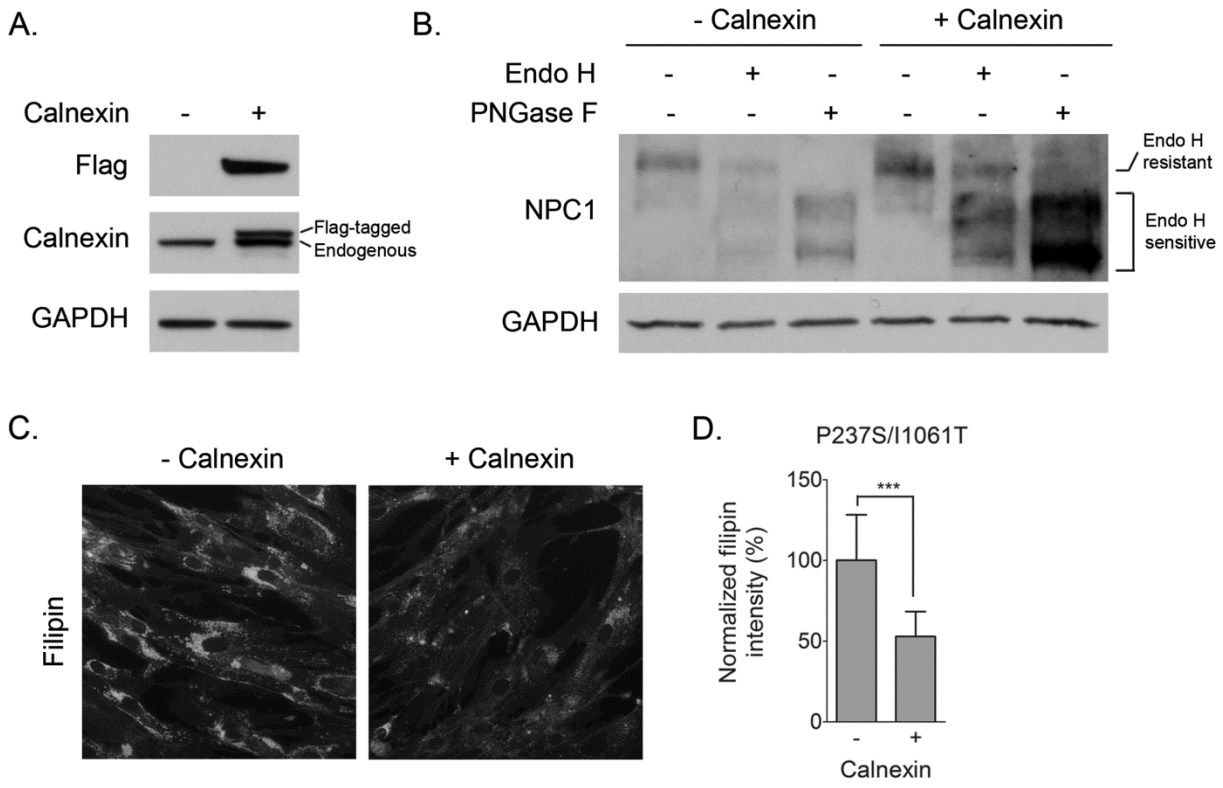

4.4 Discussion

Our findings demonstrate that RyR antagonists ameliorate lipid storage in patient fibroblasts expressing NPC1 I1061T by modifying mutant NPC1 proteostasis. By diminishing activity of this calcium efflux channel, the mutant protein is stabilized, its transit through the secretory pathway to late endosomes and lysosomes is promoted, and the storage of unesterified

cholesterol and sphingolipids is alleviated. Similar effects were observed by transiently over-expressing calnexin. Our data are consistent with the model that DHBP and other RyR antagonists inhibit the spontaneous activity of RyRs to increase ER luminal calcium concentration, which in turn increases the activity of calcium-dependent chaperones such as calnexin. Although RyR antagonists may have yet uncharacterized off-target partners in the cell, and, likewise, calnexin over-expression may invoke effects independent of its activity as an ER chaperone, the combination of these two approaches provides strong, complementary evidence for the idea that modulating the ER protein folding environment enhances proteostasis of mutant NPC1. Other calcium-dependent chaperones are also present in the ER lumen, including BiP and calreticulin, and their roles in NPC1 proteostasis remains to be defined. Although treatment with DHBP or over-expression of calnexin promoted intracellular trafficking of only a small fraction of the mutant protein, they triggered a significant decrease in cholesterol storage, indicating that relatively low levels of recovered protein have marked functional effects

Treatment of the severe, progressive neurological impairment that is characteristic of Niemann-Pick C disease remains elusive. Miglustat, the only approved treatment for this disorder, may stabilize the progression of neurological symptoms in some Niemann-Pick C patients, but is less effective for others (Patterson et al., 2007; Pineda et al., 2010; Wraith and Imrie, 2009). Compelling data demonstrate that cyclodextrin, a compound that circumvents NPC1/NPC2 to clear lipid storage from NPC lysosomes (Abi-Mosleh et al., 2009; Rosenbaum et al., 2010), delays neurodegeneration in Npc1 deficient mice (Aqul et al., 2011; Davidson et al., 2009; Griffin et al., 2004; Liu et al., 2009). However, its limited ability to cross the blood brain barrier poses therapeutic challenges and suggests that complementary approaches will be beneficial. Recent studies identified HDAC inhibitors as small molecules that alleviate lipid

storage in patient fibroblasts (Munkacsi et al., 2011; Pipalia et al., 2011). Our findings add RyR antagonists to this list of compounds with the potential to provide therapeutic benefit to some patients with Niemann-Pick C disease. We note that one of the RyR antagonists tested and proven effective here, dantrolene, is used clinically. Determining the extent to which this compound, or others, alters NPC1 proteostasis in more complex disease models is an important future objective.

Our data extend observations from Gaucher disease fibroblasts (Mu et al., 2008a; Ong et al., 2010; Wang et al., 2011) highlighting the utility of proteostasis regulators in patients with disease-causing missense mutations. Here we have demonstrated that this strategy is also applicable to a multipass transmembrane protein that traffics through the secretory pathway. As other NPC1 missense mutations also lead to protein misfolding and degradation, we suggest that this strategy may be applicable to the subset of disease-causing mutations where function is retained. These findings suggest that small molecules that remodel the protein-folding environment in the ER may be therapeutically beneficial for some Niemann-Pick C patients, and potentially, for patients with other disorders caused by missense mutations.

4.5 Materials and Methods

4.5.1 Reagents

DHBP (180858), dantrolene (D9175), diltiazem (D2521), verapamil (V4629), filipin (F9765) and cycloheximide (C4859) were from Sigma. Chloroquine (193919) and ruthenium red (156565) were from MP Biomedical. Ruthenium red and dantrolene were diluted in DMSO and other channel blockers were diluted in water. BODIPY FL C5-lactosylceramide complexed to

BSA (BODIPY-LacCer) and cholera toxin subunit B, Alexa Fluor 594 conjugate (Alexa 594-CtxB) were from Invitrogen. The calnexin-3XFlag expression plasmid was from GeneCopoeia.

4.5.2 Cell culture and transfection

Human dermal fibroblast lines GM08399 (healthy control) and GM18453 (NPC1 I1061T/I1061T), GM03123 (NPC1 P237S/I1061T), GM17926 (NPC1 Y509S/I1061T), GM17912 (NPC1 P1007A/T1036M) were from Coriell Cell Repositories. Human dermal fibroblasts homozygous for the NPC11628delC allele (NIH 98.016) (Frolov et al., 2003) were a gift from Dr. Daniel Ory. Cells were maintained in Modified Eagle's Medium (MEM, Gibco), supplemented with 15% FBS (Atlanta Biologicals), 10 μg/ml penicillin, 10 μg/ml streptomycin and 2 mM glutamine (Gibco). Control (RA25) CHO cells were a gift from Dr. T.Y. Chang, and were maintained in DMEM/F12 (Gibco) supplemented with 10% FBS. Cells were transfected with 3 μg plasmid by electroporation using a Nucleofector II (Lonza) per manufacturer's instructions.

4.5.3 Quantitative filipin staining

Cells were grown on glass chamber slides and stained with filipin as described (Pacheco et al., 2007). Images were captured on a Zeiss Axioplan 2 imaging system equipped with a Zeiss AxioCam HRc camera, with a 10x Zeiss EC Plan-NEOFLUAR objective, using AxioVision 4.8 software. Quantitative analysis of filipin images from >5 fields of cells/experiment was performed using NIH ImageJ software, following the "LSO compartment ratio assay" method (Pipalia et al., 2006). Data reported are from one of three similar experiments.

4.5.4 Amplex Red cholesterol assay

Total free cholesterol levels were determined using the Amplex Red cholesterol assay kit (Invitrogen) per manufacturer's instructions. Results were normalized to protein concentration determined by protein assay (Bio-rad).

4.5.5 Sphingolipid trafficking

BODIPY-LacCer labeling was performed as described (Sun et al., 2001). Briefly, cells were washed 3 times with MEM and then incubated with 5 μM BODIPY LacCer/BSA in MEM containing 1% FBS for 45 min at 37º C. Cells were then washed 3 times with MEM containing 1% FBS and incubated for another 60 min at 37º C. Next, cells were washed 3 times with DMEM without glucose, and then were back-exchanged at 4º C for 6X10 min with DMEM without glucose containing 5% defatted BSA. Alexa 594 CtxB labeling was carried out similarly, except Alexa 594 CtxB (1:1000) was used in the pulse labeling step and the cells were chased for 2 h at 37º C. In some experiments, after Alexa 594 CtxB labeling, cells were fixed with 4% paraformaldehyde and incubated with rabbit anti-GM130 antibody (Abcam, 1:200) to visualize the Golgi apparatus. Confocal microscopy was performed using an Olympus FluoView 500 Confocal Microscope system, with a 60X WPSF water immersion objective, using Olympus FluoView software.

4.5.6 Immunofluorescence

Cells grown on coverslips were washed with PBS and fixed with methanol for 30 min. Cells were subsequently washed with PBS and incubated with blocking buffer containing 5% donkey serum, 1% BSA and 0.2% Triton X for 1 h, followed by incubation with primary antibodies in buffer containing 1.25% donkey serum, 0.25% BSA and 0.05% Triton X at 4º C overnight. Antibodies used were rabbit anti-NPC1 (Abcam, 1:500) and mouse anti-LAMP1

H4A3 (Developmental Studies Hybridoma Bank, 1:50). Next, cells were washed with PBS containing 0.05% Triton X, incubated with Alexa fluor-conjugated secondary antibodies (Invitrogen), then washed with PBS containing 0.05% Triton X. Coverslips were mounted using Vectashield mounting medium with DAPI (Vector Laboratories). Confocal microscopy was performed using a Zeiss LSM 510-META Laser Scanning Confocal Microscopy system, with a 63x Zeiss C-Apochromat water immersion objective, NA of 1.2, using Zeiss LSM 510-META software. For analysis of NPC1 and LAMP1 co-localization, the Pearson correlation coefficient was calculated using NIH ImageJ.

4.5.7 N-linked glycan removal assays and western blot analysis

Cells were harvested, washed with PBS and lysed in RIPA buffer containing c*O*mplete Protease Inhibitor Cocktail (Roche) and phosphatase inhibitor (Thermo Scientific). For cleavage of N-linked glycans, non-denatured protein samples were treated with PNGase F (NEB) or Endo H (NEB) at 37º C for 3 hours in the supplied buffers. For western blot, non-boiled samples were electrophoresed through a 7.5% SDS-polyacrylamide gel or 4%-20% Tris-glycine gradient gel (Invitrogen) and transferred to nitrocellulose membranes (BioRad) on a semidry transfer apparatus. Immunoreactivity was detected by TMA-6 (Lumigen) or ECL (Thermo Scientific). Antibodies used were rabbit anti-NPC1 (Abcam) and rabbit anti-GAPDH (Santa Cruz).

4.5.8 Gene expression analysis

Total RNA was isolated from cells using TRIzol (Invitrogen) per the manufacturer's protocol. cDNA was synthesized using the High Capacity cDNA Archive Kit (Applied Biosystems). Quantitative real time RT-PCR was performed on 5 ng cDNA per reaction, in duplicate. Primers and probes for NPC1 (Hs00264835-m1) and 18S rRNA were purchased from Applied Biosystems. Threshold cycle (Ct) values were determined on an ABI Prism 7900HT

Sequence Detection System. Relative expression values were calculated by the standard curve method and normalized to 18S rRNA.

4.5.9 GCaMP3 Ca^{2+} imaging

18-24 h after transfection with GCaMP3-ML1 (Shen et al., 2012), CHO cells were trypsinized and plated onto glass coverslips. The fluorescence intensity at 470 nm was monitored using the EasyRatioPro system. Ionomycin (1mM) in tyrode was added at the conclusion of all experiments to induce a maximal response for comparison.

4.5.10 Statistics

Statistical significance was assessed by unpaired Student's *t* test (for comparison of two means) or ANOVA (for comparison of more than two mean). The Newman-Keuls post hoc test was performed to carry out pairwise comparisons of group means if ANOVA rejected the null hypothesis. Statistics were performed using the software package Prism 5 (GraphPad Software). *P* values less than 0.05 were considered significant.

4.6 Acknowledgements

We thank Dr. Daniel Ory for NPC1 1628delC fibroblasts and Dr. T.Y. Chang for RA25 CHO cells. This work was supported by the National Institutes of Health (NS063967 and NS078526 to A.P.L.).

Chapter 5

Conclusion

In this dissertation, I have described multiple approaches to explore the pathogenesis and therapeutic strategies for Niemann-Pick type C disease. First, I demonstrated that *Npc1* deficiency in adults is sufficient to cause disease, and that neurons, but not astrocytes, play a leading role in pathogenesis. Next, I investigated the roles of neurons and oligodendrocytes in NPC dysmyelination. This study showed that *Npc1* deficiency in either cell type is sufficient to block oligodendrocyte maturation and myelin formation, with the most severe impairment in the forebrain. In addition, I showed that *Npc1* deficiency in oligodendrocytes also leads to demyelination and secondary Purkinje neuron degeneration in adults. Finally, I tested small molecules in patient fibroblasts with the NPC1 I1061T mutation. My work showed that ryanodine recepter antagonists are effective in modulating NPC1 proteostasis and ameliorating the lipid storage defect by promoting the mutant protein's folding in the ER and trafficking to LE/LYs. In the remaining part of this chapter, I will discuss some of the unanswered questions and propose future directions.

5.1 Temporal and spatial effects of *Npc1* deficiency

In Chapter 2, I utilized a conditional knockout mouse model of NPC to study the effect of timing of *Npc1* deficiency on neurodegeneration (Yu et al., 2011). Prior studies showed that a single injection of cyclodextrin at postnatal day 7 (P7) significantly extended the lifespan of *Npc1*$^{-/-}$ mice, while injections at later stages were much less effective (Davidson et al., 2009; Griffin et al., 2004; Liu et al., 2009), raising the possibility that a developmental window exists for the need of NPC1. By inducing tamoxifen-regulated Cre deletion of *Npc1* globally at 6 weeks, my work showed that *Npc1* deficiency in adults reproduced most of the neurodegenerative phenotypes seen in mice with germline deletion, but with a slightly extended lifespan. This suggests that Npc1 is needed in adult brain for normal function, but does not exclude the possibility that Npc1 also participates in the developmental events. Indeed, in Chapter 3, I showed that Npc1 is required for CNS myelination, a developmental event that takes place in the first several postnatal weeks. Although the time-sensitive effect of cyclodextrin was later attributed to the limited accessibility of cyclodextrin to the brain as blood brain barrier forms, my results indicate that it could also result partially from improvement of myelination. Collectively, my work in Chapters 2 and 3 suggest that Npc1 is crucial both for the developmental and continuous functions of the brain. Therefore, for NPC patients, therapies need to be given as early as possible, and continuously throughout life.

Another issue in the field had been whether neurodegeneration in NPC is a neuronal cell autonomous process, as prior studies yielded conflicting results. My work with a neuron specific Cre (Sny1-Cre) and an astrocyte specific Cre (GFAP-CreER^{TM2}) (Yu et al., 2011) demonstrated that *Npc1* deficiency within neurons is sufficient to cause disease. In contrast, gene deletion restricted to astrocytes did not produce any detectable defects, arguing against a significant

contribution of mature astrocytes to neurodegeneration. These findings supported prior work from our laboratory which showed that *Npc1* deficiency in Purkinje neurons is sufficient to cause degeneration (Elrick et al., 2010). My work with an oligodendrocyte specific Cre (CNP-Cre) extended this finding by showing that a similar pattern of Purkinje neuron loss can also be triggered following demyelination, demonstrating a non-cell autonomous contribution to neurodegeneration. Taken together, these data suggest that Npc1 deficiency in neurons is sufficient to cause neuron loss, but that effects in myelinating glia also contribute to NPC neuropathology.

Progressive motor dysfunction, as exhibited by tremor, ataxia and hindlimb paralysis, is a prominent phenotypic feature of NPC mice, and was originally attributed primarily to Purkinje neuron dysfunction. However, *Npc1* deficiency restricted to Purkinje neurons only results in a mild impairment in motor function (Elrick et al., 2010), indicating that pathology elsewhere also contributes to this complex phenotype. Indeed, my work with Syn1-Cre and CNP-Cre mice demonstrated that dysfunction of other neurons, as well as oligodendrocytes, is sufficient to impair motor coordination. Therefore, motor dysfunction in NPC mice is a complex process involving pathology in both neurons of different brain regions and oligodendrocytes.

While the data presented in my thesis and studies from other laboratories have clarified the role of Npc1 deficiency in neurons and glia, little work has focused on the role of microglia, the resident macrophages in the CNS (Gehrmann et al., 1995). Microglia continually survey the brain using their branched processes, and are activated when the healthy environment is disturbed by invading pathogens or by cell damage. After proliferation and migration to the site of damage, microglia respond by phagocytosing cell debris and foreign materials, and by releasing pro-inflammatory cytokines to induce an inflammatory response. This process often

ends with the secretion of anti-inflammatory cytokines and growth factors by microglia to promote repair and regeneration of the damaged tissue. Microglial activation is a common phenomena in neurodegenerative disorders. However, the inflammatory response generated by microglia, if not controlled tightly, can be detrimental to the tissue and worsen the disease (Dheen et al., 2007). Therefore, the outcome of microglia activation in neurodegenerative diseases remains controversial, and is probably context dependent. For example, in a mouse model of Sanhoff disease, a lysosomal storage disorder caused by β-hexosaminidases deficiency, monocytes from the periphery were shown to cross the blood brain barrier to expand the pool of activated microglia in the CNS. Prevention of monocyte infiltration ameliorated the neurological symptoms and prolonged lifespan (Wu and Proia, 2004). This suggests that in Sanhoff disease, monocyte infiltration and microglial activation accelerates neurodegeneration. On the other hand, in a mouse model of type II Gaucher's disease, glucocerebrosidase deficiency in all CNS cell types except microglia resulted in a more profound activation of microglia and a more slowly progressive disease course compared to global null mutants (Enquist et al., 2007). This suggests that restoration of microglial function in Gaucher's disease might be beneficial for the clinical outcome.

In *Npc1*$^{-/-}$ mice, the initial observation was that microglial activation preceded neurodegeneration and was detected as early as 2 weeks (Baudry et al., 2003). This raised the possibility that *Npc1* deficient microglia might play a role in initiating the disease by triggering a detrimental inflammatory response or by releasing reactive oxygen species. However, my work and work by others demonstrated that *Npc1* deficiency in neurons alone is sufficient to cause microgliosis (Yu et al., 2011), and that neuroinflammation in the cerebellum can be suppressed by neuronal specific rescue of *Npc1* deficiency in Purkinje cells (Lopez et al., 2012a). These data

suggest that microglial activation is more likely a consequence than a cause of neuronal dysfunction, and therefore is unlikely to be the initiating factor in the NPC pathology. Moreover, attempts to inhibit macrophage infiltration (Lopez et al., 2012a) or to suppress neuroinflammation by inactivating genes encoding immune response factors (Lopez et al., 2012b) have failed to prevent neuronal loss or extend the lifespan in *Npc1*$^{-/-}$ mice. Furthermore, these manipulations have worsened the liver pathology of mutant mice. These observations suggest that microglia and macrophages do not significantly contribute to the progression of NPC disease, and might be beneficial for preventing further tissue damage. Consistent with these findings, neuron-microglia co-culture studies showed that the survival of cerebellar granule neurons is not affected by microglia, regardless of the *Npc1* genotype in either cell type (Peake et al., 2011). Taken together, these studies imply that microgliosis is a secondary factor in the pathogenesis of NPC, and therefore additional work using the conditional knockout model of NPC to study microglia is unlikely to yield new insights into disease mechanisms.

5.2 NPC1 and myelination

In Chapter 3, I presented multiple findings revealing the essential roles of both axonal and oligodendroglial Npc1 in myelination. First, by re-examining brain tissue from Syn-1-Cre mice at a much earlier age, P16, I unexpectedly showed that *Npc1* deficiency in neurons is sufficient to disrupt myelination in a regional specific manner. In parallel, my work with CNP-Cre mice showed that a similar pattern of dysmyelination is triggered by *Npc1* deficiency in oligodendrocytes. Furthermore, aged mice lacking oligodendrocytic Npc1 developed

demyelination and secondary Purkinje neuron loss that underlie the progressive motor incoordination in these mice.

This work leaves behind many unanswered questions. For example, how does Npc1 dysfunction in neurons block oligodendrocyte maturation and myelination? By showing that *Npc1* deficient axons are well preserved in dysmyelinated regions, my work excluded the possibility that the defect in myelin formation is caused by the lack or loss of axons in the same region. Furthermore, my data showed that Syn1-Cre mutants have decreased levels of activated Fyn kinase, a Src family member that acts in oligodendrocytes as an integrator of axonal signals for promoting myelination. Based on these findings, we favor a model in which *Npc1* deficiency in axons leads to perturbed myelination through disruption of Fyn-dependent axon-oligodendroglial communication. The immediate next question is what is the link between loss of Npc1 in neurons and disrupted Fyn activity in oligodendrocytes? At least two upstream signaling pathways have been shown to link axonal signals to Fyn activation. The first is the laminin-2/$\alpha_6\beta_1$ integrin complex, in which interaction with laminin-2 at the surface of axons activates $\alpha_6\beta_1$ integrin in oligodendrocytes to regulate Fyn activity through dephosphorylation of its inhibitory site Y531 (Colognato et al., 2002; Colognato et al., 2004; Laursen et al., 2009). Notably, mice with a deficiency in the laminin α_2 chain, a component of laminin-2, exhibit regional dysmyelination similar to that of the Syn1-Cre mutants (Chun et al., 2003). The second signaling pathway is the L1/contactin complex. Similar to the laminin-2/$\alpha_6\beta_1$ integrin complex, interaction of L1 on the surface of axons and contactin on oligodendrocytes triggers the phosphorylation of Fyn at its activating site Y420 (Laursen et al., 2009). These two complexes are shown to work synergistically to maximize the effect of Fyn activation (Laursen et al., 2009). It is possible that in Syn1-Cre mutants, sequestration of cholesterol in LE/LYs leads to decreased

cholesterol content in the plasma membrane. This change in the cholesterol level may alter the surface properties of axons (e.g. reduced levels of laminin-2 or contactin), resulting in the subsequent failure of stimulating oligodendrocyte differentiation. It is also possible that *Npc1* deficiency in neurons leads to decreased electrical activities, which have been shown to be another axonal signal for Fyn activation and myelination (Wake et al., 2011). Further work is needed to test these possibilities. In addition to upstream events, there are three well-characterized downstream pathways controlled by Fyn activation: a Rho-GTPase-dependent pathway to regulate actin cytoskeleton dynamics and oligodendrocyte morphological differentiation, recruitment of microtubule cytoskeleton (tau, α-tubulin, etc.) to establish cell polarity and facilitate cargo transport, and regulation of mRNA transport and local translation of myelin proteins such as MBP (Kramer-Albers and White, 2011). A recent remyelination study showed that pharmacological manipulation of the Fyn-Rho pathway is sufficient to overcome the inhibitory effect of myelin on oligodendrocyte differentiation *in vitro* (Baer et al., 2009). This suggests that studies to identify the downstream pathway affected by Fyn inactivation in NPC mice might shed light on future therapies targeting dysmyelination in human patients.

Another unsolved question is how *Npc1* deficiency in oligodendrocytes leads to demyelination in adult mice. In the brainstem and cerebellum, myelin is formed in CNP-Cre mutants in early postnatal days, but is later lost in aged mice. By showing that the numbers of $Olig2^{+}$ cells are the same in the cerebellum between 23-week-old CNP-Cre mutants and controls, my work excluded the possibility that the late-onset demyelination is caused by loss of oligodendrocytes. Given the fact that myelin turnover is very slow in the adult brain (Dietschy, 2009), it is less likely that demyelination reflects a defect in myelin synthesis. We favor the possibility that the myelin sheath produced by *Npc1* deficient oligodendrocytes is defective and

unstable, leading to increased degradation. To test this idea, biochemical experiments are needed to compare the chemical composition of the myelin sheath between CNP-Cre mutants and controls. For example, probing the lipid and protein profile in purified myelin would establish the extent to which the cholesterol to protein ratio is altered in CNP-Cre mutants. Examination of the mRNA levels of myelin proteins might also be helpful to differentiate "reduced myelin synthesis" versus "increased myelin breakdown".

5.3 Proteostasis regulation and therapeutic strategies

In Chapter 4, I identified ryanodine receptor (RyR) antagonists as disease-modifying compounds in patient fibroblasts carrying the I1061T mutation (Yu et al., 2012). My work showed that by increasing the ER luminal Ca^{2+} concentration, RyR antagonists enhance ER proteostasis to promote the folding and trafficking of NPC1 I1061T, thereby restoring its normal function and ameliorating the lipid storage defects. A limitation of my work is that the study was carried out in patient fibroblasts, results of which may not reflect changes of the brain pathology. Based on my work in Chapters 2 and 3 demonstrating that neurons are the most critical cell type for NPC, further work is needed to test the effects of RyR antagonists in a neuronal cell model of NPC. This neuronal model needs to carry missense mutations of *NPC1*, since the beneficial effect of RyR antagonists requires the presence of the NPC1 protein. The newly developed induced pluripotent stem cell (iPS) technology serves as a powerful tool to generate neurons from patient fibroblasts (Ito et al., 2012). This system could prove helpful in providing an *in vitro* model to test RyR antagonists and other compounds in the disease-relevant cell type. The next step would be to move from cellular models to an animal model of NPC. Again, since RyR

antagonists only rescue defects caused by missense mutations of *NPC1*, mouse models with null mutations, such as the *Npc1*^{nih} mice and the conditional knockout model, are not appropriate for this purpose. A new mouse model of NPC expressing Npc1 I1061T is being developed in Dr. Daniel Ory's laboratory and will be a useful *in vivo* model to test RyR antagonists.

My work described the beneficial effects of RyR antagonists on the most prevalent missense mutation, NPC1 I1061T. However, this mutation only accounts for ~20% of all the NPC patients (Millat et al., 1999), and it would be very informative to test how other missense mutations respond to RyR antagonists. Based on my findings of NPC1 I1061T, the prediction is that only those mutants that are misfolded but retain function if trafficked to LE/LYs may benefit from RyR antagonists. A comprehensive understanding of the biochemical behavior of individual NPC1 mutants would be of great value for directing personalized therapies for NPC patients in the future.

In addition to RyR antagonists, I also showed that over-expression of calnexin, a Ca^{2+} regulated ER chaperone involved in protein folding, is sufficient to suppress the cholesterol storage defect in patient fibroblasts with the NPC1 I1061T mutation (Yu et al., 2012). This suggests that manipulation of ER chaperones might serve as an alternative strategy to promote ER proteostasis in NPC. An in-depth investigation of the roles of different ER chaperones in promoting NPC1 I1061T folding is ongoing in our laboratory. Similarly, knowledge of the protein machinery involved in ER associated degradation of misfolded NPC1 protein might provide a clue for future drug discovery. For example, targeting the E3 ligase responsible for ubiquitinating misfolded NPC1 protein might prevent its degradation and provide more substrates for ER chaperones, and this strategy might work synergistically with RyR antagonists to provide a beneficial effect.

Inducing the unfolded protein response (UPR) is another potential strategy to modify ER proteostasis. The UPR is a series of signaling cascades that cells use to adapt to various ER stresses, including the accumulation of misfolded proteins. The three ER stress sensors IRE1, PERK and ATF6, are BiP-bound receptors for monitoring the protein folding environment in the ER lumen. Once unfolded proteins accumulate in the ER and preferentially sequester BiP, these sensors are released, leading to the activation of a cascade of downstream events. The outcomes of these pathways are attenuation of protein translation, transcriptional up-regulation of protein folding- and degradation-related genes, and activation of apoptosis if prolonged stress is detected (Wang and Kaufman, 2012). Manipulation of the UPR has been successfully applied to Gaucher's disease and other lysosomal storage disorders (Mu et al., 2008b). However, caution should be taken to keep UPR activation tightly controlled in order to avoid activation of apoptosis. Currently genetic strategies to manipulate the IRE and ATF6 arms of the UPR, which generally promote protein folding and cell survival, are being tested in NPC patient fibroblasts in our laboratory.

5.4 Concluding remarks

Niemann-Pick Type C is a rare genetic disorder that is largely neglected by the pharmaceutical industry. However, for each family who has one or more children suffering from NPC, the significance of this disorder cannot be overstated. The development of effective therapies for NPC will not be achieved without advances in the understanding of the disease pathogenesis. In this thesis, I have helped define the timing and cell type important for the NPC neuropathology. Furthermore, I have identified a new disease modifying strategy that might be

therapeutically beneficial to some NPC patients. It is my sincere hope that these studies will shed light on future NPC drug development to eventually cure this devastating disease.

References

Abi-Mosleh, L., R.E. Infante, A. Radhakrishnan, J.L. Goldstein, and M.S. Brown. 2009. Cyclodextrin overcomes deficient lysosome-to-endoplasmic reticulum transport of cholesterol in Niemann-Pick type C cells. *Proc. Natl. Acad. Sci. U. S. A.* 106:19316-21.

Abian, O., P. Alfonso, A. Velazquez-Campoy, P. Giraldo, M. Pocovi, and J. Sancho. 2011. Therapeutic strategies for Gaucher disease: miglustat (NB-DNJ) as a pharmacological chaperone for glucocerebrosidase and the different thermostability of velaglucerase alfa and imiglucerase. *Mol Pharm*. 8:2390-7.

Aggarwal, S., L. Yurlova, N. Snaidero, C. Reetz, S. Frey, J. Zimmermann, G. Pahler, A. Janshoff, J. Friedrichs, D.J. Muller, C. Goebel, and M. Simons. 2011. A size barrier limits protein diffusion at the cell surface to generate lipid-rich myelin-membrane sheets. *Dev Cell*. 21:445-56.

Allaman, I., M. Belanger, and P.J. Magistretti. 2011. Astrocyte-neuron metabolic relationships: for better and for worse. *Trends Neurosci*. 34:76-87.

Aqul, A., B. Liu, C.M. Ramirez, A.A. Pieper, S.J. Estill, D.K. Burns, J.J. Repa, S.D. Turley, and J.M. Dietschy. 2011. Unesterified cholesterol accumulation in late endosomes/lysosomes causes neurodegeneration and is prevented by driving cholesterol export from this compartment. *J. Neurosci.* 31:9404-13.

Baer, A.S., Y.A. Syed, S.U. Kang, D. Mitteregger, R. Vig, C. Ffrench-Constant, R.J. Franklin, F. Altmann, G. Lubec, and M.R. Kotter. 2009. Myelin-mediated inhibition of oligodendrocyte precursor differentiation can be overcome by pharmacological modulation of Fyn-RhoA and protein kinase C signalling. *Brain*. 132:465-81.

Barres, B.A., and M.C. Raff. 1993. Proliferation of oligodendrocyte precursor cells depends on electrical activity in axons. *Nature*. 361:258-60.

Barres, B.A., and M.C. Raff. 1999. Axonal control of oligodendrocyte development. *J Cell Biol*. 147:1123-8.

Barski, J.J., K. Dethleffsen, and M. Meyer. 2000. Cre recombinase expression in cerebellar Purkinje cells. *Genesis*. 28:93-8.

Baudry, M., Y. Yao, D. Simmons, J. Liu, and X. Bi. 2003. Postnatal development of inflammation in a murine model of Niemann-Pick type C disease: immunohistochemical observations of microglia and astroglia. *Exp Neurol*. 184:887-903.

Baumann, N., and D. Pham-Dinh. 2001. Biology of oligodendrocyte and myelin in the mammalian central nervous system. *Physiol. Rev.* 81:871-927.

Beck, M. 2007. New therapeutic options for lysosomal storage disorders: enzyme replacement, small molecules and gene therapy. *Hum Genet*. 121:1-22.

Berg, T.O., P.E. Stromhaug, T. Berg, and P.O. Seglen. 1994. Separation of lysosomes and autophagosomes by means of glycyl-phenylalanine-naphthylamide, a lysosome-disrupting cathepsin-C substrate. *Eur. J. Biochem.* 221:595-602.

Blom, T.S., M.D. Linder, K. Snow, H. Pihko, M.W. Hess, E. Jokitalo, V. Veckman, A.C. Syvanen, and E. Ikonen. 2003. Defective endocytic trafficking of NPC1 and NPC2 underlying infantile Niemann-Pick type C disease. *Hum Mol Genet*. 12:257-72.

Borbon, I., J. Totenhagen, M.T. Fiorenza, S. Canterini, W. Ke, T. Trouard, and R.P. Erickson. 2012. Niemann-Pick C1 mice, a model of "juvenile Alzheimer's disease", with normal gene expression in neurons and fibrillary astrocytes show long term survival and delayed neurodegeneration. *J Alzheimers Dis*. 30:875-87.

Bordey, A., and H. Sontheimer. 2003. Modulation of glutamatergic transmission by bergmann glial cells in rat cerebellum in situ. *J Neurophysiol*. 89:979-88.

Bornig, H., and G. Geyer. 1974. Staining of cholesterol with the fluorescent antibiotic "filipin". *Acta Histochem.* 50:110-5.

Camargo, F., R.P. Erickson, W.S. Garver, G.S. Hossain, P.N. Carbone, R.A. Heidenreich, and J. Blanchard. 2001. Cyclodextrins in the treatment of a mouse model of Niemann-Pick C disease. *Life Sci*. 70:131-42.

Carstea, E.D., J.A. Morris, K.G. Coleman, S.K. Loftus, D. Zhang, C. Cummings, J. Gu, M.A. Rosenfeld, W.J. Pavan, D.B. Krizman, J. Nagle, M.H. Polymeropoulos, S.L. Sturley, Y.A. Ioannou, M.E. Higgins, M. Comly, A. Cooney, A. Brown, C.R. Kaneski, E.J. Blanchette-Mackie, N.K. Dwyer, E.B. Neufeld, T.Y. Chang, L. Liscum, J.F. Strauss, 3rd, K. Ohno, M. Zeigler, R. Carmi, J. Sokol, D. Markie, R.R. O'Neill, O.P. van Diggelen, M. Elleder, M.C. Patterson, R.O. Brady, M.T. Vanier, P.G. Pentchev, and D.A. Tagle. 1997. Niemann-Pick C1 disease gene: homology to mediators of cholesterol homeostasis. *Science*. 277:228-31.

Casper, K.B., K. Jones, and K.D. McCarthy. 2007. Characterization of astrocyte-specific conditional knockouts. *Genesis*. 45:292-9.

Casper, K.B., and K.D. McCarthy. 2006. GFAP-positive progenitor cells produce neurons and oligodendrocytes throughout the CNS. *Mol Cell Neurosci*. 31:676-84.

Charles, P., M.P. Hernandez, B. Stankoff, M.S. Aigrot, C. Colin, G. Rougon, B. Zalc, and C. Lubetzki. 2000. Negative regulation of central nervous system myelination by polysialylated-neural cell adhesion molecule. *Proc. Natl. Acad. Sci. U S A*. 97:7585-90.

Chen, C.S., M.C. Patterson, C.L. Wheatley, J.F. O'Brien, and R.E. Pagano. 1999. Broad screening test for sphingolipid-storage diseases. *Lancet*. 354:901-5.

Chen, G., H.M. Li, Y.R. Chen, X.S. Gu, and S. Duan. 2007. Decreased estradiol release from astrocytes contributes to the neurodegeneration in a mouse model of Niemann-Pick disease type C. *Glia*. 55:1509-18.

Chien, Y.H., N.C. Lee, L.K. Tsai, A.C. Huang, S.F. Peng, S.J. Chen, and W.L. Hwu. 2007. Treatment of Niemann-Pick disease type C in two children with miglustat: initial responses and maintenance of effects over 1 year. *J Inherit Metab Dis*. 30:826.

Chin, D.J., G. Gil, D.W. Russell, L. Liscum, K.L. Luskey, S.K. Basu, H. Okayama, P. Berg, J.L. Goldstein, and M.S. Brown. 1984. Nucleotide sequence of 3-hydroxy-3-methyl-glutaryl coenzyme A reductase, a glycoprotein of endoplasmic reticulum. *Nature*. 308:613-7.

Choudhury, A., M. Dominguez, V. Puri, D.K. Sharma, K. Narita, C.L. Wheatley, D.L. Marks, and R.E. Pagano. 2002. Rab proteins mediate Golgi transport of caveola-internalized

glycosphingolipids and correct lipid trafficking in Niemann-Pick C cells. *J. Clin. Invest.* 109:1541-50.

Christopherson, K.S., E.M. Ullian, C.C. Stokes, C.E. Mullowney, J.W. Hell, A. Agah, J. Lawler, D.F. Mosher, P. Bornstein, and B.A. Barres. 2005. Thrombospondins are astrocyte-secreted proteins that promote CNS synaptogenesis. *Cell*. 120:421-33.

Chun, S.J., M.N. Rasband, R.L. Sidman, A.A. Habib, and T. Vartanian. 2003. Integrin-linked kinase is required for laminin-2-induced oligodendrocyte cell spreading and CNS myelination. *J Cell Biol*. 163:397-408.

Colognato, H., W. Baron, V. Avellana-Adalid, J.B. Relvas, A. Baron-Van Evercooren, E. Georges-Labouesse, and C. ffrench-Constant. 2002. CNS integrins switch growth factor signalling to promote target-dependent survival. *Nat Cell Biol*. 4:833-41.

Colognato, H., S. Ramachandrappa, I.M. Olsen, and C. ffrench-Constant. 2004. Integrins direct Src family kinases to regulate distinct phases of oligodendrocyte development. *J Cell Biol*. 167:365-75.

Cox, T.M. 2005. Substrate reduction therapy for lysosomal storage diseases. *Acta Paediatr Suppl*. 94:69-75; discussion 57.

Cruz, J.C., S. Sugii, C. Yu, and T.Y. Chang. 2000. Role of Niemann-Pick type C1 protein in intracellular trafficking of low density lipoprotein-derived cholesterol. *J Biol Chem*. 275:4013-21.

Danbolt, N.C. 2001. Glutamate uptake. *Prog Neurobiol*. 65:1-105.

Davidson, C.D., N.F. Ali, M.C. Micsenyi, G. Stephney, S. Renault, K. Dobrenis, D.S. Ory, M.T. Vanier, and S.U. Walkley. 2009. Chronic cyclodextrin treatment of murine Niemann-Pick C disease ameliorates neuronal cholesterol and glycosphingolipid storage and disease progression. *PLoS One*. 4:e6951.

Davies, J.P., and Y.A. Ioannou. 2000. Topological analysis of Niemann-Pick C1 protein reveals that the membrane orientation of the putative sterol-sensing domain is identical to those of 3-hydroxy-3-methylglutaryl-CoA reductase and sterol regulatory element binding protein cleavage-activating protein. *J. Biol. Chem.* 275:24367-74.

Deffieu, M.S., and S.R. Pfeffer. 2011. Niemann-Pick type C 1 function requires lumenal domain residues that mediate cholesterol-dependent NPC2 binding. *Proc. Natl. Acad. Sci. U S A.* 108:18932-6.

Demerens, C., B. Stankoff, M. Logak, P. Anglade, B. Allinquant, F. Couraud, B. Zalc, and C. Lubetzki. 1996. Induction of myelination in the central nervous system by electrical activity. *Proc Natl Acad Sci U S A.* 93:9887-92.

Dheen, S.T., C. Kaur, and E.A. Ling. 2007. Microglial activation and its implications in the brain diseases. *Curr Med Chem*. 14:1189-97.

Di Rocco, M., A. Dardis, A. Madeo, R. Barone, and A. Fiumara. 2012. Early miglustat therapy in infantile Niemann-Pick disease type C. *Pediatr Neurol*. 47:40-3.

Dietschy, J.M. 2009. Central nervous system: cholesterol turnover, brain development and neurodegeneration. *Biol Chem*. 390:287-93.

Dietschy, J.M., and S.D. Turley. 2004. Thematic review series: brain Lipids. Cholesterol metabolism in the central nervous system during early development and in the mature animal. *J. Lipid Res.* 45:1375-97.

Dietschy, J.M., and J.D. Wilson. 1968. Cholesterol synthesis in the squirrel monkey: relative rates of synthesis in various tissues and mechanisms of control. *J Clin Invest*. 47:166-74.

Dong, X.P., X. Wang, D. Shen, S. Chen, M. Liu, Y. Wang, E. Mills, X. Cheng, M. Delling, and H. Xu. 2009. Activating mutations of the TRPML1 channel revealed by proline-scanning mutagenesis. *J. Biol. Chem.* 284:32040-52.

Du, X., J. Kumar, C. Ferguson, T.A. Schulz, Y.S. Ong, W. Hong, W.A. Prinz, R.G. Parton, A.J. Brown, and H. Yang. 2011. A role for oxysterol-binding protein-related protein 5 in endosomal cholesterol trafficking. *J Cell Biol*. 192:121-35.

Dugas, J.C., T.L. Cuellar, A. Scholze, B. Ason, A. Ibrahim, B. Emery, J.L. Zamanian, L.C. Foo, M.T. McManus, and B.A. Barres. 2010. Dicer1 and miR-219 Are required for normal oligodendrocyte differentiation and myelination. *Neuron*. 65:597-611.

Dushkin, M.I., and Y.S. Schwartz. 1995. Effect of verapamil and nifedipine on cholesteryl ester metabolism and low-density lipoprotein oxidation in macrophages. *Biochem. Pharmacol.* 49:389-97.

Elrick, M.J., C.D. Pacheco, T. Yu, N. Dadgar, V.G. Shakkottai, C. Ware, H.L. Paulson, and A.P. Lieberman. 2010. Conditional Niemann-Pick C mice demonstrate cell autonomous Purkinje cell neurodegeneration. *Hum. Mol. Genet.* 19:837-47.

Elrick, M.J., T. Yu, C. Chung, and A.P. Lieberman. 2012. Impaired proteolysis underlies autophagic dysfunction in Niemann-Pick type C disease. *Hum Mol Genet*. 21:4876-87.

Emery, B. 2010. Regulation of oligodendrocyte differentiation and myelination. *Science*. 330:779-82.

Emery, B., D. Agalliu, J.D. Cahoy, T.A. Watkins, J.C. Dugas, S.B. Mulinyawe, A. Ibrahim, K.L. Ligon, D.H. Rowitch, and B.A. Barres. 2009. Myelin gene regulatory factor is a critical transcriptional regulator required for CNS myelination. *Cell*. 138:172-85.

Enquist, I.B., C. Lo Bianco, A. Ooka, E. Nilsson, J.E. Mansson, M. Ehinger, J. Richter, R.O. Brady, D. Kirik, and S. Karlsson. 2007. Murine models of acute neuronopathic Gaucher disease. *Proc Natl Acad Sci U S A*. 104:17483-8.

Erickson, R.P., W.S. Garver, F. Camargo, G.S. Hossain, and R.A. Heidenreich. 2000. Pharmacological and genetic modifications of somatic cholesterol do not substantially alter the course of CNS disease in Niemann-Pick C mice. *J Inherit Metab Dis*. 23:54-62.

Fancy, S.P., S.E. Baranzini, C. Zhao, D.I. Yuk, K.A. Irvine, S. Kaing, N. Sanai, R.J. Franklin, and D.H. Rowitch. 2009. Dysregulation of the Wnt pathway inhibits timely myelination and remyelination in the mammalian CNS. *Genes Dev*. 23:1571-85.

Farina, C., F. Aloisi, and E. Meinl. 2007. Astrocytes are active players in cerebral innate immunity. *Trends Immunol*. 28:138-45.

Fink, J.K., M.R. Filling-Katz, J. Sokol, D.G. Cogan, A. Pikus, B. Sonies, B. Soong, P.G. Pentchev, M.E. Comly, R.O. Brady, and et al. 1989. Clinical spectrum of Niemann-Pick disease type C. *Neurology*. 39:1040-9.

Fluegel, M.L., T.J. Parker, and L.J. Pallanck. 2006. Mutations of a Drosophila NPC1 gene confer sterol and ecdysone metabolic defects. *Genetics*. 172:185-96.

Friedland, N., H.L. Liou, P. Lobel, and A.M. Stock. 2003. Structure of a cholesterol-binding protein deficient in Niemann-Pick type C2 disease. *Proc Natl Acad Sci U S A*. 100:2512-7.

Frolov, A., S.E. Zielinski, J.R. Crowley, N. Dudley-Rucker, J.E. Schaffer, and D.S. Ory. 2003. NPC1 and NPC2 regulate cellular cholesterol homeostasis through generation of low density lipoprotein cholesterol-derived oxysterols. *J. Biol. Chem.* 278:25517-25.

Galanaud, D., A. Tourbah, S. Lehericy, N. Leveque, B. Heron, T. Billette de Villemeur, N. Guffon, F. Feillet, N. Baumann, M.T. Vanier, and F. Sedel. 2009. 24 month-treatment

with miglustat of three patients with Niemann-Pick disease type C: follow up using brain spectroscopy. *Mol Genet Metab*. 96:55-8.

Garver, W.S., R.A. Heidenreich, R.P. Erickson, M.A. Thomas, and J.M. Wilson. 2000. Localization of the murine Niemann-Pick C1 protein to two distinct intracellular compartments. *J. Lipid Res.* 41:673-87.

Gehrmann, J., Y. Matsumoto, and G.W. Kreutzberg. 1995. Microglia: intrinsic immuneffector cell of the brain. *Brain Res Brain Res Rev*. 20:269-87.

Gelsthorpe, M.E., N. Baumann, E. Millard, S.E. Gale, S.J. Langmade, J.E. Schaffer, and D.S. Ory. 2008. Niemann-Pick type C1 I1061T mutant encodes a functional protein that is selected for endoplasmic reticulum-associated degradation due to protein misfolding. *J Biol Chem*. 283:8229-36.

German, D.C., C.L. Liang, T. Song, U. Yazdani, C. Xie, and J.M. Dietschy. 2002. Neurodegeneration in the Niemann-Pick C mouse: glial involvement. *Neuroscience*. 109:437-50.

German, D.C., E.M. Quintero, C.L. Liang, B. Ng, S. Punia, C. Xie, and J.M. Dietschy. 2001. Selective neurodegeneration, without neurofibrillary tangles, in a mouse model of Niemann-Pick C disease. *J Comp Neurol*. 433:415-25.

Gieselmann, V. 1995. Lysosomal storage diseases. *Biochim Biophys Acta*. 1270:103-36.

Gong, J.S., M. Kobayashi, H. Hayashi, K. Zou, N. Sawamura, S.C. Fujita, K. Yanagisawa, and M. Michikawa. 2002. Apolipoprotein E (ApoE) isoform-dependent lipid release from astrocytes prepared from human ApoE3 and ApoE4 knock-in mice. *J Biol Chem*. 277:29919-26.

Grabowski, G.A., and M. Horowitz. 1997. Gaucher's disease: molecular, genetic and enzymological aspects. *Baillieres Clin Haematol*. 10:635-56.

Greer, W.L., M.J. Dobson, G.S. Girouard, D.M. Byers, D.C. Riddell, and P.E. Neumann. 1999. Mutations in NPC1 highlight a conserved NPC1-specific cysteine-rich domain. *Am J Hum Genet*. 65:1252-60.

Greer, W.L., D.C. Riddell, T.L. Gillan, G.S. Girouard, S.M. Sparrow, D.M. Byers, M.J. Dobson, and P.E. Neumann. 1998. The Nova Scotia (type D) form of Niemann-Pick disease is caused by a G3097-->T transversion in NPC1. *Am J Hum Genet*. 63:52-4.

Griffin, L.D., W. Gong, L. Verot, and S.H. Mellon. 2004. Niemann-Pick type C disease involves disrupted neurosteroidogenesis and responds to allopregnanolone. *Nat. Med.* 10:704-11.

Hawes, C.M., H. Wiemer, S.R. Krueger, and B. Karten. 2010. Pre-synaptic defects of NPC1-deficient hippocampal neurons are not directly related to plasma membrane cholesterol. *J Neurochem*. 114:311-22.

Hayashi, S., and A.P. McMahon. 2002. Efficient recombination in diverse tissues by a tamoxifen-inducible form of Cre: a tool for temporally regulated gene activation/inactivation in the mouse. *Dev. Biol.* 244:305-18.

Haydon, P.G. 2001. GLIA: listening and talking to the synapse. *Nat Rev Neurosci*. 2:185-93.

Higaki, K., D. Almanzar-Paramio, and S.L. Sturley. 2004. Metazoan and microbial models of Niemann-Pick Type C disease. *Biochim Biophys Acta*. 1685:38-47.

Higgins, J.J., M.C. Patterson, J.M. Dambrosia, A.T. Pikus, P.G. Pentchev, S. Sato, R.O. Brady, and N.W. Barton. 1992. A clinical staging classification for type C Niemann-Pick disease. *Neurology*. 42:2286-90.

Higgins, M.E., J.P. Davies, F.W. Chen, and Y.A. Ioannou. 1999. Niemann-Pick C1 is a late endosome-resident protein that transiently associates with lysosomes and the trans-Golgi network. *Mol. Genet. Metab.* 68:1-13.

Howng, S.Y., R.L. Avila, B. Emery, M. Traka, W. Lin, T. Watkins, S. Cook, R. Bronson, M. Davisson, B.A. Barres, and B. Popko. 2010. ZFP191 is required by oligodendrocytes for CNS myelination. *Genes Dev*. 24:301-11.

Hsu, Y.S., W.L. Hwu, S.F. Huang, M.Y. Lu, R.L. Chen, D.T. Lin, S.S. Peng, and K.H. Lin. 1999. Niemann-Pick disease type C (a cellular cholesterol lipidosis) treated by bone marrow transplantation. *Bone Marrow Transplant*. 24:103-7.

Hu, C.Y., W.Y. Ong, and S.C. Patel. 2000. Regional distribution of NPC1 protein in monkey brain. *J Neurocytol*. 29:765-73.

Hua, X., A. Nohturfft, J.L. Goldstein, and M.S. Brown. 1996. Sterol resistance in CHO cells traced to point mutation in SREBP cleavage-activating protein. *Cell*. 87:415-26.

Huang, X., K. Suyama, J. Buchanan, A.J. Zhu, and M.P. Scott. 2005. A Drosophila model of the Niemann-Pick type C lysosome storage disease: dnpc1a is required for molting and sterol homeostasis. *Development*. 132:5115-24.

Imrie, J., S. Vijayaraghaven, C. Whitehouse, S. Harris, L. Heptinstall, H. Church, A. Cooper, G.T. Besley, and J.E. Wraith. 2002. Niemann-Pick disease type C in adults. *J Inherit Metab Dis*. 25:491-500.

Infante, R.E., A. Radhakrishnan, L. Abi-Mosleh, L.N. Kinch, M.L. Wang, N.V. Grishin, J.L. Goldstein, and M.S. Brown. 2008a. Purified NPC1 protein: II. Localization of sterol binding to a 240-amino acid soluble luminal loop. *J Biol Chem*. 283:1064-75.

Infante, R.E., M.L. Wang, A. Radhakrishnan, H.J. Kwon, M.S. Brown, and J.L. Goldstein. 2008b. NPC2 facilitates bidirectional transfer of cholesterol between NPC1 and lipid bilayers, a step in cholesterol egress from lysosomes. *Proc Natl Acad Sci U S A*. 105:15287-92.

Ito, D., H. Okano, and N. Suzuki. 2012. Accelerating progress in induced pluripotent stem cell research for neurological diseases. *Ann Neurol*. 72:167-74.

Johnson, R.L., A.L. Rothman, J. Xie, L.V. Goodrich, J.W. Bare, J.M. Bonifas, A.G. Quinn, R.M. Myers, D.R. Cox, E.H. Epstein, Jr., and M.P. Scott. 1996. Human homolog of patched, a candidate gene for the basal cell nevus syndrome. *Science*. 272:1668-71.

Kaech, S., and G. Banker. 2006. Culturing hippocampal neurons. *Nat Protoc*. 1:2406-15.

Karten, B., H. Hayashi, G.A. Francis, R.B. Campenot, D.E. Vance, and J.E. Vance. 2005. Generation and function of astroglial lipoproteins from Niemann-Pick type C1-deficient mice. *Biochem J*. 387:779-88.

Karten, B., K.B. Peake, and J.E. Vance. 2009. Mechanisms and consequences of impaired lipid trafficking in Niemann-Pick type C1-deficient mammalian cells. *Biochim. Biophys. Acta*. 1791:659-70.

Kim, S.J., B.H. Lee, Y.S. Lee, and K.S. Kang. 2007. Defective cholesterol traffic and neuronal differentiation in neural stem cells of Niemann-Pick type C disease improved by valproic acid, a histone deacetylase inhibitor. *Biochem Biophys Res Commun*. 360:593-9.

Kirchhoff, C., C. Osterhoff, and L. Young. 1996. Molecular cloning and characterization of HE1, a major secretory protein of the human epididymis. *Biol Reprod*. 54:847-56.

Ko, D.C., J. Binkley, A. Sidow, and M.P. Scott. 2003. The integrity of a cholesterol-binding pocket in Niemann-Pick C2 protein is necessary to control lysosome cholesterol levels. *Proc Natl Acad Sci U S A*. 100:2518-25.

Ko, D.C., L. Milenkovic, S.M. Beier, H. Manuel, J. Buchanan, and M.P. Scott. 2005. Cell-autonomous death of cerebellar purkinje neurons with autophagy in Niemann-Pick type C disease. *PLoS Genet.* 1:81-95.

Koenning, M., S. Jackson, C.M. Hay, C. Faux, T.J. Kilpatrick, M. Willingham, and B. Emery. 2012. Myelin gene regulatory factor is required for maintenance of myelin and mature oligodendrocyte identity in the adult CNS. *J Neurosci*. 32:12528-42.

Kramer-Albers, E.M., and R. White. 2011. From axon-glial signalling to myelination: the integrating role of oligodendroglial Fyn kinase. *Cell. Mol. Life Sci.* 68:2003-12.

Kuwamura, M., T. Awakura, A. Shimada, T. Umemura, K. Kagota, N. Kawamura, and M. Naiki. 1993. Type C Niemann-Pick disease in a boxer dog. *Acta Neuropathol*. 85:345-8.

Kwon, H.J., L. Abi-Mosleh, M.L. Wang, J. Deisenhofer, J.L. Goldstein, M.S. Brown, and R.E. Infante. 2009. Structure of N-terminal domain of NPC1 reveals distinct subdomains for binding and transfer of cholesterol. *Cell*. 137:1213-24.

Lachmann, R.H. 2003. Miglustat. Oxford GlycoSciences/Actelion. *Curr Opin Investig Drugs*. 4:472-9.

Lachmann, R.H., D. te Vruchte, E. Lloyd-Evans, G. Reinkensmeier, D.J. Sillence, L. Fernandez-Guillen, R.A. Dwek, T.D. Butters, T.M. Cox, and F.M. Platt. 2004. Treatment with miglustat reverses the lipid-trafficking defect in Niemann-Pick disease type C. *Neurobiol Dis*. 16:654-8.

Lakso, M., J.G. Pichel, J.R. Gorman, B. Sauer, Y. Okamoto, E. Lee, F.W. Alt, and H. Westphal. 1996. Efficient in vivo manipulation of mouse genomic sequences at the zygote stage. *Proc. Natl. Acad. Sci. U S A*. 93:5860-5.

Lappe-Siefke, C., S. Goebbels, M. Gravel, E. Nicksch, J. Lee, P.E. Braun, I.R. Griffiths, and K.A. Nave. 2003. Disruption of Cnp1 uncouples oligodendroglial functions in axonal support and myelination. *Nat. Genet.* 33:366-74.

Laursen, L.S., C.W. Chan, and C. ffrench-Constant. 2009. An integrin-contactin complex regulates CNS myelination by differential Fyn phosphorylation. *J Neurosci*. 29:9174-85.

Lee, X., Z. Yang, Z. Shao, S.S. Rosenberg, M. Levesque, R.B. Pepinsky, M. Qiu, R.H. Miller, J.R. Chan, and S. Mi. 2007. NGF regulates the expression of axonal LINGO-1 to inhibit oligodendrocyte differentiation and myelination. *J. Neurosci.* 27:220-5.

Lehre, K.P., and N.C. Danbolt. 1998. The number of glutamate transporter subtype molecules at glutamatergic synapses: chemical and stereological quantification in young adult rat brain. *J Neurosci*. 18:8751-7.

Li, J., G. Brown, M. Ailion, S. Lee, and J.H. Thomas. 2004. NCR-1 and NCR-2, the C. elegans homologs of the human Niemann-Pick type C1 disease protein, function upstream of DAF-9 in the dauer formation pathways. *Development*. 131:5741-52.

Liao, G., S. Cheung, J. Galeano, A.X. Ji, Q. Qin, and X. Bi. 2009. Allopregnanolone treatment delays cholesterol accumulation and reduces autophagic/lysosomal dysfunction and inflammation in Npc1-/- mouse brain. *Brain Res.* 1270:140-51.

Ligon, K.L., S. Kesari, M. Kitada, T. Sun, H.A. Arnett, J.A. Alberta, D.J. Anderson, C.D. Stiles, and D.H. Rowitch. 2006. Development of NG2 neural progenitor cells requires Olig gene function. *Proc Natl Acad Sci U S A*. 103:7853-8.

Liou, H.L., S.S. Dixit, S. Xu, G.S. Tint, A.M. Stock, and P. Lobel. 2006. NPC2, the protein deficient in Niemann-Pick C2 disease, consists of multiple glycoforms that bind a variety of sterols. *J Biol Chem*. 281:36710-23.

Liscum, L., and J.R. Faust. 1989. The intracellular transport of low density lipoprotein-derived cholesterol is inhibited in Chinese hamster ovary cells cultured with 3-beta-[2-(diethylamino)ethoxy]androst-5-en-17-one. *J Biol Chem*. 264:11796-806.

Liscum, L., R.M. Ruggiero, and J.R. Faust. 1989. The intracellular transport of low density lipoprotein-derived cholesterol is defective in Niemann-Pick type C fibroblasts. *J Cell Biol*. 108:1625-36.

Liu, B., H. Li, J.J. Repa, S.D. Turley, and J.M. Dietschy. 2008. Genetic variations and treatments that affect the lifespan of the NPC1 mouse. *J Lipid Res*. 49:663-9.

Liu, B., S.D. Turley, D.K. Burns, A.M. Miller, J.J. Repa, and J.M. Dietschy. 2009. Reversal of defective lysosomal transport in NPC disease ameliorates liver dysfunction and neurodegeneration in the npc1-/- mouse. *Proc. Natl. Acad. Sci. U. S. A.* 106:2377-82.

Loftus, S.K., R.P. Erickson, S.U. Walkley, M.A. Bryant, A. Incao, R.A. Heidenreich, and W.J. Pavan. 2002. Rescue of neurodegeneration in Niemann-Pick C mice by a prion-promoter-driven Npc1 cDNA transgene. *Hum Mol Genet*. 11:3107-14.

Loftus, S.K., J.A. Morris, E.D. Carstea, J.Z. Gu, C. Cummings, A. Brown, J. Ellison, K. Ohno, M.A. Rosenfeld, D.A. Tagle, P.G. Pentchev, and W.J. Pavan. 1997. Murine model of Niemann-Pick C disease: mutation in a cholesterol homeostasis gene. *Science*. 277:232-5.

Lopez, M.E., A.D. Klein, U.J. Dimbil, and M.P. Scott. 2011. Anatomically defined neuron-based rescue of neurodegenerative Niemann-Pick type C disorder. *J. Neurosci.* 31:4367-78.

Lopez, M.E., A.D. Klein, J. Hong, U.J. Dimbil, and M.P. Scott. 2012a. Neuronal and epithelial cell rescue resolves chronic systemic inflammation in the lipid storage disorder Niemann-Pick C. *Hum Mol Genet*. 21:2946-60.

Lopez, M.E., A.D. Klein, and M.P. Scott. 2012b. Complement is dispensable for neurodegeneration in Niemann-Pick disease type C. *J Neuroinflammation*. 9:216.

Louwette, S., L. Regal, C. Wittevrongel, C. Thys, G. Vandeweeghde, E. Decuyper, P. Leemans, R. De Vos, C. Van Geet, J. Jaeken, and K. Freson. 2012. NPC1 defect results in abnormal platelet formation and function: studies in Niemann-Pick disease type C1 patients and zebrafish. *Hum Mol Genet*.

Lowenthal, A.C., J.F. Cummings, D.A. Wenger, M.A. Thrall, P.A. Wood, and A. de Lahunta. 1990. Feline sphingolipidosis resembling Niemann-Pick disease type C. *Acta Neuropathol*. 81:189-97.

Lu, Q.R., T. Sun, Z. Zhu, N. Ma, M. Garcia, C.D. Stiles, and D.H. Rowitch. 2002. Common developmental requirement for Olig function indicates a motor neuron/oligodendrocyte connection. *Cell*. 109:75-86.

Lund, E.G., J.M. Guileyardo, and D.W. Russell. 1999. cDNA cloning of cholesterol 24-hydroxylase, a mediator of cholesterol homeostasis in the brain. *Proc Natl Acad Sci U S A*. 96:7238-43.

Lund, E.G., C. Xie, T. Kotti, S.D. Turley, J.M. Dietschy, and D.W. Russell. 2003. Knockout of the cholesterol 24-hydroxylase gene in mice reveals a brain-specific mechanism of cholesterol turnover. *J Biol Chem*. 278:22980-8.

Malathi, K., K. Higaki, A.H. Tinkelenberg, D.A. Balderes, D. Almanzar-Paramio, L.J. Wilcox, N. Erdeniz, F. Redican, M. Padamsee, Y. Liu, S. Khan, F. Alcantara, E.D. Carstea, J.A. Morris, and S.L. Sturley. 2004. Mutagenesis of the putative sterol-sensing domain of yeast Niemann Pick C-related protein reveals a primordial role in subcellular sphingolipid distribution. *J Cell Biol*. 164:547-56.

Marcaggi, P., D. Billups, and D. Attwell. 2003. The role of glial glutamate transporters in maintaining the independent operation of juvenile mouse cerebellar parallel fibre synapses. *J Physiol*. 552:89-107.

Masliah, E., E. Rockenstein, I. Veinbergs, M. Mallory, M. Hashimoto, A. Takeda, Y. Sagara, A. Sisk, and L. Mucke. 2000. Dopaminergic loss and inclusion body formation in alpha-synuclein mice: implications for neurodegenerative disorders. *Science*. 287:1265-9.

Mauch, D.H., K. Nagler, S. Schumacher, C. Goritz, E.C. Muller, A. Otto, and F.W. Pfrieger. 2001. CNS synaptogenesis promoted by glia-derived cholesterol. *Science*. 294:1354-7.

Maue, R.A., R.W. Burgess, B. Wang, C.M. Wooley, K.L. Seburn, M.T. Vanier, M.A. Rogers, C.C. Chang, T.Y. Chang, B.T. Harris, D.J. Graber, C.A. Penatti, D.M. Porter, B.S. Szwergold, L.P. Henderson, J.W. Totenhagen, T.P. Trouard, I.A. Borbon, and R.P. Erickson. 2012. A novel mouse model of Niemann-Pick type C disease carrying a D1005G-Npc1 mutation comparable to commonly observed human mutations. *Hum Mol Genet*. 21:730-50.

Maxfield, F.R., and G. van Meer. 2010. Cholesterol, the central lipid of mammalian cells. *Curr Opin Cell Biol*. 22:422-9.

Millat, G., N. Bailo, S. Molinero, C. Rodriguez, K. Chikh, and M.T. Vanier. 2005. Niemann-Pick C disease: use of denaturing high performance liquid chromatography for the detection of NPC1 and NPC2 genetic variations and impact on management of patients and families. *Mol Genet Metab*. 86:220-32.

Millat, G., C. Marcais, M.A. Rafi, T. Yamamoto, J.A. Morris, P.G. Pentchev, K. Ohno, D.A. Wenger, and M.T. Vanier. 1999. Niemann-Pick C1 disease: the I1061T substitution is a frequent mutant allele in patients of Western European descent and correlates with a classic juvenile phenotype. *Am J Hum Genet*. 65:1321-9.

Millat, G., C. Marcais, C. Tomasetto, K. Chikh, A.H. Fensom, K. Harzer, D.A. Wenger, K. Ohno, and M.T. Vanier. 2001. Niemann-Pick C1 disease: correlations between NPC1 mutations, levels of NPC1 protein, and phenotypes emphasize the functional significance of the putative sterol-sensing domain and of the cysteine-rich luminal loop. *Am J Hum Genet*. 68:1373-85.

Miyawaki, S., S. Mitsuoka, T. Sakiyama, and T. Kitagawa. 1982. Sphingomyelinosis, a new mutation in the mouse: a model of Niemann-Pick disease in humans. *J Hered*. 73:257-63.

Morris, M.D., C. Bhuvaneswaran, H. Shio, and S. Fowler. 1982. Lysosome lipid storage disorder in NCTR-BALB/c mice. I. Description of the disease and genetics. *Am J Pathol*. 108:140-9.

Mu, T.W., D.M. Fowler, and J.W. Kelly. 2008a. Partial restoration of mutant enzyme homeostasis in three distinct lysosomal storage disease cell lines by altering calcium homeostasis. *PLoS Biol.* 6:e26.

Mu, T.W., D.S. Ong, Y.J. Wang, W.E. Balch, J.R. Yates, 3rd, L. Segatori, and J.W. Kelly. 2008b. Chemical and biological approaches synergize to ameliorate protein-folding diseases. *Cell*. 134:769-81.

Munkacsi, A.B., F.W. Chen, M.A. Brinkman, K. Higaki, G.D. Gutierrez, J. Chaudhari, J.V. Layer, A. Tong, M. Bard, C. Boone, Y.A. Ioannou, and S.L. Sturley. 2011. An "exacerbate-reverse" strategy in yeast identifies histone deacetylase inhibition as a correction for cholesterol and sphingolipid transport defects in human Niemann-Pick type C disease. *J Biol Chem*. 286:23842-51.

Mutka, A.L., S. Lusa, M.D. Linder, E. Jokitalo, O. Kopra, M. Jauhiainen, and E. Ikonen. 2004. Secretion of sterols and the NPC2 protein from primary astrocytes. *J Biol Chem*. 279:48654-62.

Naureckiene, S., D.E. Sleat, H. Lackland, A. Fensom, M.T. Vanier, R. Wattiaux, M. Jadot, and P. Lobel. 2000. Identification of HE1 as the second gene of Niemann-Pick C disease. *Science*. 290:2298-301.

Neufeld, E.B., M. Wastney, S. Patel, S. Suresh, A.M. Cooney, N.K. Dwyer, C.F. Roff, K. Ohno, J.A. Morris, E.D. Carstea, J.P. Incardona, J.F. Strauss, 3rd, M.T. Vanier, M.C. Patterson, R.O. Brady, P.G. Pentchev, and E.J. Blanchette-Mackie. 1999. The Niemann-Pick C1 protein resides in a vesicular compartment linked to retrograde transport of multiple lysosomal cargo. *J. Biol. Chem.* 274:9627-35.

Okamura, N., S. Kiuchi, M. Tamba, T. Kashima, S. Hiramoto, T. Baba, F. Dacheux, J.L. Dacheux, Y. Sugita, and Y.Z. Jin. 1999. A porcine homolog of the major secretory protein of human epididymis, HE1, specifically binds cholesterol. *Biochim Biophys Acta*. 1438:377-87.

Ong, D.S., T.W. Mu, A.E. Palmer, and J.W. Kelly. 2010. Endoplasmic reticulum Ca2+ increases enhance mutant glucocerebrosidase proteostasis. *Nat. Chem. Biol.* 6:424-32.

Paciorkowski, A.R., M. Westwell, S. Ounpuu, K. Bell, J. Kagan, C. Mazzarella, and R.M. Greenstein. 2008. Motion analysis of a child with Niemann-Pick disease type C treated with miglustat. *Mov Disord*. 23:124-8.

Park, W.D., J.F. O'Brien, P.A. Lundquist, D.L. Kraft, C.W. Vockley, P.S. Karnes, M.C. Patterson, and K. Snow. 2003. Identification of 58 novel mutations in Niemann-Pick disease type C: correlation with biochemical phenotype and importance of PTC1-like domains in NPC1. *Hum Mutat*. 22:313-25.

Patel, S.C., S. Suresh, U. Kumar, C.Y. Hu, A. Cooney, E.J. Blanchette-Mackie, E.B. Neufeld, R.C. Patel, R.O. Brady, Y.C. Patel, P.G. Pentchev, and W.Y. Ong. 1999. Localization of Niemann-Pick C1 protein in astrocytes: implications for neuronal degeneration in Niemann- Pick type C disease. *Proc Natl Acad Sci U S A*. 96:1657-62.

Patterson, M.C., A.M. Di Bisceglie, J.J. Higgins, R.B. Abel, R. Schiffmann, C.C. Parker, C.E. Argoff, R.P. Grewal, K. Yu, P.G. Pentchev, and et al. 1993. The effect of cholesterol-lowering agents on hepatic and plasma cholesterol in Niemann-Pick disease type C. *Neurology*. 43:61-4.

Patterson, M.C., D. Vecchio, E. Jacklin, L. Abel, H. Chadha-Boreham, C. Luzy, R. Giorgino, and J.E. Wraith. 2010. Long-term miglustat therapy in children with Niemann-Pick disease type C. *J Child Neurol*. 25:300-5.

Patterson, M.C., D. Vecchio, H. Prady, L. Abel, and J.E. Wraith. 2007. Miglustat for treatment of Niemann-Pick C disease: a randomised controlled study. *Lancet Neurol*. 6:765-72.

Peake, K.B., R.B. Campenot, D.E. Vance, and J.E. Vance. 2011. Niemann-Pick Type C1 deficiency in microglia does not cause neuron death in vitro. *Biochim Biophys Acta*. 1812:1121-9.

Pentchev, P.G., M.E. Comly, H.S. Kruth, M.T. Vanier, D.A. Wenger, S. Patel, and R.O. Brady. 1985. A defect in cholesterol esterification in Niemann-Pick disease (type C) patients. *Proc Natl Acad Sci U S A*. 82:8247-51.

Phillips, S.E., E.A. Woodruff, 3rd, P. Liang, M. Patten, and K. Broadie. 2008. Neuronal loss of Drosophila NPC1a causes cholesterol aggregation and age-progressive neurodegeneration. *J Neurosci*. 28:6569-82.

Pineda, M., M.S. Perez-Poyato, M. O'Callaghan, M.A. Vilaseca, M. Pocovi, R. Domingo, L.R. Portal, A.V. Perez, T. Temudo, A. Gaspar, J.J. Penas, S. Roldan, L.M. Fumero, O.B. de la Barca, M.T. Silva, J. Macias-Vidal, and M.J. Coll. 2010. Clinical experience with miglustat therapy in pediatric patients with Niemann-Pick disease type C: a case series. *Mol Genet Metab*. 99:358-66.

Pineda, M., J.E. Wraith, E. Mengel, F. Sedel, W.L. Hwu, M. Rohrbach, B. Bembi, M. Walterfang, G.C. Korenke, T. Marquardt, C. Luzy, R. Giorgino, and M.C. Patterson. 2009. Miglustat in patients with Niemann-Pick disease Type C (NP-C): a multicenter observational retrospective cohort study. *Mol Genet Metab*. 98:243-9.

Pipalia, N.H., C.C. Cosner, A. Huang, A. Chatterjee, P. Bourbon, N. Farley, P. Helquist, O. Wiest, and F.R. Maxfield. 2011. Histone deacetylase inhibitor treatment dramatically reduces cholesterol accumulation in Niemann-Pick type C1 mutant human fibroblasts. *Proc. Natl. Acad. Sci. U. S. A.* 108:5620-5.

Pipalia, N.H., A. Huang, H. Ralph, M. Rujoi, and F.R. Maxfield. 2006. Automated microscopy screening for compounds that partially revert cholesterol accumulation in Niemann-Pick C cells. *J. Lipid Res.* 47:284-301.

Platt, F.M., G.R. Neises, R.A. Dwek, and T.D. Butters. 1994. N-butyldeoxynojirimycin is a novel inhibitor of glycolipid biosynthesis. *J Biol Chem*. 269:8362-5.

Powers, E.T., R.I. Morimoto, A. Dillin, J.W. Kelly, and W.E. Balch. 2009. Biological and chemical approaches to diseases of proteostasis deficiency. *Annu Rev Biochem*. 78:959-91.

Pressey, S.N., D.A. Smith, A.M. Wong, F.M. Platt, and J.D. Cooper. 2012. Early glial activation, synaptic changes and axonal pathology in the thalamocortical system of Niemann-Pick type C1 mice. *Neurobiol Dis*. 45:1086-100.

Ramirez, C.M., B. Liu, A.M. Taylor, J.J. Repa, D.K. Burns, A.G. Weinberg, S.D. Turley, and J.M. Dietschy. 2010. Weekly cyclodextrin administration normalizes cholesterol metabolism in nearly every organ of the Niemann-Pick type C1 mouse and markedly prolongs life. *Pediatr Res*. 68:309-15.

Richardson, W.D., N. Kessaris, and N. Pringle. 2006. Oligodendrocyte wars. *Nat. Rev. Neurosci.* 7:11-8.

Rodriguez-Lafrasse, C., R. Rousson, P.G. Pentchev, P. Louisot, and M.T. Vanier. 1994. Free sphingoid bases in tissues from patients with type C Niemann-Pick disease and other lysosomal storage disorders. *Biochim Biophys Acta*. 1226:138-44.

Rosen, D.R., T. Siddique, D. Patterson, D.A. Figlewicz, P. Sapp, A. Hentati, D. Donaldson, J. Goto, J.P. O'Regan, H.X. Deng, and et al. 1993. Mutations in Cu/Zn superoxide dismutase gene are associated with familial amyotrophic lateral sclerosis. *Nature*. 362:59-62.

Rosenbaum, A.I., G. Zhang, J.D. Warren, and F.R. Maxfield. 2010. Endocytosis of beta-cyclodextrins is responsible for cholesterol reduction in Niemann-Pick type C mutant cells. *Proc. Natl. Acad. Sci. U. S. A.* 107:5477-82.

Runz, H., D. Dolle, A.M. Schlitter, and J. Zschocke. 2008. NPC-db, a Niemann-Pick type C disease gene variation database. *Hum Mutat*. 29:345-50.

Saher, G., B. Brugger, C. Lappe-Siefke, W. Mobius, R. Tozawa, M.C. Wehr, F. Wieland, S. Ishibashi, and K.A. Nave. 2005. High cholesterol level is essential for myelin membrane growth. *Nat. Neurosci.* 8:468-75.

Santos, M.L., S. Raskin, D.S. Telles, A. Lohr, Jr., P.B. Liberalesso, S.C. Vieira, and M.L. Cordeiro. 2008. Treatment of a child diagnosed with Niemann-Pick disease type C with miglustat: a case report in Brazil. *J Inherit Metab Dis*. 31 Suppl 2:S357-61.

Sarna, J.R., M. Larouche, H. Marzban, R.V. Sillitoe, D.E. Rancourt, and R. Hawkes. 2003. Patterned Purkinje cell degeneration in mouse models of Niemann-Pick type C disease. *J Comp Neurol*. 456:279-91.

Sawkar, A.R., W. D'Haeze, and J.W. Kelly. 2006a. Therapeutic strategies to ameliorate lysosomal storage disorders--a focus on Gaucher disease. *Cell Mol Life Sci*. 63:1179-92.

Sawkar, A.R., M. Schmitz, K.P. Zimmer, D. Reczek, T. Edmunds, W.E. Balch, and J.W. Kelly. 2006b. Chemical chaperones and permissive temperatures alter localization of Gaucher disease associated glucocerebrosidase variants. *ACS Chem Biol*. 1:235-51.

Schuller, U., V.M. Heine, J. Mao, A.T. Kho, A.K. Dillon, Y.G. Han, E. Huillard, T. Sun, A.H. Ligon, Y. Qian, Q. Ma, A. Alvarez-Buylla, A.P. McMahon, D.H. Rowitch, and K.L. Ligon. 2008. Acquisition of granule neuron precursor identity is a critical determinant of progenitor cell competence to form Shh-induced medulloblastoma. *Cancer Cell*. 14:123-34.

Schwend, T., E.J. Loucks, D. Snyder, and S.C. Ahlgren. 2011. Requirement of Npc1 and availability of cholesterol for early embryonic cell movements in Zebrafish. *J Lipid Res*.

Shen, D., X. Wang, X. Li, X. Zhang, Z. Yao, S. Dibble, X.P. Dong, T. Yu, A.P. Lieberman, H.D. Showalter, and H. Xu. 2012. Lipid storage disorders block lysosomal trafficking by inhibiting a TRP channel and lysosomal calcium release. *Nat Commun*. 3:731.

Shen, S., J. Li, and P. Casaccia-Bonnefil. 2005. Histone modifications affect timing of oligodendrocyte progenitor differentiation in the developing rat brain. *J Cell Biol*. 169:577-89.

Shin, D., J.Y. Shin, M.T. McManus, L.J. Ptacek, and Y.H. Fu. 2009. Dicer ablation in oligodendrocytes provokes neuronal impairment in mice. *Ann Neurol*. 66:843-57.

Shulman, L.M., N.J. David, and W.J. Weiner. 1995. Psychosis as the initial manifestation of adult-onset Niemann-Pick disease type C. *Neurology*. 45:1739-43.

Sleat, D.E., J.A. Wiseman, M. El-Banna, S.M. Price, L. Verot, M.M. Shen, G.S. Tint, M.T. Vanier, S.U. Walkley, and P. Lobel. 2004. Genetic evidence for nonredundant functional cooperativity between NPC1 and NPC2 in lipid transport. *Proc Natl Acad Sci U S A*. 101:5886-91.

Sokol, J., J. Blanchette-Mackie, H.S. Kruth, N.K. Dwyer, L.M. Amende, J.D. Butler, E. Robinson, S. Patel, R.O. Brady, M.E. Comly, and et al. 1988. Type C Niemann-Pick disease. Lysosomal accumulation and defective intracellular mobilization of low density lipoprotein cholesterol. *J Biol Chem*. 263:3411-7.

Somers, K.L., D.E. Brown, R. Fulton, P.C. Schultheiss, D. Hamar, M.O. Smith, R. Allison, H.E. Connally, C. Just, T.W. Mitchell, D.A. Wenger, and M.A. Thrall. 2001. Effects of dietary cholesterol restriction in a feline model of Niemann-Pick type C disease. *J Inherit Metab Dis*. 24:427-36.

Soriano, P. 1999. Generalized lacZ expression with the ROSA26 Cre reporter strain. *Nat. Genet.* 21:70-1.

Sperber, B.R., E.A. Boyle-Walsh, M.J. Engleka, P. Gadue, A.C. Peterson, P.L. Stein, S.S. Scherer, and F.A. McMorris. 2001. A unique role for Fyn in CNS myelination. *J. Neurosci.* 21:2039-47.

Sugimoto, Y., H. Ninomiya, Y. Ohsaki, K. Higaki, J.P. Davies, Y.A. Ioannou, and K. Ohno. 2001. Accumulation of cholera toxin and GM1 ganglioside in the early endosome of Niemann-Pick C1-deficient cells. *Proc. Natl. Acad. Sci. U. S. A.* 98:12391-6.

Sun, X., D.L. Marks, W.D. Park, C.L. Wheatley, V. Puri, J.F. O'Brien, D.L. Kraft, P.A. Lundquist, M.C. Patterson, R.E. Pagano, and K. Snow. 2001. Niemann-Pick C variant detection by altered sphingolipid trafficking and correlation with mutations within a specific domain of NPC1. *Am. J. Hum. Genet.* 68:1361-72.

Sym, M., M. Basson, and C. Johnson. 2000. A model for niemann-pick type C disease in the nematode Caenorhabditis elegans. *Curr Biol*. 10:527-30.

Takahashi, M., Y. Kovalchuk, and D. Attwell. 1995. Pre- and postsynaptic determinants of EPSC waveform at cerebellar climbing fiber and parallel fiber to Purkinje cell synapses. *J Neurosci*. 15:5693-702.

Takikita, S., T. Fukuda, I. Mohri, T. Yagi, and K. Suzuki. 2004. Perturbed myelination process of premyelinating oligodendrocyte in Niemann-Pick type C mouse. *J. Neuropathol. Exp. Neurol.* 63:660-73.

Tawk, M., J. Makoukji, M. Belle, C. Fonte, A. Trousson, T. Hawkins, H. Li, S. Ghandour, M. Schumacher, and C. Massaad. 2011. Wnt/beta-catenin signaling is an essential and direct driver of myelin gene expression and myelinogenesis. *J Neurosci*. 31:3729-42.

Trouard, T.P., R.A. Heidenreich, J.F. Seeger, and R.P. Erickson. 2005. Diffusion tensor imaging in Niemann-Pick Type C disease. *Pediatr. Neurol.* 33:325-30.

Umemori, H., S. Sato, T. Yagi, S. Aizawa, and T. Yamamoto. 1994. Initial events of myelination involve Fyn tyrosine kinase signalling. *Nature*. 367:572-6.

Vance, J.E., H. Hayashi, and B. Karten. 2005. Cholesterol homeostasis in neurons and glial cells. *Semin Cell Dev Biol*. 16:193-212.

Vanier, M.T. 1999. Lipid changes in Niemann-Pick disease type C brain: personal experience and review of the literature. *Neurochem Res*. 24:481-9.

Vanier, M.T. 2010. Niemann-Pick disease type C. *Orphanet J. Rare Dis.* 5:16.

Vanier, M.T., S. Duthel, C. Rodriguez-Lafrasse, P. Pentchev, and E.D. Carstea. 1996. Genetic heterogeneity in Niemann-Pick C disease: a study using somatic cell hybridization and linkage analysis. *Am J Hum Genet*. 58:118-25.

Vanier, M.T., and G. Millat. 2003. Niemann-Pick disease type C. *Clin Genet*. 64:269-81.

Vanier, M.T., C. Rodriguez-Lafrasse, R. Rousson, S. Duthel, K. Harzer, P.G. Pentchev, A. Revol, and P. Louisot. 1991. Type C Niemann-Pick disease: biochemical aspects and phenotypic heterogeneity. *Dev Neurosci*. 13:307-14.

Vanier, M.T., D.A. Wenger, M.E. Comly, R. Rousson, R.O. Brady, and P.G. Pentchev. 1988. Niemann-Pick disease group C: clinical variability and diagnosis based on defective cholesterol esterification. A collaborative study on 70 patients. *Clin Genet*. 33:331-48.

Verheijen, M.H., N. Camargo, V. Verdier, K. Nadra, A.S. de Preux Charles, J.J. Medard, A. Luoma, M. Crowther, H. Inouye, H. Shimano, S. Chen, J.F. Brouwers, J.B. Helms, M.L. Feltri, L. Wrabetz, D. Kirschner, R. Chrast, and A.B. Smit. 2009. SCAP is required for timely and proper myelin membrane synthesis. *Proc. Natl. Acad. Sci. U S A*. 106:21383-8.

Wake, H., P.R. Lee, and R.D. Fields. 2011. Control of local protein synthesis and initial events in myelination by action potentials. *Science*. 333:1647-51.

Walterfang, M., M. Fahey, P. Desmond, A. Wood, M.L. Seal, C. Steward, C. Adamson, C. Kokkinos, M. Fietz, and D. Velakoulis. 2010. White and gray matter alterations in adults with Niemann-Pick disease type C: a cross-sectional study. *Neurology*. 75:49-56.

Wang, F., G. Agnello, N. Sotolongo, and L. Segatori. 2011. Ca2+ homeostasis modulation enhances the amenability of L444P glucosylcerebrosidase to proteostasis regulation in patient-derived fibroblasts. *ACS Chem. Biol.* 6:158-68.

Wang, S., and R.J. Kaufman. 2012. The impact of the unfolded protein response on human disease. *J Cell Biol*. 197:857-67.

Wang, S., A.D. Sdrulla, G. diSibio, G. Bush, D. Nofziger, C. Hicks, G. Weinmaster, and B.A. Barres. 1998. Notch receptor activation inhibits oligodendrocyte differentiation. *Neuron*. 21:63-75.

Weintraub, H., A. Abramovici, U. Sandbank, A.D. Booth, P.G. Pentchev, and B. Sela. 1987. Dysmyelination in NCTR-Balb/C mouse mutant with a lysosomal storage disorder. Morphological survey. *Acta Neuropathol.* 74:374-81.

Weintraub, H., A. Abramovici, U. Sandbank, P.G. Pentchev, R.O. Brady, M. Sekine, A. Suzuki, and B. Sela. 1985. Neurological mutation characterized by dysmyelination in NCTR-Balb/C mouse with lysosomal lipid storage disease. *J. Neurochem.* 45:665-72.

Weng, Q., Y. Chen, H. Wang, X. Xu, B. Yang, Q. He, W. Shou, Y. Higashi, V. van den Berghe, E. Seuntjens, S.G. Kernie, P. Bukshpun, E.H. Sherr, D. Huylebroeck, and Q.R. Lu. 2012. Dual-mode modulation of Smad signaling by Smad-interacting protein Sip1 is required for myelination in the central nervous system. *Neuron*. 73:713-28.

Winchester, B., A. Vellodi, and E. Young. 2000. The molecular basis of lysosomal storage diseases and their treatment. *Biochem Soc Trans*. 28:150-4.

Wojtanik, K.M., and L. Liscum. 2003. The transport of low density lipoprotein-derived cholesterol to the plasma membrane is defective in NPC1 cells. *J Biol Chem*. 278:14850-6.

Wraith, J.E., M.R. Baumgartner, B. Bembi, A. Covanis, T. Levade, E. Mengel, M. Pineda, F. Sedel, M. Topcu, M.T. Vanier, H. Widner, F.A. Wijburg, and M.C. Patterson. 2009. Recommendations on the diagnosis and management of Niemann-Pick disease type C. *Mol Genet Metab*. 98:152-65.

Wraith, J.E., and J. Imrie. 2009. New therapies in the management of Niemann-Pick type C disease: clinical utility of miglustat. *Ther Clin Risk Manag*. 5:877-87.

Wu, Y.P., and R.L. Proia. 2004. Deletion of macrophage-inflammatory protein 1 alpha retards neurodegeneration in Sandhoff disease mice. *Proc Natl Acad Sci U S A*. 101:8425-30.

Xie, C., D.K. Burns, S.D. Turley, and J.M. Dietschy. 2000. Cholesterol is sequestered in the brains of mice with Niemann-Pick type C disease but turnover is increased. *J Neuropathol Exp Neurol*. 59:1106-17.

Xie, X., M.S. Brown, J.M. Shelton, J.A. Richardson, J.L. Goldstein, and G. Liang. 2011. Amino acid substitution in NPC1 that abolishes cholesterol binding reproduces phenotype of complete NPC1 deficiency in mice. *Proc Natl Acad Sci U S A*. 108:15330-5.

Xu, M., K. Liu, M. Swaroop, F.D. Porter, R. Sidhu, S. Firnkes, D.S. Ory, J.J. Marugan, J. Xiao, N. Southall, W.J. Pavan, C. Davidson, S.U. Walkley, A.T. Remaley, U. Baxa, W. Sun, J.C. McKew, C.P. Austin, and W. Zheng. 2012. delta-Tocopherol Reduces Lipid Accumulation in Niemann-Pick Type C1 and Wolman Cholesterol Storage Disorders. *J Biol Chem*.

Xu, S., B. Benoff, H.L. Liou, P. Lobel, and A.M. Stock. 2007. Structural basis of sterol binding by NPC2, a lysosomal protein deficient in Niemann-Pick type C2 disease. *J Biol Chem*. 282:23525-31.

Yamada, A., M. Saji, Y. Ukita, Y. Shinoda, M. Taniguchi, K. Higaki, H. Ninomiya, and K. Ohno. 2001. Progressive neuronal loss in the ventral posterior lateral and medial nuclei of thalamus in Niemann-Pick disease type C mouse brain. *Brain Dev*. 23:288-97.

Yamamoto, T., K. Iwasawa, T. Tokoro, Y. Eto, and K. Maekawa. 1994. [A possible same genetic defect in two Niemann-Pick disease model mice]. *No To Hattatsu*. 26:318-22.

Yazawa, I., B.I. Giasson, R. Sasaki, B. Zhang, S. Joyce, K. Uryu, J.Q. Trojanowski, and V.M. Lee. 2005. Mouse model of multiple system atrophy alpha-synuclein expression in oligodendrocytes causes glial and neuronal degeneration. *Neuron*. 45:847-59.

Ye, F., Y. Chen, T. Hoang, R.L. Montgomery, X.H. Zhao, H. Bu, T. Hu, M.M. Taketo, J.H. van Es, H. Clevers, J. Hsieh, R. Bassel-Duby, E.N. Olson, and Q.R. Lu. 2009. HDAC1 and HDAC2 regulate oligodendrocyte differentiation by disrupting the beta-catenin-TCF interaction. *Nat Neurosci*. 12:829-38.

Yu, T., C. Chung, D. Shen, H. Xu, and A.P. Lieberman. 2012. Ryanodine receptor antagonists adapt NPC1 proteostasis to ameliorate lipid storage in Niemann-Pick type C disease fibroblasts. *Hum Mol Genet*. 21:3205-14.

Yu, T., V.G. Shakkottai, C. Chung, and A.P. Lieberman. 2011. Temporal and cell-specific deletion establishes that neuronal Npc1 deficiency is sufficient to mediate neurodegeneration. *Hum. Mol. Genet.* 20:4440-51.

Zervas, M., K. Dobrenis, and S.U. Walkley. 2001a. Neurons in Niemann-Pick disease type C accumulate gangliosides as well as unesterified cholesterol and undergo dendritic and axonal alterations. *J Neuropathol Exp Neurol*. 60:49-64.

Zervas, M., K.L. Somers, M.A. Thrall, and S.U. Walkley. 2001b. Critical role for glycosphingolipids in Niemann-Pick disease type C. *Curr Biol*. 11:1283-7.

Zhang, M., D. Strnatka, C. Donohue, J.L. Hallows, I. Vincent, and R.P. Erickson. 2008. Astrocyte-only Npc1 reduces neuronal cholesterol and triples life span of Npc1-/- mice. *J Neurosci Res*. 86:2848-56.

Zhang, M., M. Sun, N.K. Dwyer, M.E. Comly, S.C. Patel, R. Sundaram, J.A. Hanover, and E.J. Blanchette-Mackie. 2003. Differential trafficking of the Niemann-Pick C1 and 2 proteins highlights distinct roles in late endocytic lipid trafficking. *Acta Paediatr Suppl*. 92:63-73; discussion 45.

Zhao, X., X. He, X. Han, Y. Yu, F. Ye, Y. Chen, T. Hoang, X. Xu, Q.S. Mi, M. Xin, F. Wang, B. Appel, and Q.R. Lu. 2010. MicroRNA-mediated control of oligodendrocyte differentiation. *Neuron*. 65:612-26.

Zhu, Y., M.I. Romero, P. Ghosh, Z. Ye, P. Charnay, E.J. Rushing, J.D. Marth, and L.F. Parada. 2001. Ablation of NF1 function in neurons induces abnormal development of cerebral cortex and reactive gliosis in the brain. *Genes Dev.* 15:859-76.